People's Democratic Republic of Algeria
Ministry of Higher Education and Scientific Research

N° Série : ………/2024

# Kasdi Merbah Ouargla University

Faculty of Hydrocarbons, Renewables Energies,
And earth and Universe Sciences

**Department of Hydrocarbons Production**

## MASTER THESIS

**To obtain the Master's Degree**

**Major: Academic Production**

Presented By:

**Raida HAOUED MOUISSA, Isra ABBAS**

-THEME-

# Simulation of the impact of boosting method on gas reservoir recovery (TAGS) at Brides field, Gassi Touil Region.

Defended on: 11 / 06 / 2024 Ouargla University

Jury:

| | | |
|---|---|---|
| President: | Mr.BOUTALBI Med.Chaker | University. Ouargla |
| Examiner: | Mr.FROUHAT Rachid | University. Ouargla |
| Supervisor: | Mr.CHETTI Djamal Eddine | University. Ouargla |
| Co-Supervisor: | Mrs.BOULAADJOUL Soumia | University. Ouargla |
| Co-Supervisor: | Mr.HATHAT Imad | DP Sonatrach |
| Co-Supervisor: | Mr.DEROUICHE Abderrahim | DP Sonatrach |

Ouargla Academic year 2023/2024

# Acknowledgement

As we bring this manuscript and years of research at the Hyrocarbons faculty of KASDI MERBAH University to a close, we would like to express our deepest gratitude to our supervisors, Mr. **DJAMAL EDDINE CHETTI** and Mrs. **BOULAADJOUL SOUMIA**, for his unwavering trust and encouragement throughout our journey.

We are also honored to extend our sincere appreciation to Mr. **BOUTALBI CHAKER** for accepting to chair our thesis defense jury.

Our gratitude extends to Mr. **FROUHAT RACHID** for his willingness to review our work.

Finally, in these last lines, we would like to express our heartfelt thanks go to the dean **DOBBI ABDELMADJID**, the Department head **BEN SASSI ABDELATIF**, and the Administrators **BOUFADESS DJAMILA**, **ARBAOUI ALI**, **ADJOU ZAKARIA**, and **GAZAN SALIM** .

# شكر وتقدير لعمال سوناطراك البواسل

## إلى عمال سوناطراك الكرام،

يسعدنا ، ونحن نختتم هذا العمل، أن نتوجه إليكم بوافر الشكر والتقدير، عرفاناً بجميل ما قدمتموه لنا من عونٍ وسندٍ خلال مسيرة إنجازه

لقد كنتم خيرَ رفقاءِ دربٍ، وسندٍ قويٍّ، شاركتمونا بِخِبراتِكم الواسعة وعلمِكم الغزير، مُثْرِينَ إيانا بِمَعَارِفَ شاملةٍ أفادتنا في تكوينِنا وتطويرِ مهاراتِنا

لا يسعنا إلا أن نعترف بأنّ هذا العمل لم يكن ليُكتمل بِهَذِهِ الصورةِ اللائقةِ لولا جهودكم الجبّارة وتفانيكم الصادق. فقد أبديتمْ صبرًا جميلاً وتواضعًا مُقَدّرًا في تعاملكم معنا، ممّا زادَ من شعورِنا بالامتنانِ والتقديرِ لكم.

إنّنا لن ننسى أبدًا وقوفكم معنا في كلّ خطوةٍ من خطواتِ هذا العمل، ودعمكم المتواصل لنا. فكنتم خيرَ سندٍ لنا، وخيرَ عونٍ على إنجازهِ بِأعلى دقةٍ واتقان

جزيل الشكر والتقدير لكم، أيها العمال البواسل، على ما بذلتموه من جهدٍ وعطاءٍ مخلص، وعلى ما قدمتموه لنا من دعمٍ معنويٍ وماديٍ لا يُقدر بثمن

بذلك لاننسى ان نخصص شكرا لكل من الافاضل بوحجة محمد,عماد هتهات,درويش عبدالرحيم,عبو احمد وطارق بوغباش.

مع خالص التمنيات لكم بالتوفيق والسداد في مسيرتكم المهنية المُشرّفة

*I dedicate this humble work of mine to my parents, who have stopped at nothing to support me.*

*To my siblings, who fill my life with chaos and companionship.*

*To my best friend, and partner in crime, Raida.*

*"We were girls together "*

*And lastly, the one who shaped my very being and who has been my rock and silent protector my entire life, my dear sister, Halla.*

*ISRA*

# اهداء

الى ابي نور عيناي وكل عائلة حودمية ،

لعويسات وبوعبيد .

الى أعظم هبات الله لي في هذه الحياة ، وسبب
وجودي والاستمرار فيها ، وفي وسط العتمة نور، حتى
الحروف لن تصف شروق شمس بجمال
ابتسامتك ولا غروبها بدونها "أمي".

الى اختاي اللتان لم تنجبهما امي خلود واسراء .

راعة

## Abstract

In oil and gas production, Boosters play a crucial role in ensuring efficient transport of well fluids from the reservoir to processing facilities. Our research involves studying the impact of this method on the production of 7 wells in the Brides field, Gassi Touil region. This study is based on the analysis and interpretation of modelling results and production predictions using the MBAL and PIPESIME software. Our findings demonstrate that implementing the booster will result in a significant increase in gas and condensate flow rates. Furthermore, our economic assessment reveals an exceptionally short payback period of around 41 days into the project.

**Keywords:**

Booster, modelling, predictions, Brides field, MBAL software, PIPESIME software.

## Résumé

Dans la production pétrolière et gazière, les Boosters jouent un rôle crucial en assurant un transport efficace des fluides de puits du réservoir aux installations de traitement. Notre recherche consiste à étudier l'impact de cette méthode sur la production de 7 puits dans le champ Brides, région de Gassi Touil. Cette étude s'appuie sur l'analyse et l'interprétation des résultats de modélisation et des prévisions de production à l'aide des logiciels MBAL et PIPESIME. Nos résultats démontrent que la mise en œuvre du surpresseur entraînera une augmentation significative des débits de gaz et de condensats. De plus, notre évaluation économique révèle un délai de récupération exceptionnellement court d'environ 41 jours après le début du projet.

**Les mots clés :**

Booster, modélisation, prédictions, champ de Brides, Logiciel MBAL, Logiciel PIPESIME.

## مستخلص

في إنتاج النفط والغاز، تلعب المعززات دورًا حاسمًا في ضمان النقل الفعال لسوائل الآبار من المكمن إلى مرافق المعالجة. يتضمن بحثنا دراسة تأثير هذه الطريقة على إنتاج 7 آبار بحقل بريداس منطقة قاسي الطويل. اعتمدت هذه الدراسة على تحليل وتفسير نتائج النمذجة وتنبؤات الإنتاج باستخدام برنامج MBAL وPIPESIME. توضح النتائج التي توصلنا إليها أن تنفيذ المعزز سيؤدي إلى زيادة كبيرة في معدلات تدفق الغاز والمكثفات. علاوة على ذلك، يكشف تقييمنا الاقتصادي عن فترة استرداد قصيرة للغاية تبلغ حوالي 41 يومًا من بدء المشروع.

**الكلمات المفتاحية:**

المعزز، النمذجة، منطقة بريداس، التنبؤ بالإنتاج، برنامج MBAL، برنامج PIPESIME.

# Table of Contents

# List of Figures

# List of Tables

# List of Equations

# Symbols and Abbreviations

**$n_p$:** Moles of gas produced.

**$n_i$:** Moles of gas initially in the reservoir.

**$n_f$:** Moles of gas remaining in the reservoir.

**$P_i$:** Initial reservoir pressure.

**$G_p$:** Cumulative gas production, **scf.**

**P :** Current reservoir pressure.

**V:** Original gas volume, ft3.

**$z_i$:** Gas deviation factor at pi.

**z:** Gas deviation factor at p.

**T:** Temperature, °**R.**

**$W_e$:** Cumulative water influx, **ft3**.

**$W_p$:** Cumulative water production, **ft3**.

**G:** Initial gas in place (**SCF**).

**q:** Flow rate.

**Pwf**: Bottomhole flowing pressure.

**Pwh:** Wellhead pressure.

**ΔP:** Pressure drop in each segment.

**$q_g$:** Flow rate, **Mcf/D**.

**k:** Permeability**, md**.

**h:** Net vertical thickness, **ft.**

**$\bar{p}_r$:** Average formation pressure (shut-in BHP), **psia.**

**$p_{wfs}$:** Sandface flowing BHP, **psia**.

**µ:** Viscosity, **cp**.

**T**: Temperature, °**R**.

**Z:** Supercompressibility, dimensionless.

$\mathbf{r_e}$**:** Drainage radius, **ft**.

$\mathbf{r_w}$: Wellbore radius, **ft**.

**S:** skin factor, dimensionless.

**MF**: Manifold.

**HP**: High pressure.

**LP**: Low pressure.

# Introduction

# Introduction

Natural gas is a clean-burning source of energy extracted from geological formations. It is widely used for various purposes such as heating, cooling, electricity generation, and the production of essential materials like steel and concrete. The natural gas industry is an important contributor to Algeria's Gross Domestic Product (GDP). In 2019, natural gas rents in the country accounted for approximately 2% of the country's economy.

Oil and gas companies have sought to maximize the recovery of the reserves in place and to extend the life of the mature oil and natural gas sites to meet the global demand for these fossil energies, which constitute almost all of the energy consumed worldwide.

Enhancement of the production of oil and gas is considered a must during the lifespan of any hydrocarbon reservoir, as their production naturally declines over time. Thanks to significant technological advancements, the petroleum industry has introduced various methods to increase the total recovery of oil and gas. These methods include artificial recovery techniques such as gas lift, CO2 injection, as well as stimulation methods. Additionally, it is also important to take into consideration other different elements that may cause a decline in production such as the location, and operating environment of the wells. Production optimization techniques may not always be a sufficient solution in these cases.

In our research, we are focusing on the Boosting technique. The compression unit "Booster", is a multiphase pressure boosting technology, is designed to increase the pressure of the well fluids (oil, gas, and water mix) ensuring efficient transportation from the reservoir to processing facilities. This boosting system can offer a cost-effective solution to well intervention and contributes to the recovery of more hydrocarbons by overcoming pressure drops in pipelines, ultimately prolonging the life of the hydrocarbon field.

We aim to achieve the following objectives in our study:

- Identifying the "Boosting" technology and its various applications on the production system and discussing the potential improvements that this technique could bring.
- Employing MBAL software to model reservoirs.
- Utilizing PIPSIME software to model the Boosting unit production system.
- Optimizing the flow and analyzing the impact of the Booster on the overall system and future production.

Our research consists of 4 chapters. The first chapter is a general overview of the Gassi Touil region, where our study took place. In the second chapter, we delve into the concept of production prediction and the general knowledge required to realize our study. The third chapter discusses the criteria for selecting the 7 candidate wells that have been chosen to be boosted and provides a detailed description of the Boosting unit proposed. The fourth and final chapter will contain the result of our research, detailing the use of MBAL and PIPESIM software to model and predict the potential outcomes of implementing a Boosting unit on the candidate wells.

# Chapter I

## *General Information on Gassi Touil Region*

## I.1 Sonatrach Production Division (DP)

Sonatrach is the Algerian national company responsible for research, production, pipeline transportation, processing, and marketing of hydrocarbons and derivatives. It's also involved in other sectors like power generation, renewable energies, and desalination. Sonatrach operates in Algeria and around the world.

It's the leading company in Africa and holds a prominent position globally. Its total production (all products combined) was 191 million TEP (Tonnes Equivalent Pétrole) in 2015. Its activities contribute to about 31% of Algeria's Gross National Product (GNP). Sonatrach employs 120,000 people across the group.

Sonatrach is divided into four Activities: Exploration & Production, Downstream, Pipeline Transportation, and Marketing. The Production Division (DP) is an integral part of the Exploration & Production Activity.

## I.2 Presentation of the Gassi Touil Site

The Gassi Touil Regional Directorate is one of ten Regional Directorates that constitute the Production Division of the Exploitation Production branch / Exploration & Production Activity of the Sonatrach group.

Petroleum, gas, and dry gas extracted from deposits in the perimeters of Brides, Nezla (North and South), Gassi El Adem, Gassi Touil, Toual, Hassi Touareg (North and South), Hassi Chergui (North and South), and Rhourd El Khelf. **[1]**

The Regional Directorate has various base facilities, including:

- Two production units (one for crude oil treatment and one for gas treatment).
- Oil and gas fields.
- An agricultural area (launched as part of the Saharan agriculture development policy)**.**

The Gassi Touil region is situated in the Ouargla wilaya, approximately 1000 km from Algiers and 150 km southeast of Hassi Messaoud. It encompasses an area of roughly 170 km in length and 105 km in width. **[2]**

**a) Geographical Coordinates:**

X: 06° 28’ 7’’ E

Y: 30° 31’ 0’’ N

**b) UTM Coordinates:**

X = 257,100

Y = 3,378,550

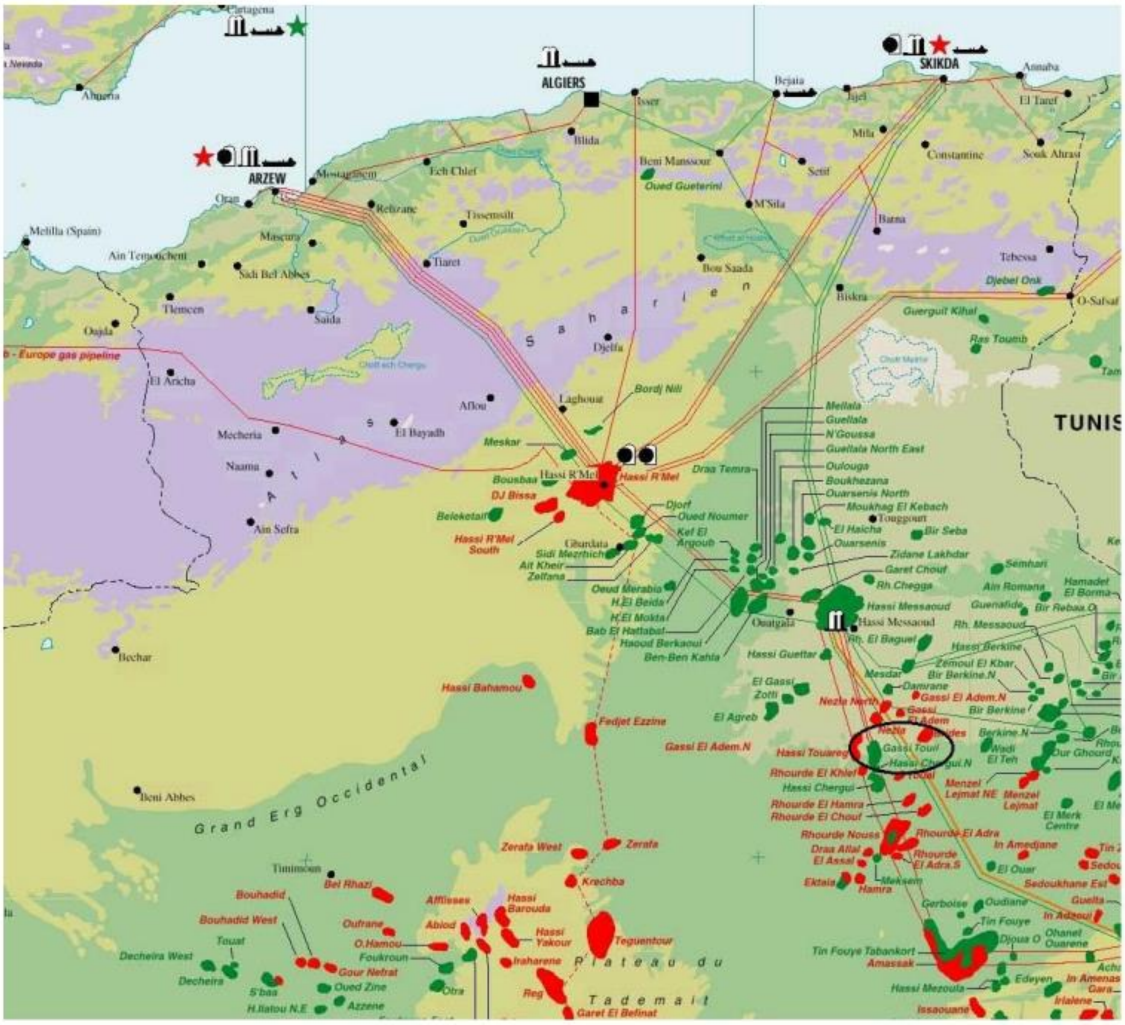


**Figure I.1**: Geographique localisation Gassi Touil region. **[3]**

## I.3 History of Gassi Touil region

The Gassi Touil region is composed of several fields, with the main ones being:

- **Gassi Touil (GT)**, discovered in 1961, confirming the presence of oil and gas

with 80 gas wells drilled.

- **Nezla Nord (NZN)**, discovered in 1958, indicating the presence of oil and gas with 10 oil and gas wells drilled
- **Nezla Sud (NZS)**, discovered in 1958, revealing the presence of gas with 30 gas wells drilled
- **Hassi Touareg (HTG)**, discovered in 1958, confirming the presence of gas with 13 gas wells drilled
- **Hassi Chergui (HC)** , discovered in 1962, confirming the presence of oil with 10 oil wells drilled.
- **Gassi El Adem (GEA)**, discovered in 1967, with 9 gas wells drilled.

The fields under development are:

- **Brides (BRD)** , discovered in 1958, indicating the presence of dry gas with 12 gas wells drilled.
- **Toual (TOU)**, discovered in 1958, revealed the presence of gas and condensate with 32 gas and condensate wells drilled. **[1]**

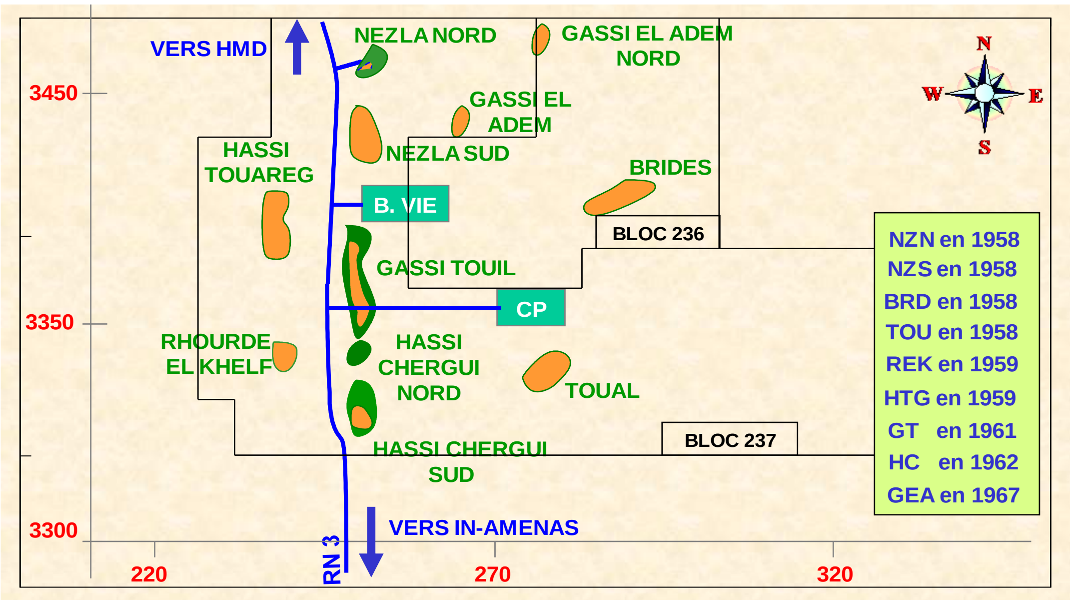


**Figure I.2** : The positioning of the Gassi Touil region fields.. **[4]**

**Table I.1**: The reservoirs of Gassi Touil region fields. **[5]**

| Field | Reservoir |
|---|---|
| BRIDES | Q.H |
| BRIDES | T.A.G.S |
| BRIDES | T.A.G.S |
| BRIDES | T.A.G.S |
| GASSI EL ADEM | Q.H |
| GASSI TOUIL | T.A.G.S |
| GASSI TOUIL | T.A.G.I |
| HASSI CHERGUI | T.A.G.S |
| HASSI CHERGUI | T.A.G.S |
| HASSI TOUAREG | T.A.G.S |
| HASSI TOUAREG | T.A.G.S |
| NEZLA | T.A.G.S |
| NEZLA | Q.H+G.O+T.A.G.I |
| NEZLA | T.A.G.S |
| TOUAL | T.A.G.I |
| TOUAL | T.A.G.S |

## I.4 Brides Field Overview

The Trias Argilo-Gréseux Supérieur (TAGS) formation in the Brides region can reach thicknesses exceeding 150 meters in some places. However, only the basal 40 to 50 meters show potential reservoir intervals, characterized by core samples with porosities ranging from 2 to 16% and variable permeabilities of 0.1 to 177 md. Its lateral extension in the Brides region is estimated to be hectometric (on the scale of hundreds of meters). The results of the Brides exploration wells (BRD-1, 2, 3, 4, 5, and 6) have revealed a significant gas condensate deposit based on the Gas-Water Contact (GWC) located at -3222 meters TVDSS (True Vertical Depth Subsea) in the TAGS reservoir. **[6]**

- **BRD 1 (1963):** The first well drilled in the BRD area, BRD 1, encountered gas within the TAGS formation in 1963.
- **BRD 2** Drilled in 1971, **BRD 3 (1974)**, and these three wells, drilled between 1987 and 1995 **BRD 4 (09/87 - 01/90), BRD 5 (02/92 - 01/94), and BRD 6 (05/94 - 08/95)**

There are three TAGS reservoirs in BRIDES:

- **TAGS MAIN** (BRD1, BRD12, BRD13, BRD14, BRD15).

- **TAGS WEST** (BDSN-2)
- **TAGS NORTH** (BDSN-1)

### I.4.2 Coordinates

**Geographic Coordinates:**

- X: 6°55'00" to 7°05'00"
- Y: 30°35'00" to 30°21'00"

**UTM Coordinates:**

- X: 308 200 to 315 600
- Y: 3 394 500 to 3 378 300

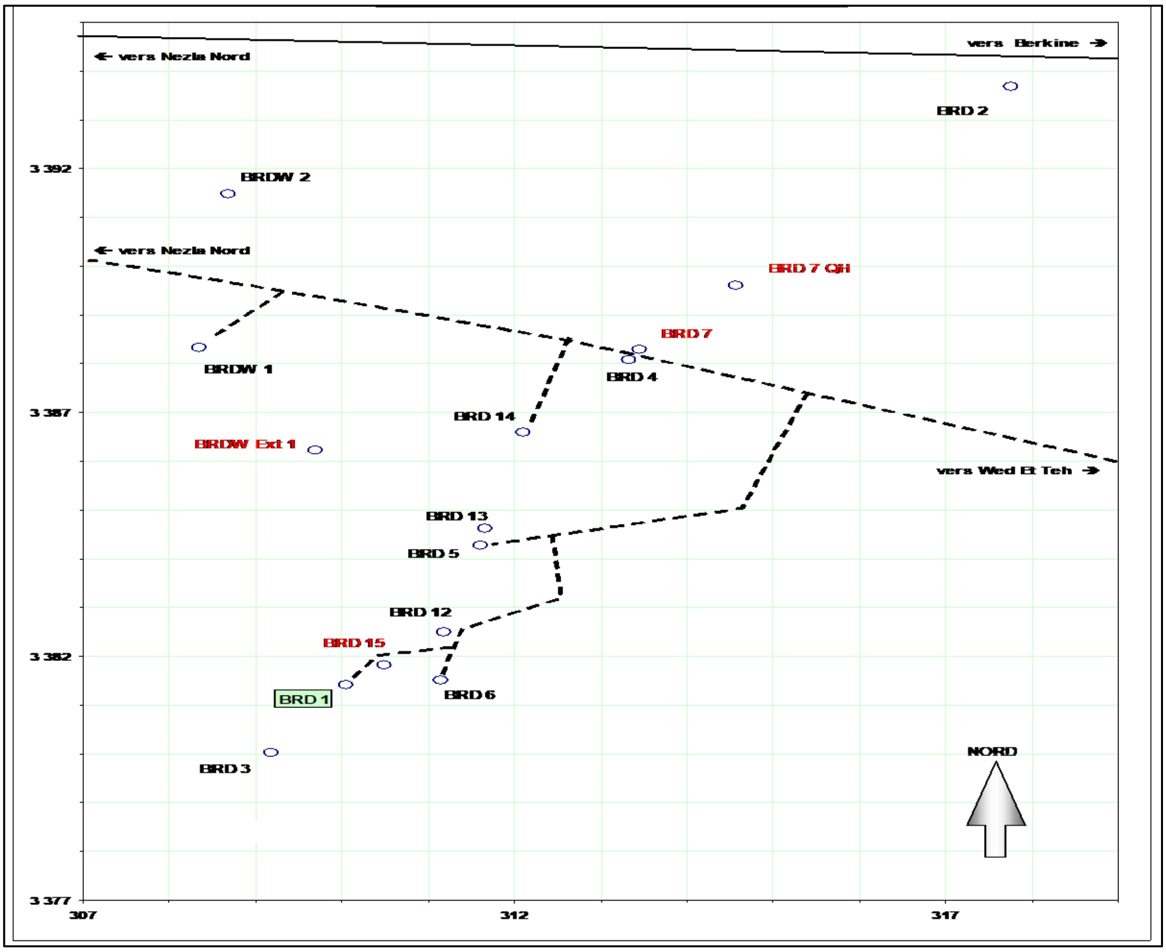


**Figure I.4**: Geographique situation of Brides field. [1]

## I.5 Lithological description of the Brides Field

- The Brides region is located in the northwestern part of the Triassic Southeast province.
- This fault has a strong vertical throw at the Ordovician level and attenuates rapidly upwards in the series.
- At the Ordovician level, the structure, of Aptian age, seems to have been strongly reactivated after the Senonian.
- The stratigraphic column of Bridès presents terrains from the Cenozoic, Mesozoic and Paleozoic eras that would rest on a Precambrian basement.
- The Cenozoic is represented by the Miopliocene.
- The Mesozoic is composed of Cretaceous, Jurassic and Triassic terrains and rests unconformably on the Lower Paleozoic terrains which are present at Bridès through the Silurian formations, and partially of the Ordovician.
- The Cambrian would be underlying the Ordovician. **[1]**

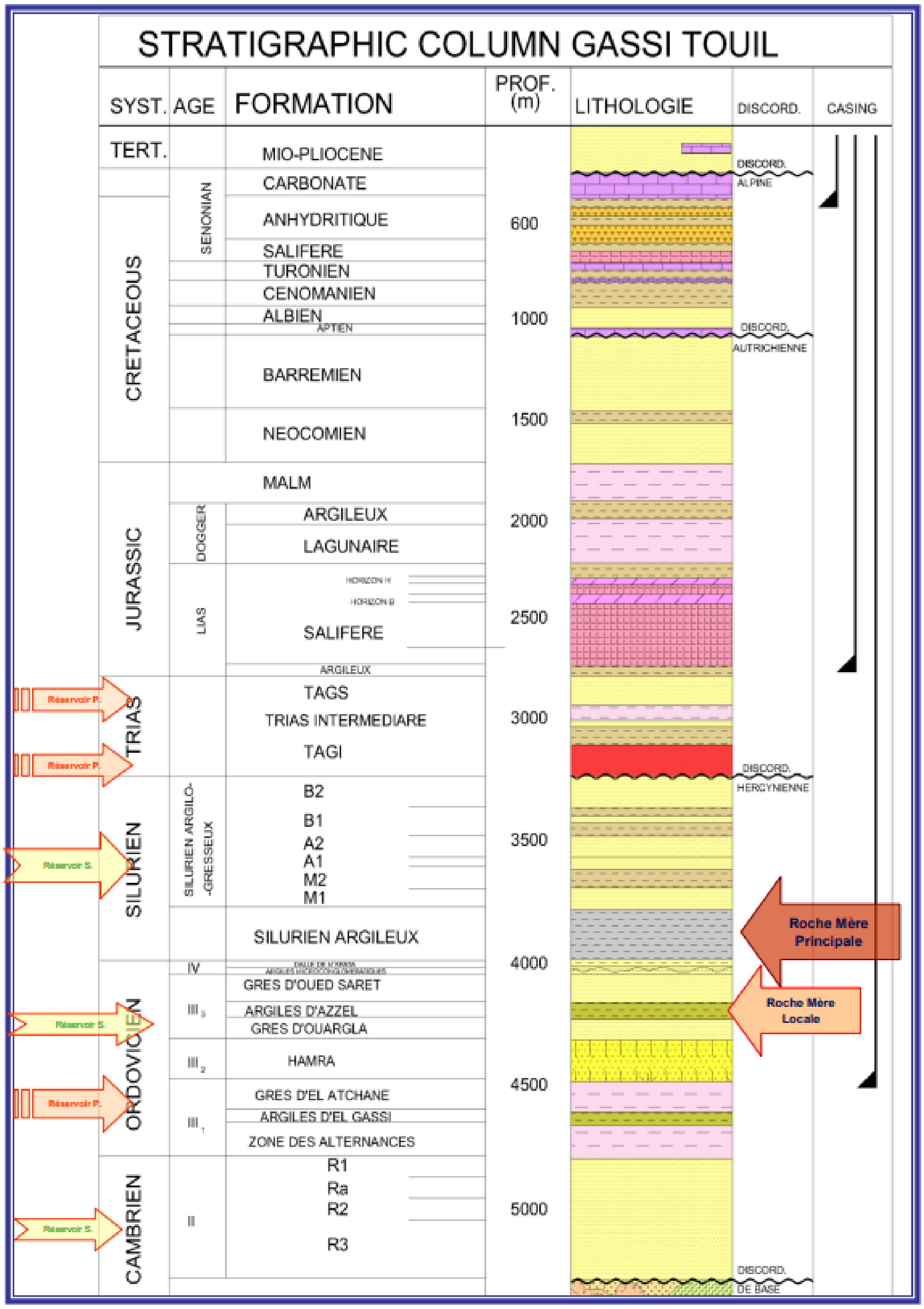


**Figure I.5**: Lithological Description Brides Field. **[4]**

# Chapter II

## *Production Prediction Methods*

# II. Introduction

Each reservoir is composed of a unique combination of geometric form, geological rock properties, fluid characteristics, and primary drive mechanism. Although no two reservoirs are identical in all aspects, they can be grouped according to the primary recovery mechanism by which they produce. It has been observed that each drive mechanism has certain typical performance characteristics in terms of:

- Ultimate recovery factor.
- Pressure decline rate.
- Gas-oil ratio.
- Water production.

The term "primary recovery" refers to the production of hydrocarbons from a reservoir without the use of any process (such as fluid injection) to supplement the natural energy of the reservoir. **[7]**

We must make a distinction between ***Conventional*** and ***Unconventional Gas Reservoirs***.

- Conventional gas reservoirs are reservoirs with sufficiently high permeability to allow for production using conventional well technologies.
- Unconventional reservoirs are reservoirs with low permeabilities that require special production technologies that allow for economic recoveries of gas (Typically, permeability less than 0.1 md). These unconventional reservoirs include:
    - shale gas and shale oil reservoirs.
    - coal seam methane reservoirs.
    - tight oil and gas sandstones or carbonates.

## II.1Primary recovery mechanisms of gas reservoirs

The determination of the drive mechanism is crucial in the early life of the reservoir, as its recognition can significantly improve the management and recovery of reserves from the reservoir in its middle and later life and can help reach a proper understanding of reservoir behaviour. For gas reservoirs, three drive mechanisms are associated with conventional ones and a fourth is associated with unconventional ones. These are:

### II.1.1 Gas Expansion is the primary drive mechanism in most conventional gas reservoirs. This mechanism is very efficient and commonly results in recoveries as high as 85 percent of the original gas in place. In this type of reservoir, the principal source of energy is a result of the subsequent expansion of the solution gas as the reservoir pressure is reduced.

### II.1.2 Rock and Fluid Expansion in gas reservoirs is identical to that in oil reservoirs. It occurs due to the slightly compressible nature of the Connate Water and the reservoir rock. This expansion adds energy to the reservoir and acts to keep the reservoir pressure higher than it would be otherwise. This expansion mechanism is always dominated by gas expansion and may only be significant in cases of over-pressured reservoirs.

### II.1.3 Aquifer Drive (water encroachment) The final drive mechanism is associated with conventional gas reservoirs. Like oil reservoirs, this drive mechanism occurs when the reservoir communicates with a water-bearing aquifer. As the reservoir pressure declines, the rock and water in the aquifer expand, and water is expelled from the aquifer and into the reservoir. This invasion of water into the reservoir provides pressure support.

### II.1.4 Gas Desorption A drive mechanism that is associated with certain unconventional gas reservoirs is. shale gas reservoirs and coal seam methane reservoirs have a high content of organic material in the reservoir rock. This organic-rich rock material has the ability to Absorb gas onto its surface (gas stored by adhesion onto the surface). As pressure is depleted, this adsorbed gas is released to the pore volume of the reservoir by the Desorption Process. This desorption of gas may dominate production from the unconventional gas reservoirs in which it occurs. **[8]**

## II.2 Reservoir Pressure Depletion

During the life of a producing hydrocarbon field, several production stages are encountered. Initially, when a field is brought into production, hydrocarbons flow naturally to the surface due to current reservoir pressure in the primary stage. The primary production rate will decline over time due to reservoir pressure depletion associated with fluid production. The drop is rapid, continuous, and usually very gradual. This behaviour is attributed to the fact that no extraneous fluids or gas caps are available to replenish the extracted gas and oil.

## II.3 Prediction of Reservoir Performance

Prediction of reservoir performance is a vital aspect of the oil and gas industry which guides management's decision of how the reservoir will behave in the future. This implies that its success will depend solely on the accurate description of the reservoir rock properties, fluid properties, rock-fluid properties and flow performance. Reservoir characterization is an ongoing process throughout the field's lifespan, aimed at reducing or identifying uncertainties associated with the static and dynamic reservoir model.

Volumetric, material balance and Decline Curve Analysis (DCA) are the three main techniques used to provide insight into estimating the amount of oil and gas initially in place (OOIP/GIIP) within a reservoir and predict future production.

**TABLE II.1**: Comparison between the 3 main methods used to Predict reservoir performance.

| Method | Description | Data Requirements | Advantages | Limitations |
|---|---|---|---|---|
| **Volumetric** | Estimates OOIP/GIIP using the geometry, porosity, and saturation of the reservoir. | Reservoir dimensions, porosity, saturation | Simple, minimal data required | Accuracy depends on data quality, ignores complexities |
| **Material Balance (MBAL)** | Applies law of conservation of mass to track hydrocarbons. | Production history, pressure data, FVF, GOR | Considers production history & pressure changes | Requires more data, pressure data crucial, may not be reliable early on |
| **Decline Curve Analysis (DCA)** | Analyzes historical production data to forecast future rates. | Historical production data (oil/gas rates vs. time) | Relatively simple, quick estimates & forecasting | Depends on data quality & length, doesn't account for reservoir properties, future behavior may deviate |

In practice, a combination of these methods is often used to get a more robust estimation of reserves. The choice of method depends on the available data and the specific characteristics of the reservoir.

In this study, the prediction methods used incorporated the material balance equation (MBE) which is predominantly pressure-temperature-volume (PVT) properties.

# II.4 Material Balance Equation (MBE)

The material balance equation (MBE) is the classical mathematical representation of the reservoir. The concept of the MBE was presented by Schilthuis in 1936 and is based on the principle of the volumetric balance. **[9]**

The material balance equation (MBE) has long been recognized as one of the basic tools for interpreting and predicting reservoir performance. The MBE can be used to:

- Estimate initial hydrocarbon volumes in place.
- Predict reservoir pressure.
- Calculate water influx.
- Predict future reservoir performance.
- Predict ultimate hydrocarbon recovery under various types of primary drive mechanisms.

The accuracy of the calculated values depends on the reliability of the available data, and whether the reservoir characteristics meet the assumptions that are associated with the development of the MBE. The equation is structured to keep an inventory of all materials entering, leaving, and accumulating in the reservoir.

## II.4.1 Basic Assumptions in the MBE

The MBE equation is based on premises used to simplify and eliminate the elements hindering the calculation process while maintaining result accuracy. The basic assumptions in the MBE are:

a) **Constant Temperature:** Pressure-volume changes in the reservoir are assumed to occur without any temperature changes. If any temperature changes occur, they are usually sufficiently small to be ignored without significant error.

b) **Reservoir Characteristics:** The reservoir has uniform porosity, permeability, and thickness characteristics. In addition, the shifting in the gas-oil contact or oil-water contact is uniform throughout the reservoir.

c) **Fluid Recovery:** The fluid recovery is considered independent of the rate, number of wells, or location of the wells. The time element is not explicitly expressed in the material balance when applied to predict future reservoir performance.

d) **Pressure Equilibrium:** All parts of the reservoir have the same pressure, and fluid properties are therefore constant throughout.

e) **Constant Reservoir Volume:** Reservoir volume is assumed to be constant except for those conditions of rock and water expansion or water influx that are specifically considered in the equation.

f) It is assumed that the PVT samples or datasets represent the actual fluid compositions and that reliable and representative laboratory procedures have been used. **[9]**

### II.4.2 Development of the General Material Balance Equation

The law of conservation of mass is the basis of material balance calculations. Material balance is an accounting of material entering or leaving a system. In its simplest form, the equation can be written on a volumetric basis as:

**Initial volume = Volume remaining + Volume removed**

The MBE is designed to treat the reservoir as a ***single tank*** or a region that is characterized by homogeneous rock properties and described by an average pressure, i.e., no pressure variation throughout the reservoir at any particular time or stage of production. Therefore, the MBE is commonly referred to as a tank model or a zero-dimensional (0-D) model. These assumptions are of course unrealistic since reservoirs are generally considered heterogeneous with considerable variation in pressures throughout the reservoir.

However, it is shown that the tank-type model accurately predicts the behaviour of the reservoir in most cases if accurate average pressures and production data are available.

### II.4.3 Gas Reservoir Material Balance

The initial gas in place G, the initial reservoir pressure pi, and the gas reserves are possible to calculate if enough production-pressure history is available for a gas reservoir. This is accomplished by forming a mass or mole balance on the gas as:

$$\mathbf{n_p = n_i - n_f} \qquad \textbf{(II.1)}$$

Figure II-1 represents a gas reservoir as an idealized gas container, the equation II.1 gas moles can be replaced by their equivalents using the real gas law to give:

$$\frac{P_{sc}G_p}{RT_{sc}} = \frac{VP_i}{z_iRT} - \frac{P[V-(W_e-W_p)]}{zRT} \quad \textbf{(II.2)}$$

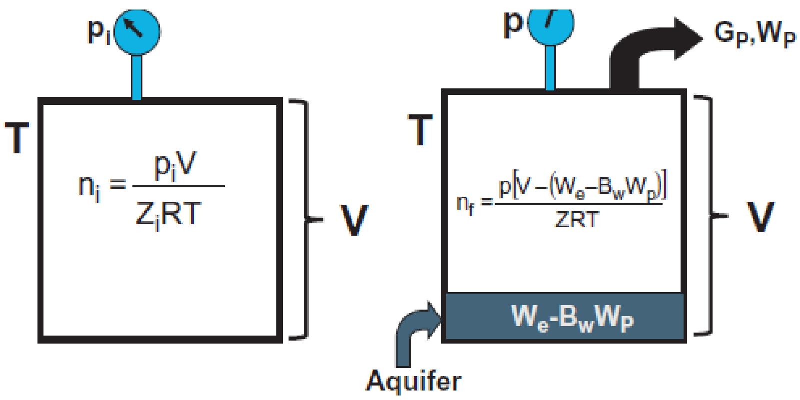


**Figure II-1** An idealized water-drive gas reservoir. **[4]**

Essentially equation II.2 is the general material balance equation (MBE). There are several ways to express equation II.2 depending on the application type and the driving mechanism. In general, there are two types of dry gas reservoirs:

- Volumetric gas reservoirs
- Water-drive gas reservoirs

For a volumetric reservoir and assuming no water production, equation II.2 becomes:

$$\frac{P_{sc}G_p}{T_{sc}} = \left(\frac{P_i}{z_iT}\right)V - \left(\frac{P}{zT}\right)V \quad \textbf{(II.3)}$$

Rearranging equation II.3 and solving for p/z gives:

$$\frac{P}{z} = \frac{P_i}{z_i} - \left(\frac{P_{sc}T}{T_{sc}V}\right)G_p \quad \textbf{(II.4)}$$

As illustrated in Figure II-2, equation II.4 generates a straight line when (p/z) is plotted versus the cumulative gas production Gp. This straight-line relationship is perhaps one of the most widely used relationships in gas reserve determination.

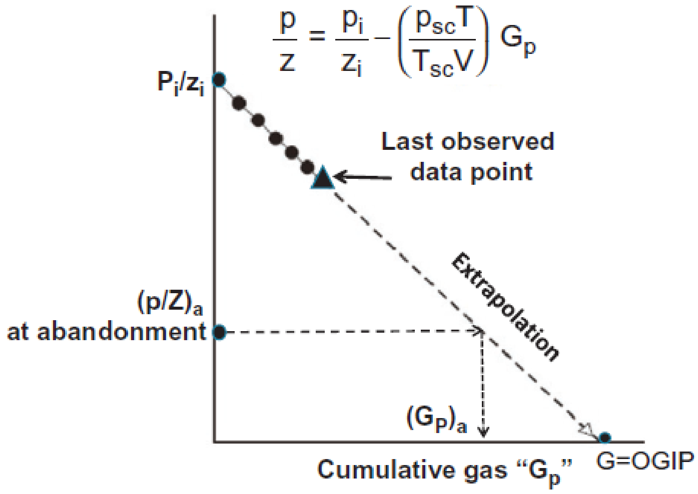


**Figure II-2** Gas material balance equation "Tank Model." **[4]**

## II.5 Nodal analysis

Nodal analysis is a technique used to analyze the flow behaviour and pressure distribution throughout a production by dividing the system into segments or nodes allows for the analysis of this system and ensures transportation of oil and gas from the reservoir to the surface takes place through a system of pipes, including the porous medium, tubing, and the surface gathering network with minimal losses. It is relatively straightforward to calculate the pressure drop for each of these segments if we know the flow rate either the upstream or downstream pressure, and the physical properties of the segment. This allows us to:

- Identify bottlenecks.
- Predict flow rates.
- Optimize production strategies.
- Improve artificial lift.
- Ensure flow assurance.

When we graph these two curves on the same graph, we refer to this as the "system graph". The intersection of the inflow curve and the outflow curve gives the one unique flow rate at which the well will produce a specified set of reservoir and wellbore properties. The point of intersection will also give the unique bottom-hole pressure at which this rate will occur:

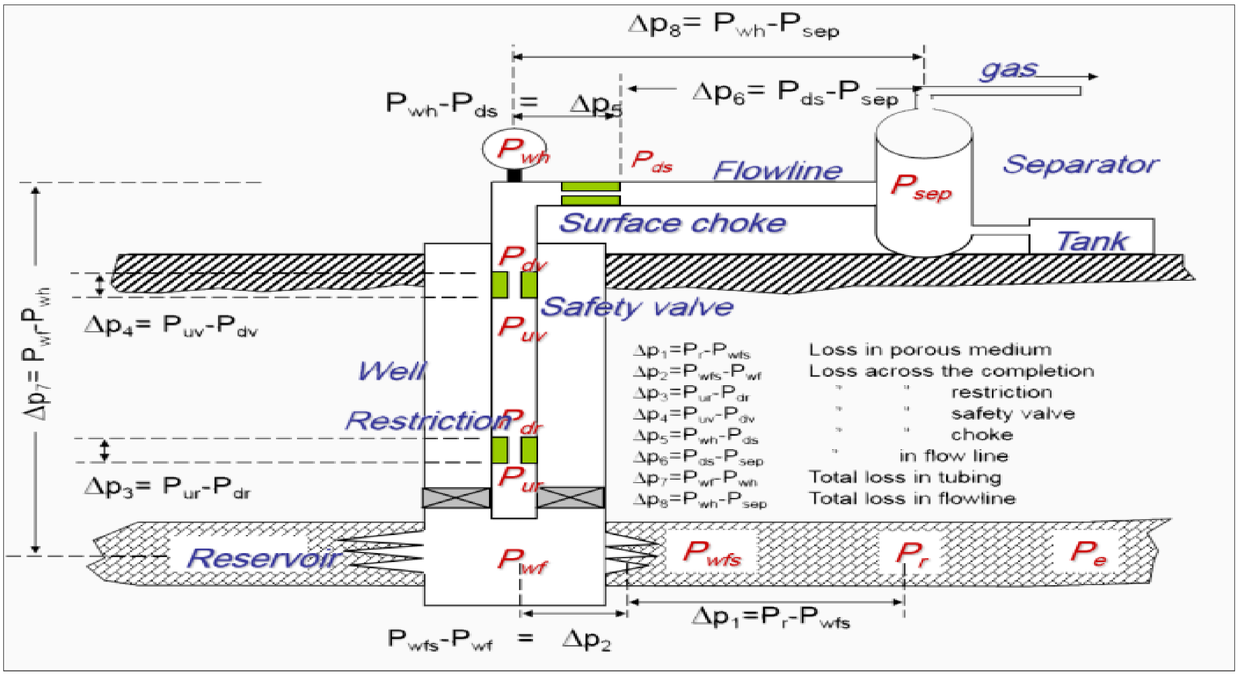


**Figure II.3:** Different Pressure Loses in the production system (Reservoir to separator).

Types of Pressure Losses in the production system:

- Reservoir Skin: ($\Delta P_1 = p_R - p_{wfs}$ )
- Wellbore Friction: ($\Delta P_2 = p_{wfs} - p_{wf}$ ).
- Tubing and Flowline Friction: ($\Delta P_3 = p_{ur} - p_{dr}$ .
- Safety Valve Pressure Drop: ($\Delta P_4 = P_{usv} - P_{dsv}$ .
- Choke Pressure Drop: ($\Delta P_5 = P_{wh} - P_{dsc}$ ).
- Surface Line Friction: ($\Delta P_6 = P_{dsc} - P_{Sep}$ ).
- Total Pressure Loss in Tubing: ($\Delta P_7$= Pwf – Pwh).
- Separator Pressure Drop: ($\Delta P_8 = P_{WH} - P_{sep}$).

The system is divided into two parts based on the nodal point:

## II.5.1 Inflow Performance Relationship (IPR)

The inflow curve describes the relationship between the bottomhole pressure and the flow rate for the reservoir.

- Reservoir pressure
- Reservoir quality (permeability and thickness).
- Completion efficiency (or skin).

- Relative permeability (change in permeability as water production starts).

### II.5.2 Tubing Performance Curves (TPC)

The outflow curve describes the relationship between the pressure (Pwf) at the solution node and the flow rate (Qs) out of the node the flowing bottom-hole pressure and the flowrate for the wellbore, and acceleration within the tubing, pipes, and lines.

**TPC:** $$\mathbf{Pwf} = Pwh - \Delta P\ tubing - \Delta P\ annulus - \Delta P\ restrictions \qquad \textbf{(II.5)}$$

If we had chosen a different point as our solution node, the shapes of the curves would have been different. The intersection of the inflow and outflow curves would have given the pressure at the new solution node. The flow rate at which the curves intersect, however, will be the same no matter where the solution node is taken. Calculated intersection points may differ slightly because of numerical errors.

### II.5.3 The Intersection: The Operating Point

The operating point is the intersection of the IPR and TPC curves. This point represents the production rate and flowing bottomhole pressure at which the well is currently operating.

The system for transporting the fluid can be divided into three parts:

- Flow in the porous medium;
- Flow in vertical or directional pipes;
- Flow in horizontal pipelines.

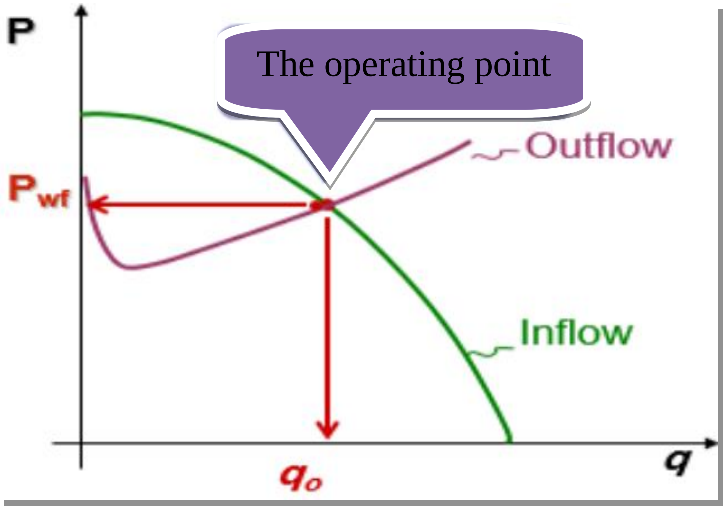


**Figure II.4**: The operating point.

The choice and sizing of the different components is very important, but due to the interaction between the components, a change in one of them can change the behavior of the fluid in the others. This is why the production system (reservoir + well + surface collection) must be analyzed as a single unit. Analyzing each part separately does not lead to good results.

The production of a well can often be limited by the performance of a single component of the system. If the effect of each component on the system performance can be isolated, then the system performance can be optimized in the most economical way.

## II.6 Back pressure equation

The back pressure equation is referred to as the oil and gas deliverability equation method that can be used to specify the Inflow Performance Relationship (IPR) for completion. This equation is also a fundamental concept in fluid mechanics used to estimate the pressure remaining at a specific point in a pipeline system. It's particularly relevant in the context of gas well boosting, where we want to ensure sufficient pressure at the end of the pipeline (treatment facility) after transporting gas from the wellhead. This equation is represented in the following form:

$$Q = C\left(p_{ws}^2 - p_{wf}^2\right)^n \quad \textbf{(II.6)}$$

Where:

$$C = \frac{703 \text{ x } 10-6 \text{ kh}}{\mu TZ\left[ln\left(\frac{r_e}{r_w}\right)-\frac{4}{3}+s\right]} \quad \textbf{(II.7)}$$

**NB:**

- The exponent "n" value ranges between 0.5 (for completely turbulent flow) to 1.0 (for pure laminar flow).
- The coefficient "C" represents the Productivity Index of the reservoir. 1.0 is often due to non-darcy flow effects.

Typically, backpressure tests consist of a series of at least three stabilized flow rates and the measurement of bottomhole flowing pressures as a function of time during these flow intervals.

The simplified back pressure equation is helpful for initial estimations, but it doesn't account for all factors influencing pressure drop. For more accurate calculations, it needs to consider the detailed flow rate calculation and pressure drop formulas with relevant fluid properties.

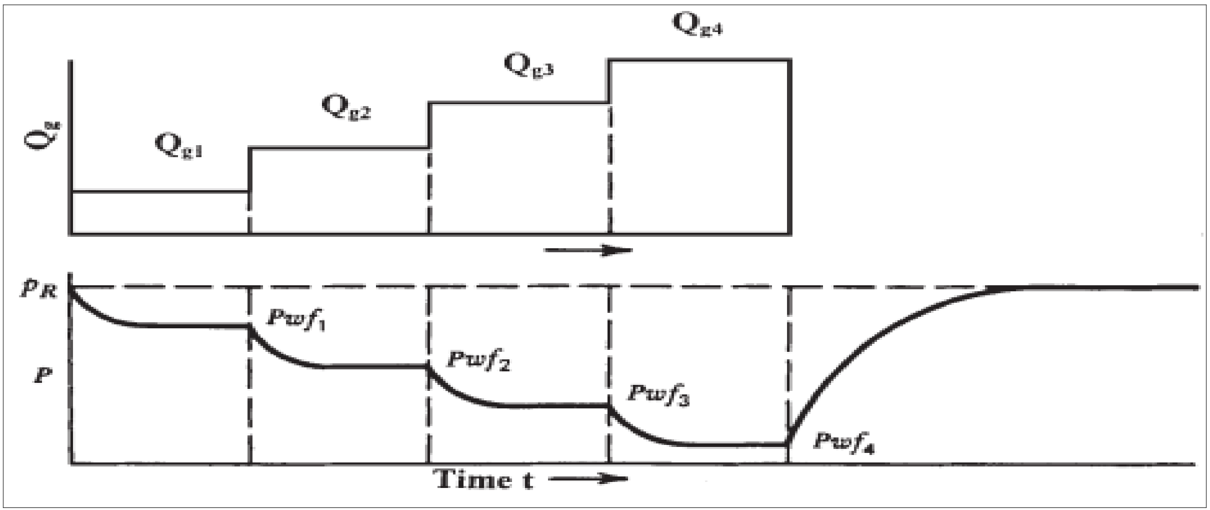


**Figure II.5:** Conventional Back-Pressure Test.

# Chapter III

## *Boosting Method and the Candidate Wells*

# III. Introduction

In this chapter, we will list the wells that have been suggested for potential boosting and outline the specific criteria that need to be met for their selection. Additionally, we will provide a detailed overview of the chosen booster, including its equipment and key characteristics.

## III.1 Selection of candidate wells

With the aim to determine the possibility of installing a Booster appropriate for wells with low potential in the Brides field. It is essential to study the compatibility of the compression unit with the wells' characteristics, location, and operating environment as well as any potential operational restrictions. The requirement to recover the total investment cost lost must also be taken into account.

The low potential wells in the Brides field are BDSN-1, BDSN-2, BRD1, BRD12, BRD15, BRDS-1, BRDS-2 and BRDS-EXT02. which are connected to a high-pressure manifold BRDMF01, and they are currently unable to produce at the existing manifold pressure of 80 bar due to their pressure decline as shown in figure III.1. To address this issue, installing a booster to elevate their pressure has been proposed, allowing them to continue production at the same manifold pressure.

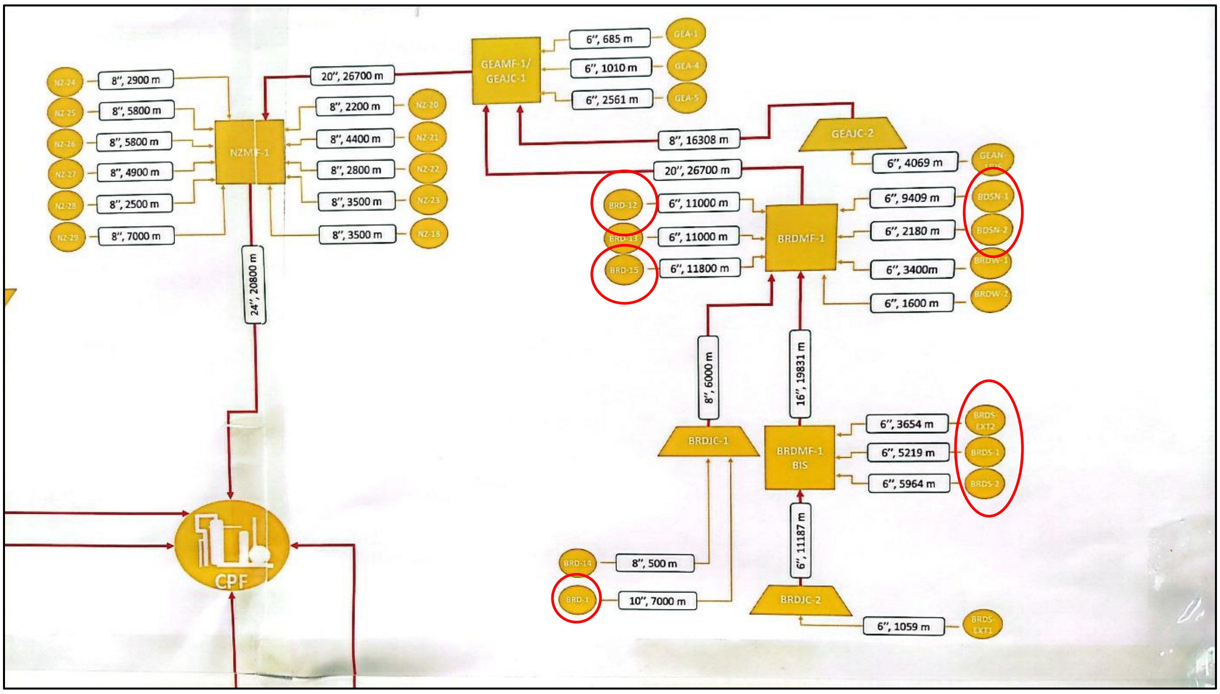


**Figure III-1** Connection of manifolds and wells placement. **[10]**

As it is evident in the diagram above, the well BRD-1 is connected to a junction with BRD-14, which operates at a higher pressure than BRD-1 and has the capability to produce at the existing manifold pressure. Therefore, we will exclude it from the wells programmed to be boosted.

### III.1.1 History of candidate wells

The Brides field was put into operation on 04/12/2013 with the opening of 03 wells (BRD12-13-15). Later, the wells BRDS-1, BRDS-2, BRDS-Ext2, BDSN-1 and BDSN-2 began production in January 2022.

**Table III.1**: history of candidate wells. **[10] [11]**

| Wells | Observations | Start of production date |
|---|---|---|
| **BRD-15** | 04/06/2012 TO 20/06/2012 Well completion in main TAGS reservoir | 04/12/2013 |
| **BRD-12** | 04/06/2012 TO 18/06/2012 Well completion in main TAGS reservoir | 04/12/2013 |
| **BDSN-1** | Drilling: from 11/01/2014 to 25/05/2014 Completion: 25/06/2014 | 01/02/2022 |
| **BDSN-2** | Drilling: from 21/03/2016 to 26/07/2016 Completion: 26/07/2016 | 01/01/2022 |
| **BRDS-1** | Start of drilling: 01/05/2009, End of drilling: 14/04/2010, TD depth sounder: 5534m<br>Work Over "ENF 34" (From 02/07 to 03/22/2018): Completion of the well in the Silurian B2 reservoir. | 01/01/2022 |
| **BRDS-2** | Start of Drilling: 11/04/2015, End of Drilling: 17/10/2015<br>Start of completion 17/10/2015, End of completion 31/10/2015 | 01/02/2022 |
| **BRDS-Ext2** | Start of drilling: 12/11/2015; end of drilling: 04/10/2016 Start of completion: 12/25/2018; end of completion: 02/14/2019 | 01/03/2022 |

### III.1.2 DATA of candidate wells

The table below presents a collection of well test data for candidate wells acquired from gauging tests:

**Table III.2**: well test data for candidate wells. **[12]**

| Wellbore | Date | Choke (-/64) | Q Gas (Sm3/J) | Q Cond (m3/J) | Q Water (m3/J) | Whp (Barg) | WHT (°C) | Bhfp (psig) | BWFT (°C) | Depth (m) |
|---|---|---|---|---|---|---|---|---|---|---|
| **BDSN-1** | 23/07/2023 | 24 | 73 560 | 52,7 | 0 | 112,32 | 48 | 2644,70 | 105,82 | 2925 |
| **BDSN-1** | 24/07/2023 | 32 | 93 264 | 61,97 | 1,63 | 76,26 | 45 | 1948,75 | 103,55 | 2925 |
| **BDSN-1** | 25/07/2023 | 40 | 102 144 | 65,3 | 1,97 | 55,92 | 48 | 1527,04 | 101,21 | 2925 |
| **BDSN-1** | 19/10/2023 | - | 64 632 | 29,74 | 3,98 | 230,01 | 36 | - | - | - |
| **BDSN-2** | 20/06/2023 | 24 | 40 320 | 32,54 | 0 | 55,99 | 43 | 1817,33 | 107,19 | 2923 |
| **BDSN-2** | 21/06/2023 | 32 | 45 240 | 17,18 | 7,49 | 37,23 | 44 | 1281,62 | 106,23 | 2923 |
| **BDSN-2** | 22/06/2023 | 40 | 54 816 | 21,7 | 6,22 | 27,37 | 38 | 959,53 | 104,75 | 2923 |
| **BDSN-2** | 20/10/2023 | - | 62 376 | 19,27 | 0 | 59,98 | 38 | - | - | - |
| **BRD-12** | 15/02/2018 | 55 | 373 296 | 72,94 | 0 | 172,37 | 70 | - | - | - |
| **BRD-12** | 22/12/2018 | 24 | 174 853 | 39,02 | 0,53 | 170,30 | 54 | - | - | - |
| **BRD-12** | 10/07/2023 | 24 | 11 232 | 0 | 0 | 44,61 | 46 | - | - | - |
| **BRD-15** | 16/02/2018 | 12 | 260 080 | 57,41 | 0 | 149,96 | 67 | - | - | - |
| **BRD-15** | 08/07/2023 | 12 | 64 664 | 0 | 0 | 48,75 | 53 | - | - | - |
| **BRD-15** | 09/07/2023 | 42 | 62 160 | 0 | 0 | 44,54 | 60 | - | - | - |
| **BRDS-1** | 02/07/2023 | 24 | 107 400 | 59,06 | 2,21 | 156,03 | 53 | 3420,86 | 123,73 | 3891 |
| **BRDS-1** | 03/07/2023 | 32 | 158 280 | 63,43 | 5,47 | 122,11 | 55 | 2582,93 | 121,57 | 3891 |
| **BRDS-1** | 04/07/2023 | 40 | 187 488 | 62,16 | 4,03 | 96,18 | 60 | 2031,64 | 119,06 | 3891 |
| **BRDS-1** | 13/10/2023 | - | 97 920 | 0,82 | 0 | 121,97 | 37 | - | - | - |
| **BRDS-1** | 14/10/2023 | - | 120 072 | 0,79 | 0 | 215,12 | 37 | - | - | - |
| **BRDS-1** | 15/10/2023 | - | 127 344 | 0 | 0 | 188,64 | 35 | - | - | - |
| **BRDS-2** | 25/06/2023 | 24 | 34 752 | 26,04 | 0 | 58,19 | 49 | 1637,16 | 111,01 | 3585 |
| **BRDS-2** | 26/06/2023 | 32 | 37 632 | 26,04 | 26,04 | 31,72 | 50 | 1119,15 | 105,51 | 3585 |
| **BRDS-2** | 27/06/2023 | 40 | 40 248 | 27,29 | 0 | 22,27 | 46 | 891,25 | 102,77 | 3585 |
| **BRDS-2** | 16/10/2023 | - | 66 984 | 0 | 0 | 56,99 | 38 | - | - | - |
| **BRDS-Ext2** | 16/01/2020 | 24 | 131 249 | 117,42 | 0,79 | 149,42 | 39 | 3700,64 | 132,50 | 4407 |
| **BRDS-Ext2** | 17/01/2020 | 32 | 150 748 | 125,39 | 2,04 | 104,61 | 43 | 2612,12 | 127,80 | 4407 |
| **BRDS-Ext2** | 18/01/2020 | 36 | 150 953 | 111,54 | 2,45 | 83,99 | 46 | 2156,24 | 124,80 | 4407 |
| **BRDS-Ext2** | 17/10/2023 | - | 51 192 | 0 | 0 | 43,99 | 39 | - | - | - |
| **BRDS-Ext2** | 18/10/2023 | - | 22 200 | 0 | 0 | 73,98 | 41 | - | - | - |

# III.2 The operating procedures for Boosting unit

## III.2.1 Pressure Boosting:

In oil and gas production, multiphase pressure boosting acts like a heartbeat, ensuring efficient transport of well fluids (oil, gas, and water mix) from the reservoir to processing facilities. This boosting system is crucial for maximizing production. It can be a cost-effective alternative to well intervention and helps recover more hydrocarbons by overcoming pressure drops in pipelines, ultimately extending the life of the oilfield. However, for stable operation, the system requires careful consideration beyond just the booster itself. Monitoring the reservoir, designing pipelines for the specific flow conditions, and selecting the right boosting technology are all essential for ensuring smooth flow and maximizing production efficiency.

The main goal is to maintain a steady flow of oil and gas. As production circumstances change, well fluids need to travel long distances to reach processing facilities. Here, boosting wellhead pressure becomes essential to overcome the backpressure created by the downstream gas flow system.

## III.2.2 Natural Reservoir Pressure Depletion

In some cases, natural reservoir pressure might be insufficient for production, particularly for:

- Gas-condensate fields (reservoirs with a mix of natural gas and light liquid hydrocarbons)
- Natural gas extracted from underground reservoirs often has insufficient pressure to travel long distances through pipelines.

## III.2.3 Requirement for Boosting:

There are three main categories of transport limitations:

- **Natural depletion is insufficient:** The natural pressure in the reservoir is not strong enough to push the oil to the surface efficiently.
- **Reservoir pressure needs maintenance:** The reservoir pressure needs to be maintained to achieve a desired production rate.

- **Transport of well fluids needs Boosting:** The distance to processing facilities or other factors hinder the natural flow of oil and require additional assistance.

### III.2.4 Factors Affecting Lift Method Selection

The choice of an artificial lift method depends on several factors:

**a) Reservoir conditions :**

- Initial reservoir pressure.
- Driving mechanisms (e.g., gas cap, water drive).
- Properties of the fluids (oil viscosity, gas-to-oil ratio).

**b) "Geographical" conditions :**

- Distance to processing facilities.
- Water depth (offshore).
- Seabed topography (offshore). **[13] [14]**

## III.3 Boosting equipment

The gas engine compressors do not require any electrical source hence they can be installed quickly and the running cost is low.

On-demand compression unit includes:

- Separating the Condensate / Gas phases
- Boosting the gas production for export and overcoming the downstream back pressure.
- Transfer the recovered condensate to an export line (same as a gas export line or separate line). **[15]**

There are various types of Boosters used for gas wells, including:

- **Reciprocating compressors:** Use pistons to compress the gas in stages. These compressors use rotating impellers to accelerate the gas, converting kinetic energy into pressure gain.

- **Centrifugal compressors:** Use rotating impellers to increase gas pressure. They employ centrifugal force generated by high speed.
- **Screw compressors:** Utilize intermeshing screws to trap and compress the gas as they rotate. They offer continuous flow and are well-suited for high-pressure applications. **[16]**

Here are some additional components that are often used in conjunction with gas-boosting equipment:

- **Inlet separators:** These remove liquids and impurities from the gas stream before they enter the compressor to protect the equipment.
- **Scrubber:** A scrubber is typically a device used to remove unwanted components from a gas stream. This could involve removing liquids, solids, or specific gas components depending on the application.
- **Aftercoolers:** These cool down the gas after compression as the compression process generates heat. Cooling the gas reduces its volume and improves its efficiency in the pipeline.
- **Discharge separators:** These remove any liquids or condensates that may form after cooling the gas.
- **Control valves:** These regulate the flow of gas through the system and maintain the desired pressure.
- **Piping and valves:** These connect the various components of the gas boosting system and allow for controlled flow of the gas. **[17]**

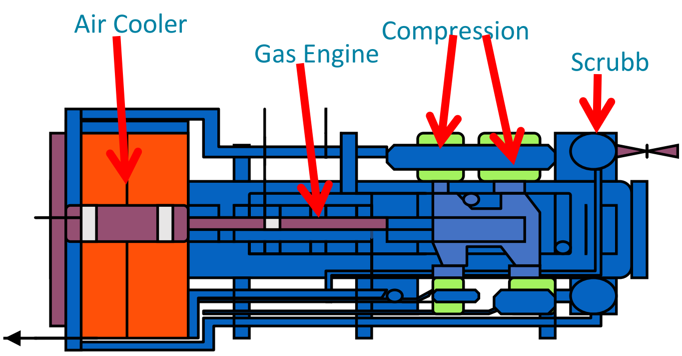


**Figure III.2**: Compressor unit components. **[15]**

## III.4 Specific Features of the Chosen Booster

As previously mentioned, the wells are linked to the high-pressure manifold (HP MF). When the pressure in the reservoir drops, the boosting method is essential to sustain the production of the wells at a high pressure to uphold the pressure of the wellhead and the flowline, an artificial method becomes necessary. by elevating the pressure of fluid to align with the original pressure of the manifold, which stands at approximately 90 Bar, whereas the pressure reaching the manifold is only 40 Bar.

The following are the features of the Booster, which have been selected based on the available data and features:

| **Capacity** | **Suction Pressure** | **Discharge Pressure** | **Fuel gas consumption** | **Compressor Frame** |
|---|---|---|---|---|
| 600,000 to 900,000 $Sm^3$/day | 40 to 60 Barg | 105 Barg | 8000 $Sm^3$/day | 1117 Kw |

**Table III.3:** Specific features of the chosen Boosting unit.

**NB:** To ensure the efficiency of the compression unit, an optimum flow rate of 300,000 Sm3/d is necessary during the production.

COMPRESSOR


SEPARATOR


PUMPS

**Figure III.3:** Main equipment of the Boosting unit. [15]

## III.5 Boosting unit operation

The role of the Boosting unit is to increase the pressure of the fluids from the candidate wells so that they can reach the processing centre. This is achieved by separating the liquid phase from the gaseous phase using an on-site 3-phase separator. The gaseous phase then goes through a compressor, while the liquid phase passes through a pump, elevating the fluids' pressure to 90 bars. After this, the two phases are combined at a junction point. The fluid, now at a higher pressure, is then injected into the manifold and sent to the CPF (centre processing facility).

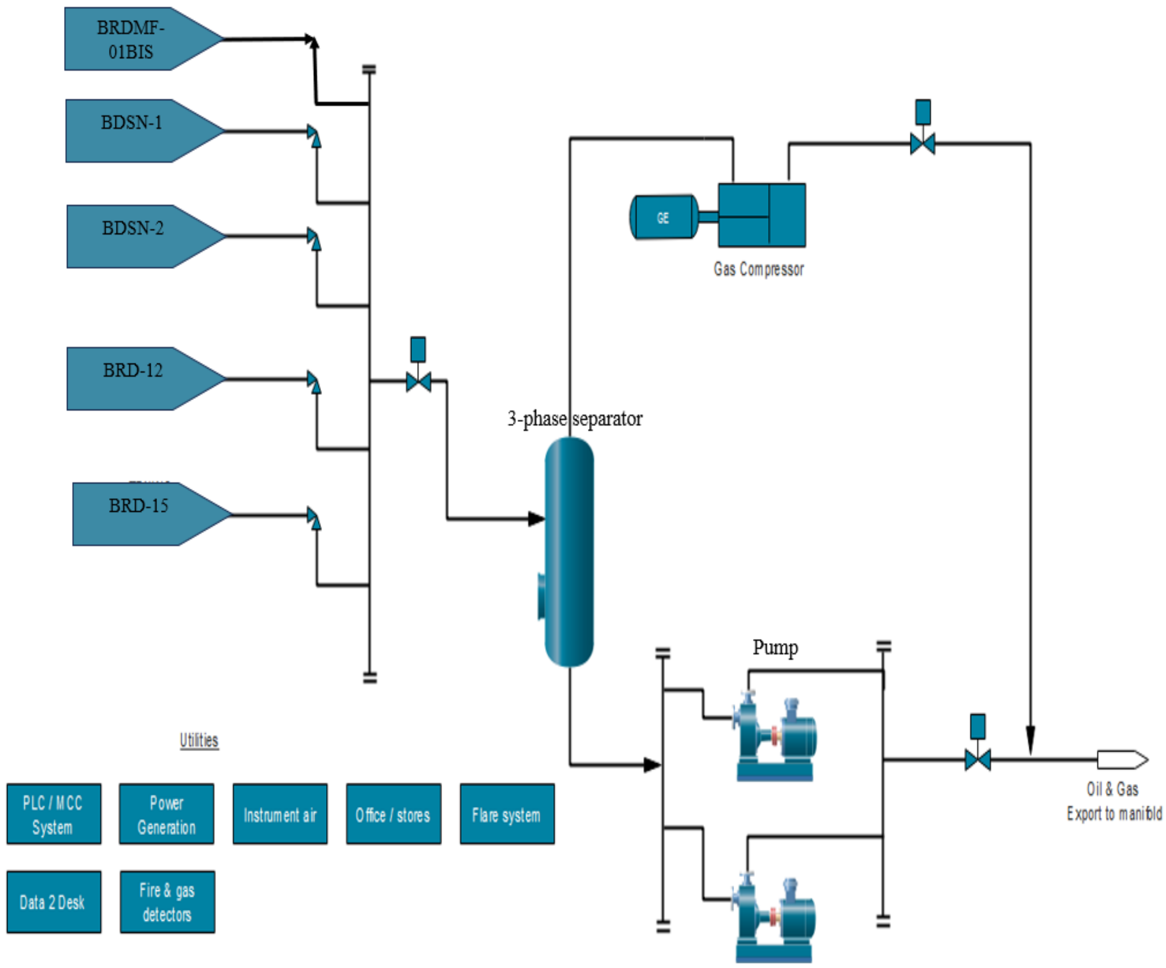


**NB:** BRDMF-01BIS is a manifold that contains three wells which are: BRDS-1, BRDS-2 and BRDS-Ext2.

**Figure III.4:** diagram of the Boosting process.

## III.6 Factors affecting Booster selection

Key factors influencing the booster selection are:

- Wellhead pressure.
- The pressure required for the gas to reach its destination.
- The flow rate of gas that needs to be transported per unit time.
- Cost of installation, operation, and maintenance. **[13] [14]**

## III.7 Various applications of Boosting

Gas boosting has various applications across different industries. Here's some key areas where gas boosting plays a vital role:

- Boosting stations are positioned at strategic points along gas gathering and to maintain sufficient pressure for continued flow.
- Boosters are essentially compressors that take in low-pressure gas from the gas well and compress it to a higher pressure. **[15]**

## III.8 The advantages of Boosting technology

Gas well boosting plays a critical role in maximizing natural gas production, enabling efficient transportation over long distances, and facilitating the development of previously inaccessible gas reserves. Here are some advantages of this technology:

- Sustain and enhance gas recovery.
- Reduce backpressure on wells.
- Keep/back to the required inlet pressure of the main facility (sustain inlet design pressure).
- Self-powered and fully automated
- Temporary replacement compressor for units that are under maintenance.
- Enables Long-Distance Transportation
- Environnemental Benefits.

# Chapter IV

## *Modeling and Forecasting of the Impact of the Booster on Candidate Wells*

# IV. Introduction

In this chapter, we will delve into the result of our research, providing a detailed analysis of the use of MBAL software and PIPESIM software to model and forecast the potential impacts of implementing a Boosting unit on the candidate wells. Furthermore, we will assess the financial ramifications of implementing a Boosting unit.

## IV.1 Using MBAL Software

### IV.1.1 Introduction to the MBAL Software

Accurate production prediction is paramount for optimizing field development and maximizing recoverable resources. MBAL (Material Balance) software - commercialised in the early 1990s- developed by Petroleum Experts as a component of their Integrated Production Modeling (IPM) suite, stands as a prominent tool for achieving this objective. **[18]**

Aside from ***Material Balance***, other tools also available are:

- Decline Curve Analysis.
- 1D model.
- Monte Carlo Simulations.
- Coal Bed Methane.
- Reservoir Allocation.
- Tight Reservoir Modelling.
- Streamlines.

All available techniques can be used in isolation or in combination to achieve various objectives. **[18]**

Notably, MBAL offers three primary deployment strategies for reservoir production prediction:

a) **Integration Within a Comprehensive Reservoir Model:** MBAL seamlessly integrates with various other IPM tools to establish a robust reservoir model. This model incorporates a wide array of data, including:
   - **Production History:** tracking of Oil, gas, and water production volumes over time.
   - **PVT Analysis:** detailed characterization of reservoir fluid properties at different pressures and temperatures.

- **Rock Properties:** comprehensive analysis of the reservoir's rock formations, including porosity, permeability, and other critical characteristics.

b) **Standalone Reservoir Analysis Tool:** MBAL exhibits its versatility by functioning independently for basic reservoir analysis. it leverages historical production data and PVT analysis results to generate production forecasts.

c) **Applications in Reservoir Production Prediction:** MBAL provides comprehensive tools to predict reservoir production accurately:

- **History Matching:** The history matching is carried out utilizing the graphical and analytical approaches. It involves adjusting model parameters to align with past production data closely. MBAL facilitates this process, ensuring the model accurately reflects the reservoir's historical behaviour**. [19] [20]**
- **Bottomhole Pressure Analysis:** The MBAL algorithm evaluates reservoir bottomhole pressure using measured pressure and production data, utilizing material balance equations to estimate background pressure.
- **Reservoir Property Estimation:** Using production data and material balance calculations, MBAL can estimate Original Oil in Place (OOIP), Original Gas in Place (OGIP), and aquifer properties.
- **Production Forecasting:** MBAL excels at forecasting future production under various scenarios after estimating reservoir properties and completing history matching. This helps to optimize production strategies.

## IV.1.2 MBAL Models Inputs

### a) PVT Description:

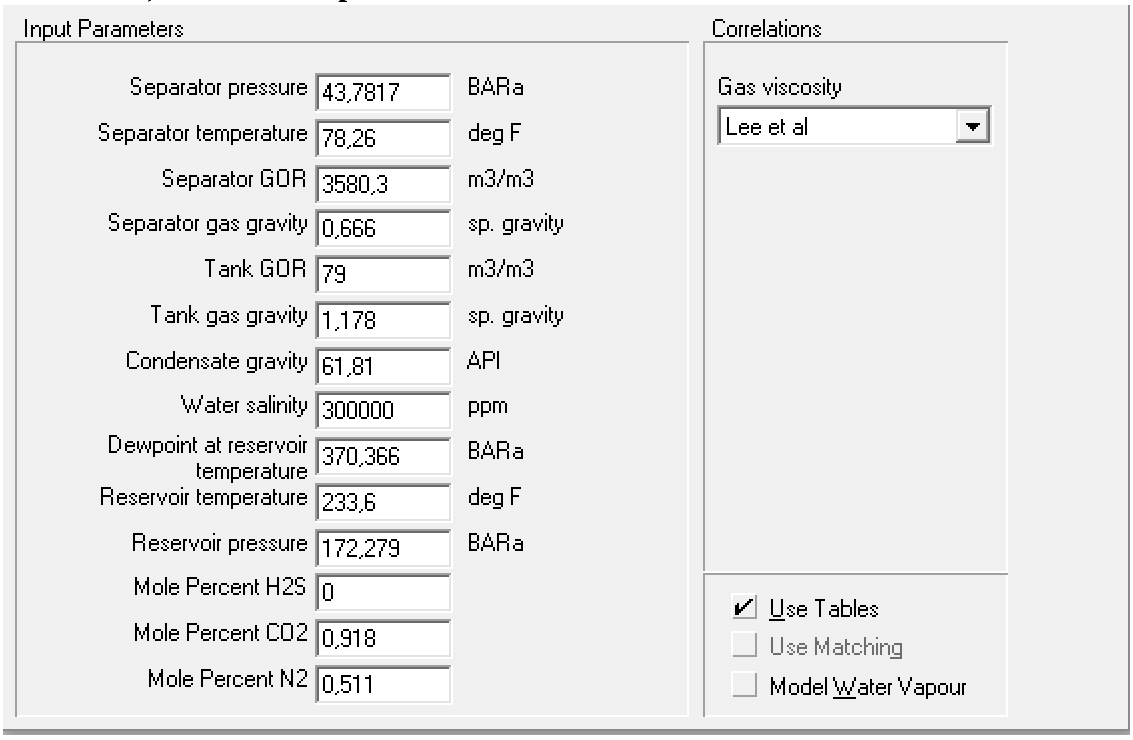


**Figure IV.1:** PVT inputs of Main TAGS reservoir.

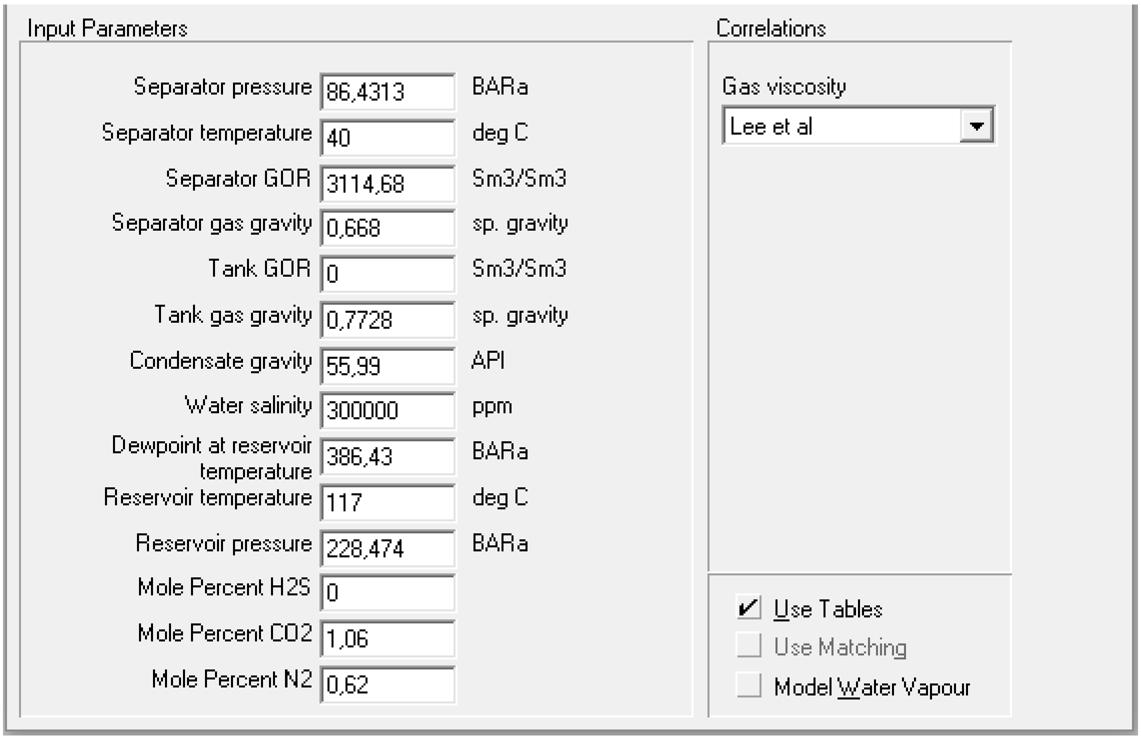


**Figure IV.2:** PVT inputs of West TAGS reservoir.

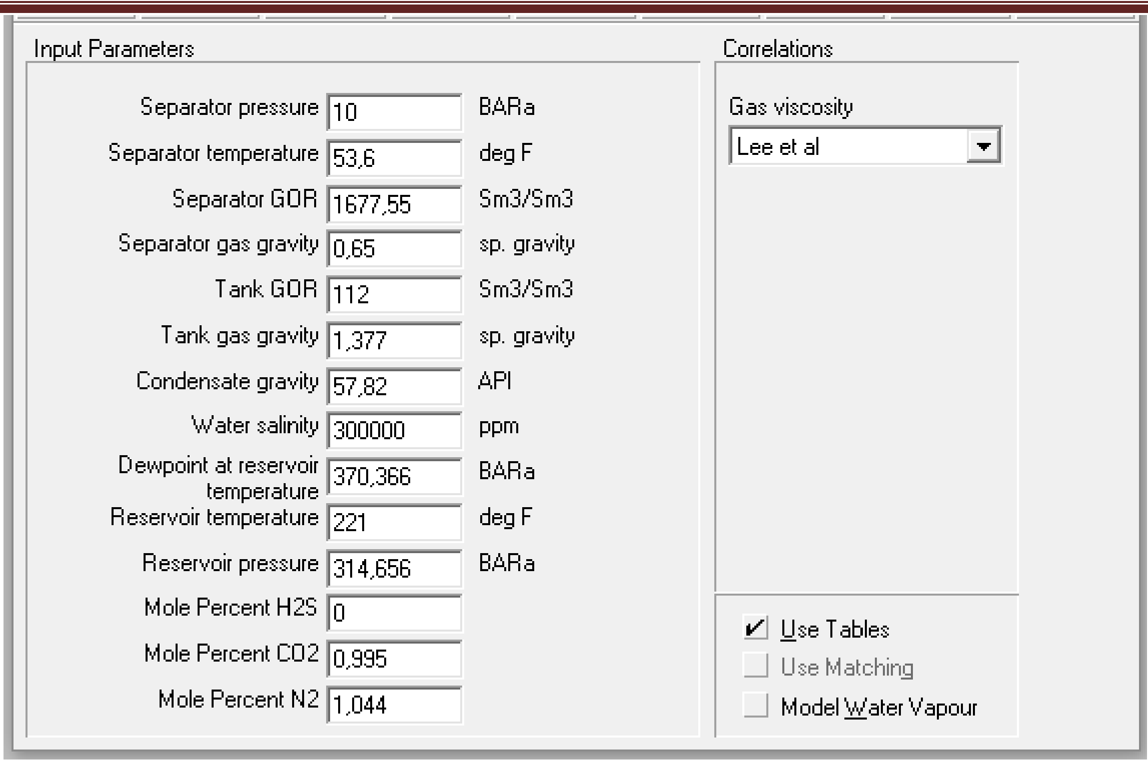


**Figure IV.3:** PVT inputs of North TAGS reservoir.

### b) Reservoir Description

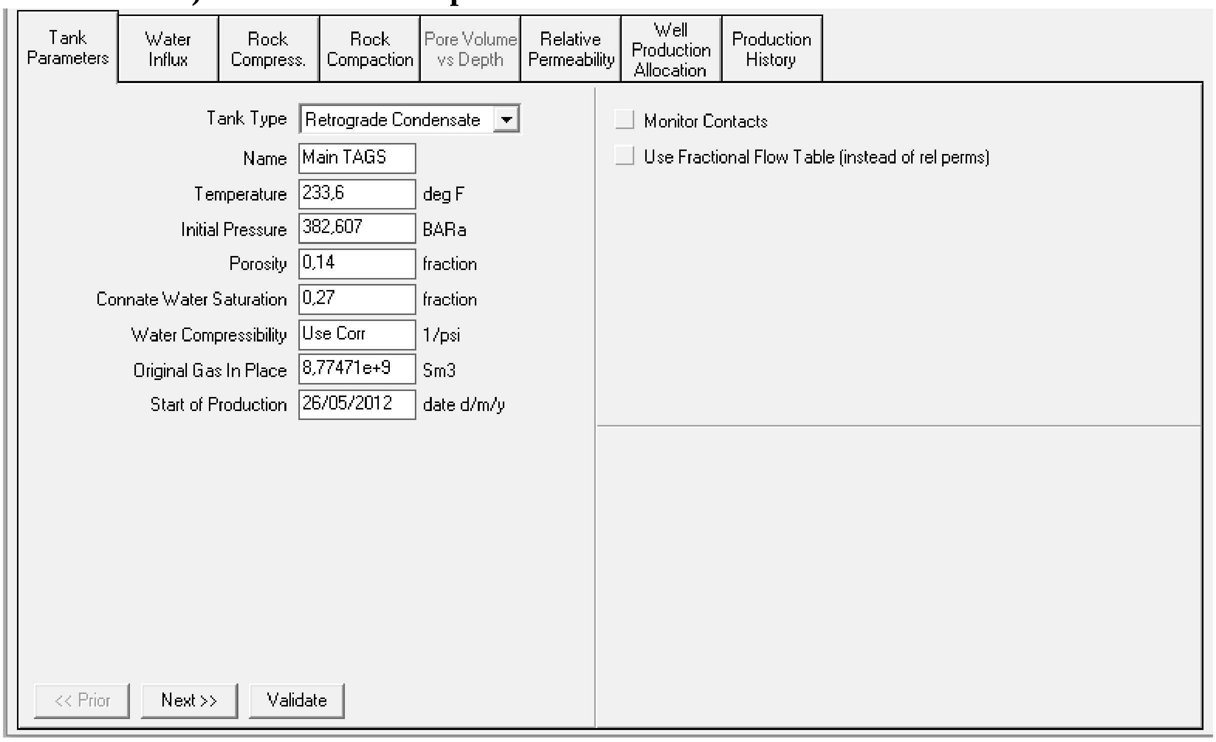


**Figure IV.4:** Tank inputs of Main TAGS reservoir.

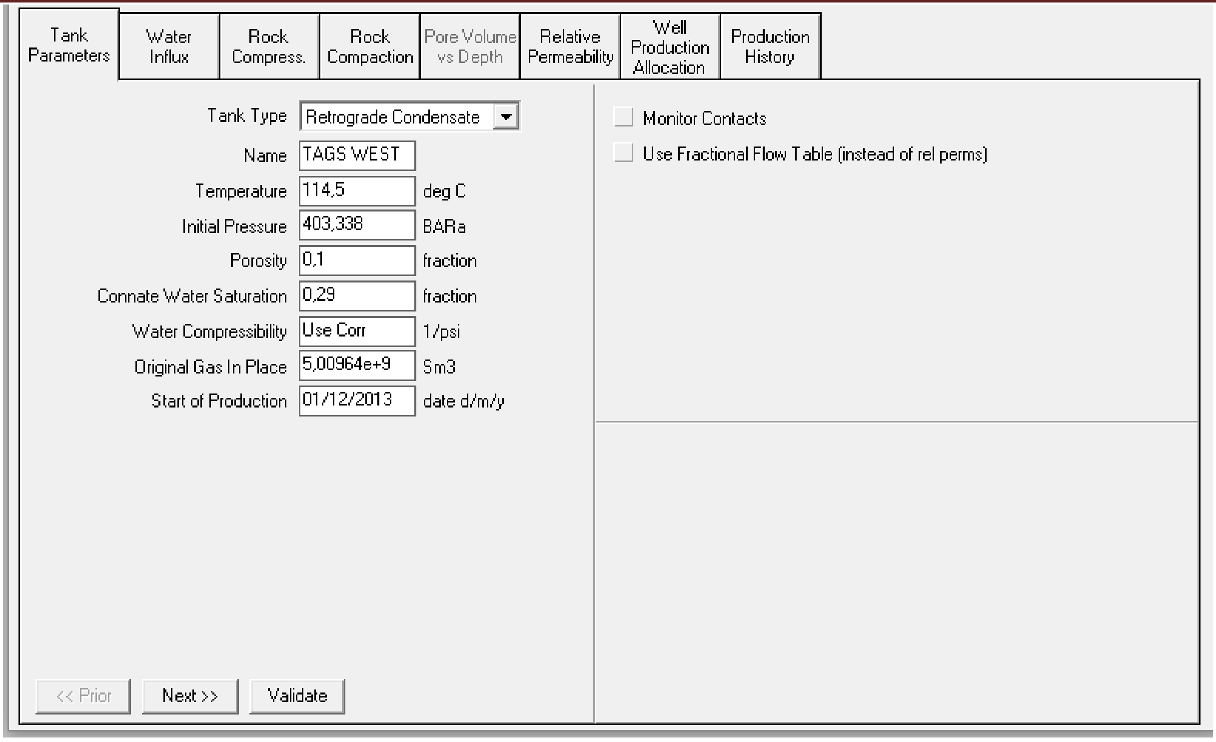


**Figure IV.5:** Tank inputs of West TAGS reservoir.

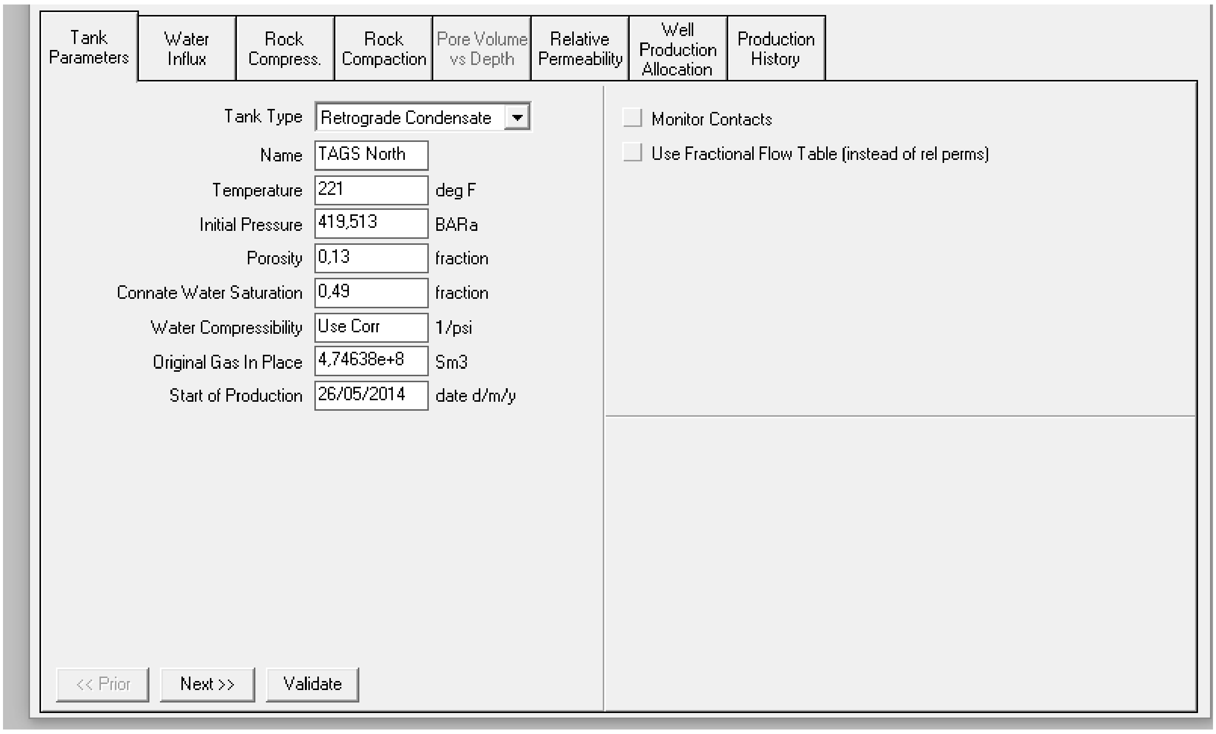


**Figure IV.6:** Tank inputs of North TAGS reservoir.

## IV.1.3 History Matching for the MBAL Models

### a. Analytical Method

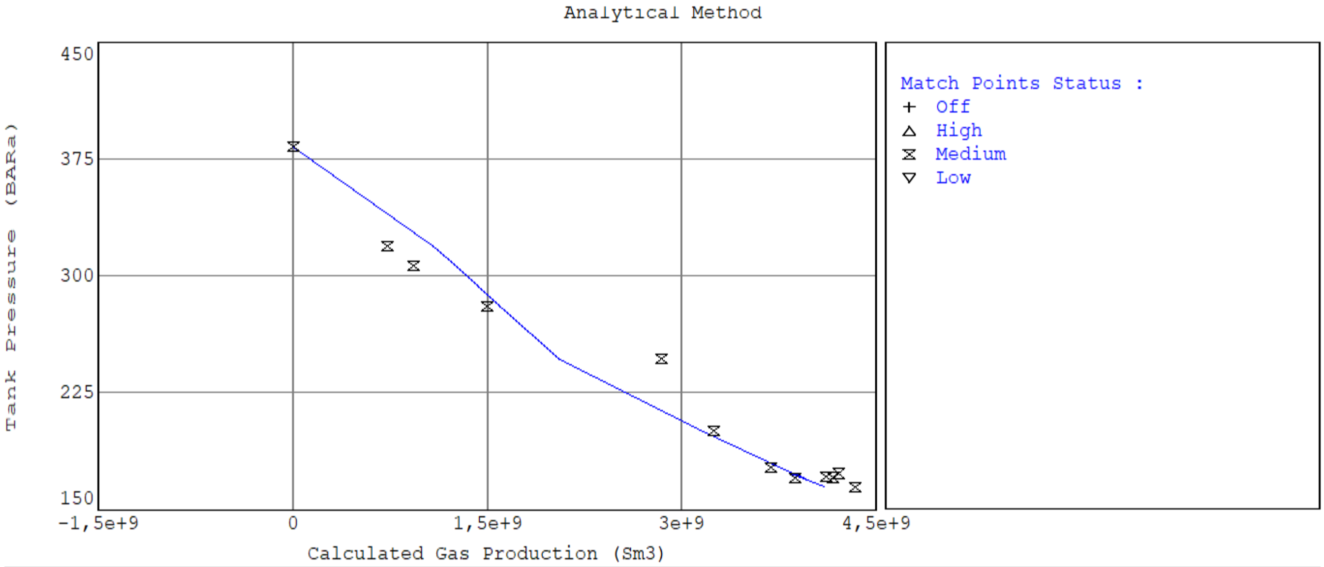


**Figure IV.7:** Analytical plot of Main TAGS reservoir after regression.

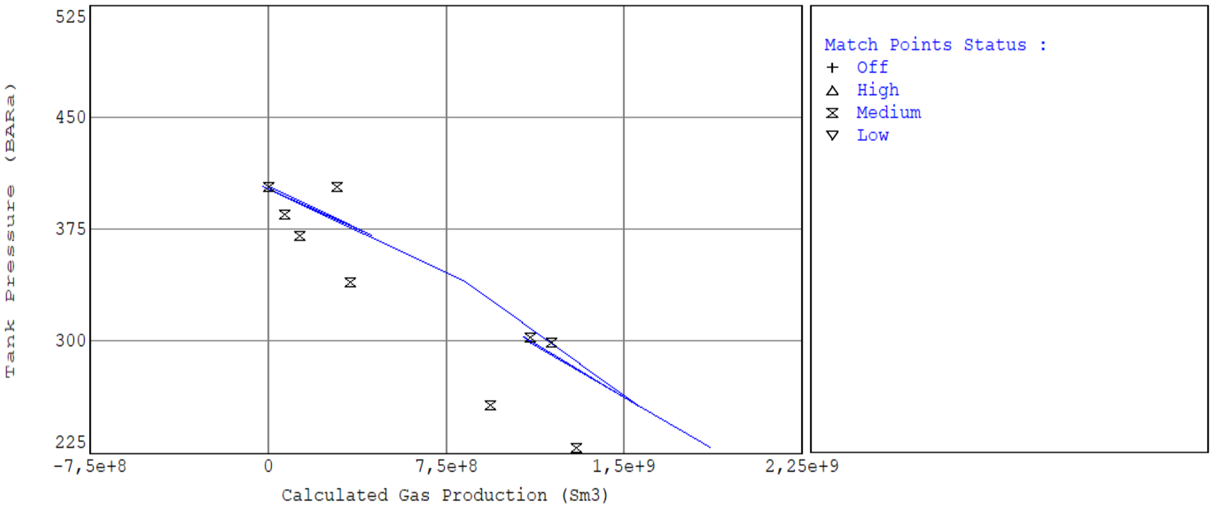


**Figure IV.8:** Analytical plot of West TAGS reservoir after regression.

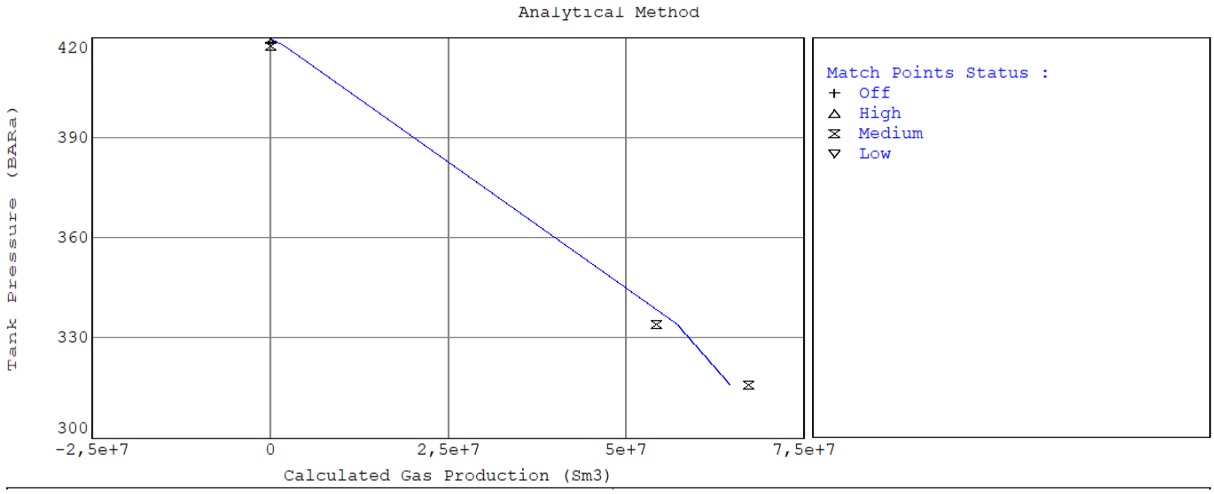


**Figure IV.9:** Analytical plot of North TAGS reservoir after regression.

### b. Graphical Method

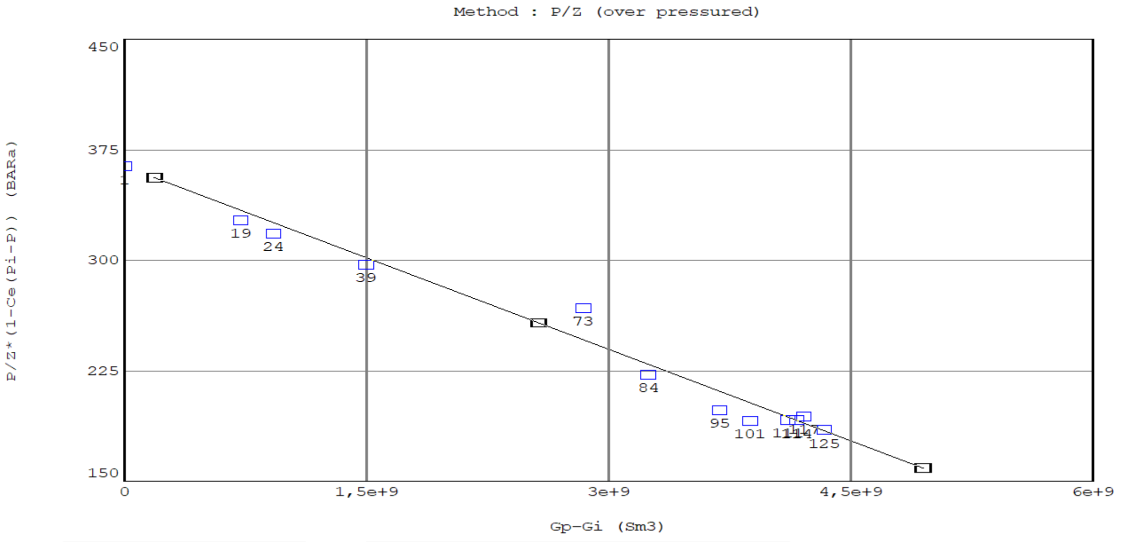


**Figure IV.10:** Graphical plot of Main TAGS reservoir after regression.

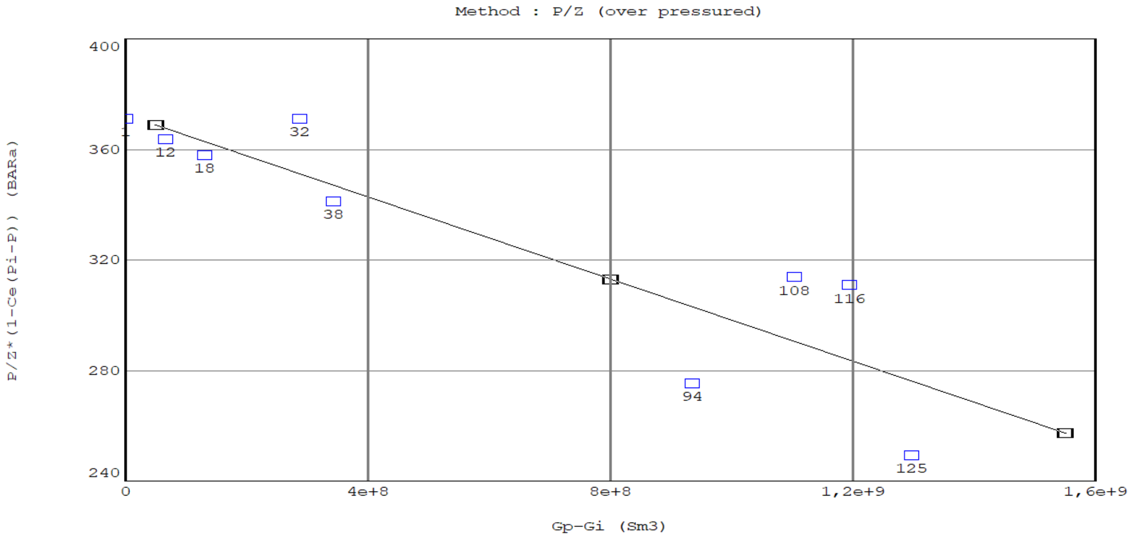


**Figure IV.11:** Graphical plot of West TAGS reservoir after regression.

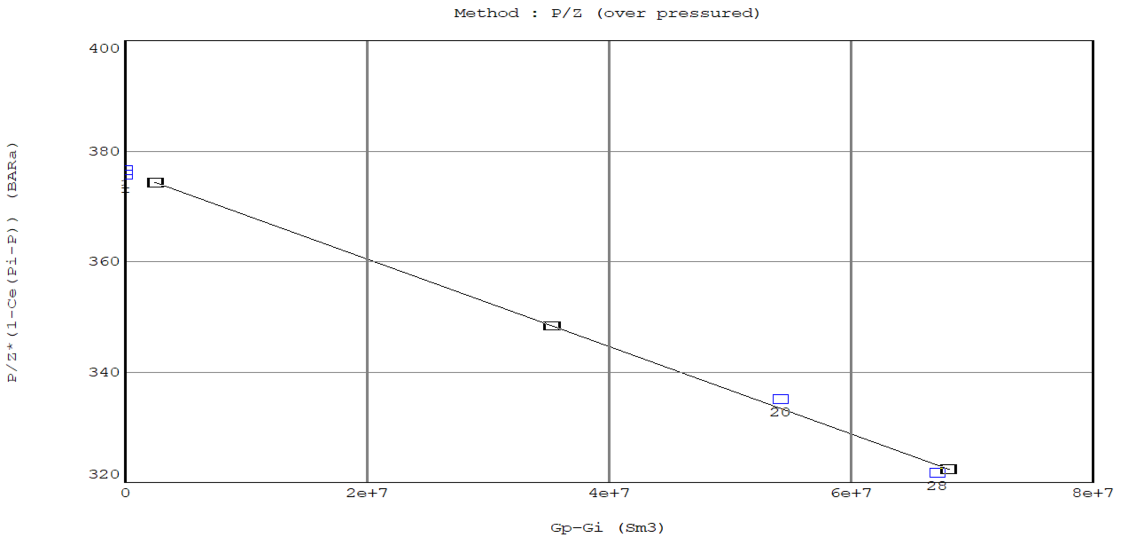


**Figure IV.12:** Graphical plot of North TAGS reservoir after regression.

## IV.1.4 Reservoirs Pressure and Production Predictions

The graphical representation of historical production data is utilized to construct a model that accurately reflects the behavior of the reservoirs, enabling the performance of predictive analysis on the reservoirs.

a. **Reservoirs Pressure**

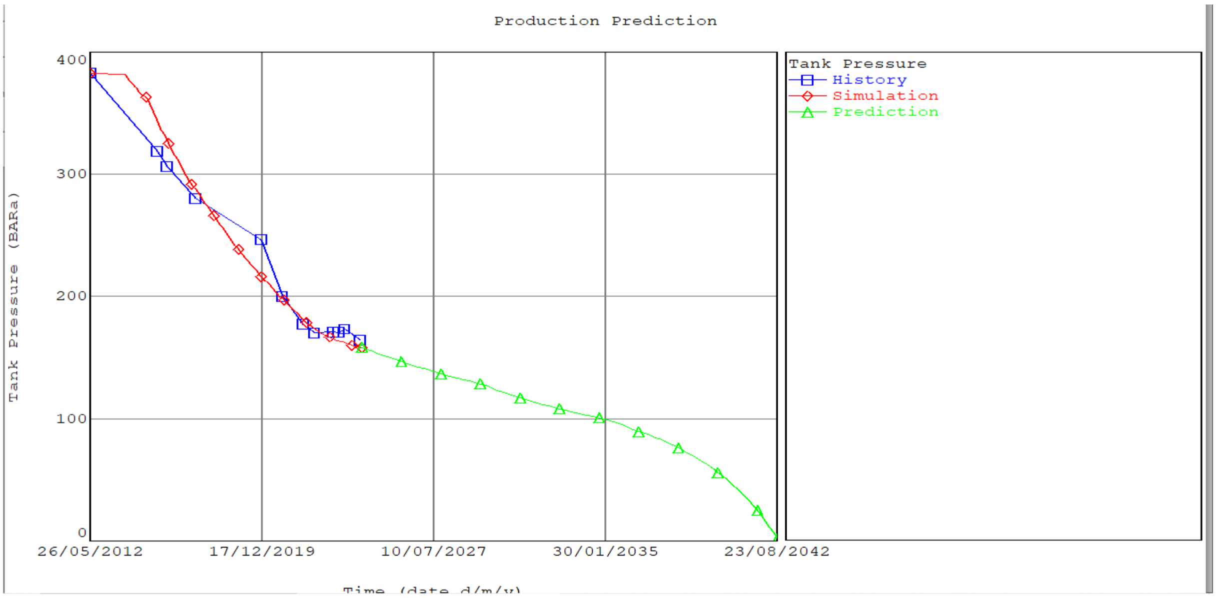


**Figure IV.13:** Production prediction of tank pressure from the end of history data to the year 2042 Main TAGS.

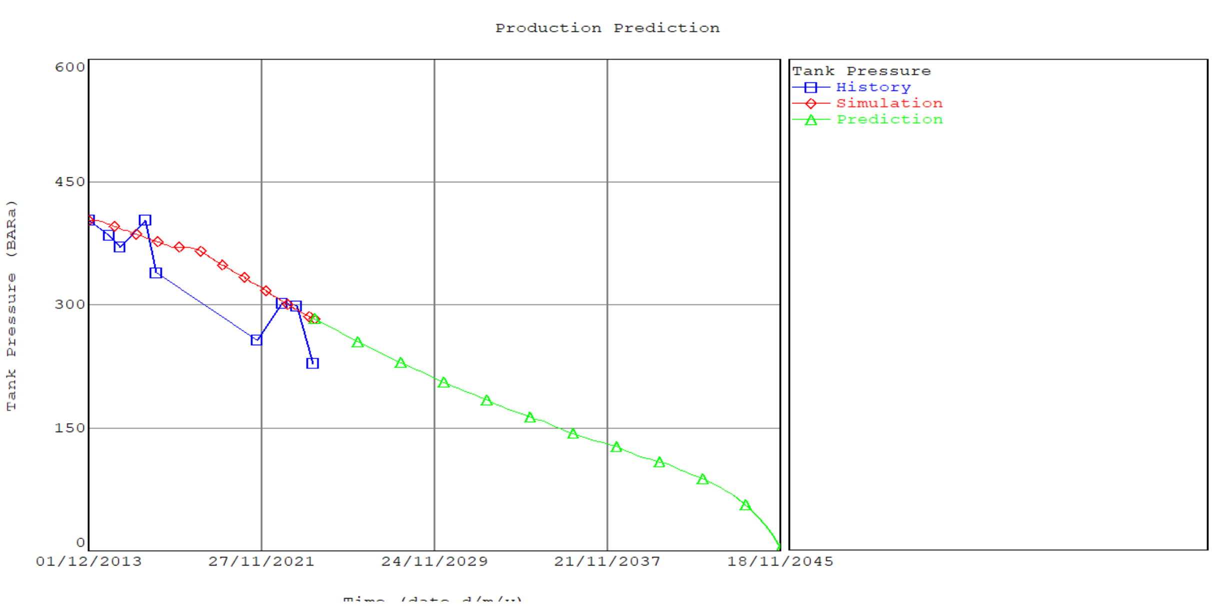


**Figure IV.14:** Production prediction of tank pressure from the end of history data to the year 2045 West TAGS.

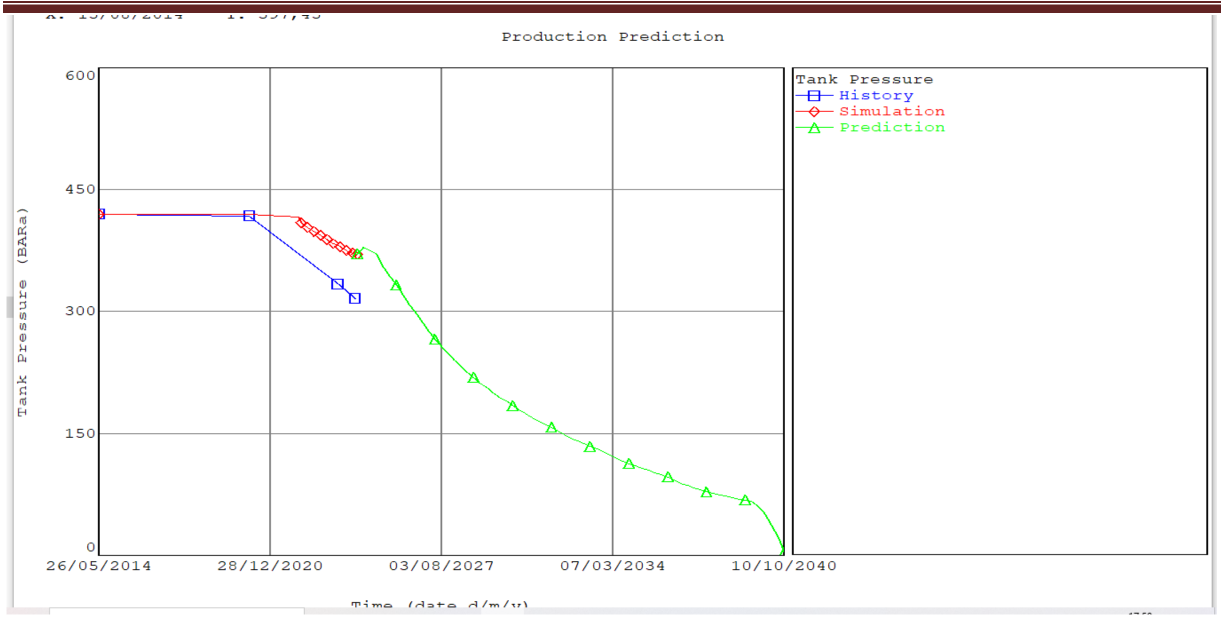


**Figure IV.15:** Production prediction of tank pressure from the end of history data to the year 2040 North TAGS.

## b. Cumulative gas and condensate production

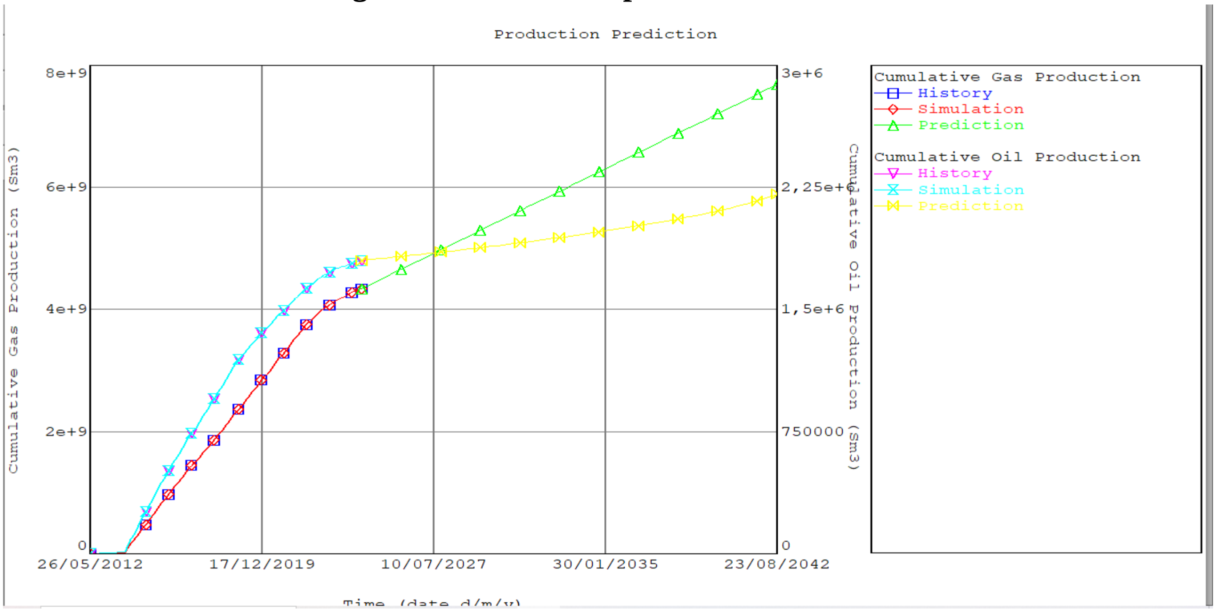


**Figure IV.16:** Production prediction of cumulative gas and condensate production from the end of history data to the year 2042 Main TAGS.

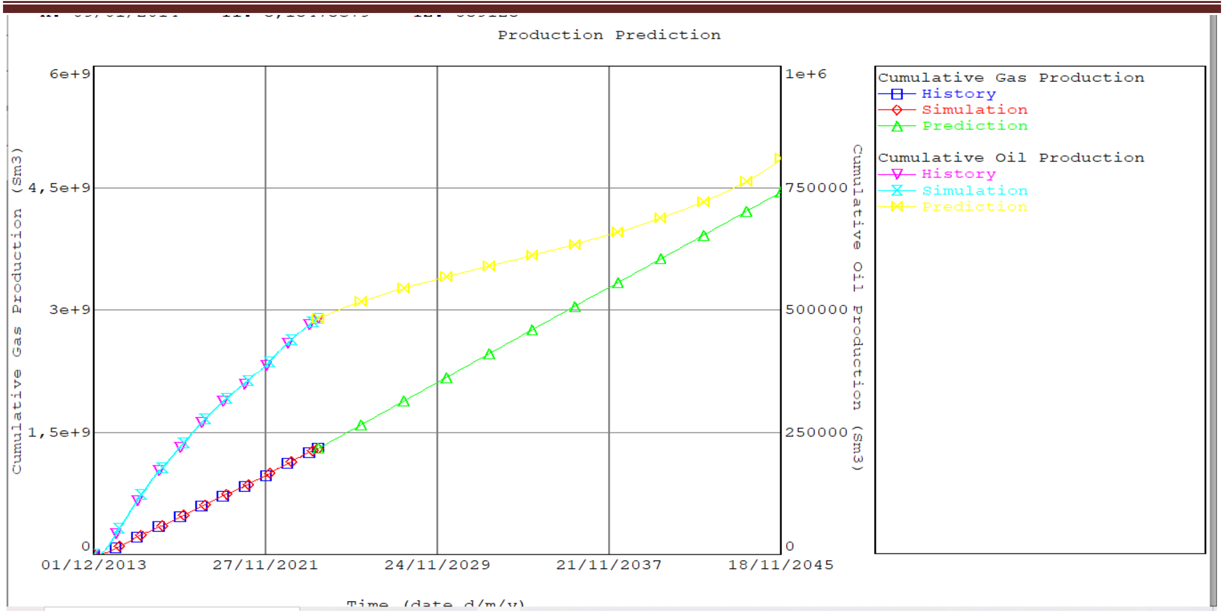


**Figure IV.17:** Production prediction of cumulative gas and condensate production from the end of history data to the year 2045 West TAGS.

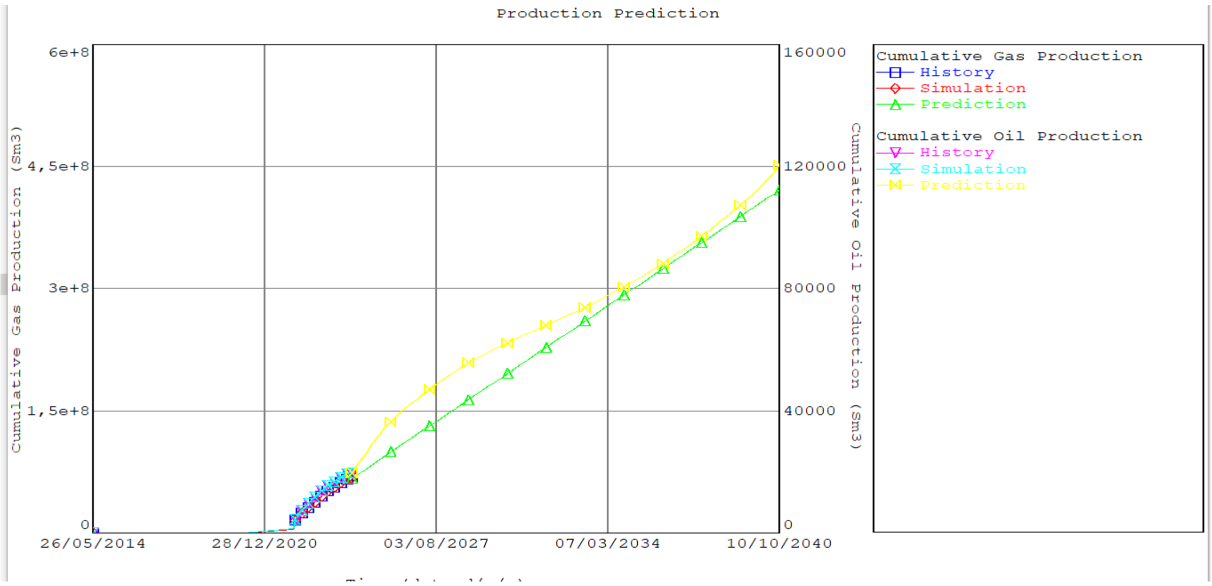


**Figure IV.18:** Production prediction of cumulative gas and condensate production from the end of history data to the year 2040 North TAGS.

## IV.1.5 Results and commentary

We were able to determine the following values of initial gas volume within our reservoir by utilizing the Mbal software:

**Table IV.1:** Original gas in place using Mbal software.

| reservoir | Original gas in place (MMsm3) |
|---|---|
| Main TAGS | 8,77 |
| West TAGS | 5 |
| North TAGS | 0,47 |

The reservoir pressure prediction of Mbal software enables us to determine the approximate future date that our reservoirs can no longer produce under the current production conditions. Implementation of a booster system holds the potential to extend the productive lifespan of these reservoirs by adapting them to operate under new conditions.

If we took these facts into consideration, we could calculate approximately the cumulative hydrocarbon expected to be produced during the time we gained by using a booster:

**Table IV.2:** cumulative hydrocarbon expected to be produced by using a Booster.

| reservoir | expected gained time | cumulative gas Produced | cumulative condensate Produced |
|---|---|---|---|
| | year | Msm3 | Msm3 |
| Main TAGS | 5 | 864,50 | 0,13 |
| West TAGS | 2 | 400,40 | 0,06 |
| North TAGS | 4 | 80,40 | 0,03 |

# IV.2 Using PIPESIM Software

## IV.2.1 Introduction to the PIPESIM Software

PIPESIM is a valuable steady-state multiphase flow simulator software developed by Schlumberger for oil and gas engineers involved in pipeline design, flow assurance analysis, and production system optimization, that empowers to optimize well performance and ensure the efficient operation of complex production systems and reservoir engineers to accurately predict flow and temperature behavior within wellbores and pipelines. Its robust capabilities enable users to:

- **Well Performance Analysis:** It facilitates the creation of accurate and representative well models.
- **Network Analysis:** Pipesim enables the simulation of an entire well network's behaviour by analyzing the impact of various network parameters.
- **Optimize existing designs:** By simulating various scenarios and tweaking parameters like choke settings, tubing sizes, and artificial lift methods, PIPESIM helps identify bottlenecks and uncover hidden potential for production improvement.
- **Predict the effects of future changes:** The ever-changing nature of oil and gas production demands proactive planning, enabling proactive decision-making.
- **Model and simulate production systems:** Once calibrated with real-world field data, it can be used to model and simulate the behavior of complex production systems.
- **Study system sensitivity:** PIPESIM facilitates comprehensive sensitivity analysis, and identifies critical factors.
- **Gap Between Theory and Reality:** It allows to calibrate their models with real-world field data. Once calibrated, predict their behavior under various conditions, and identify areas for optimization. **[21] [22]**

Here's an overview of Pipesim's key functionalities:

- Multiphase Flow Modeling.
- Steady-State Analysis.
- Pipeline Modeling.
- Wellbore Modeling.
- Facility Modeling.
- Production System Analysis.
- Artificial Lift Design. **[21]**

## IV.2.2 Modeling of the Candidate wells

This is crucial for accurately simulating production systems of multiphase flow, considering the behaviour of oil, gas, and water mixtures within the network. So, we can see the matching of the candidates wells (BDSN-1, BDSN-2, BRDS-1, BRDS-2, BRD-12, BRD-15, BRDS-

Ext2) to the manifold BRDMF01, the booster that is located there verses GEA-MF to NZ-MF directly to the processing facility (Cpf), as is showed in the figure

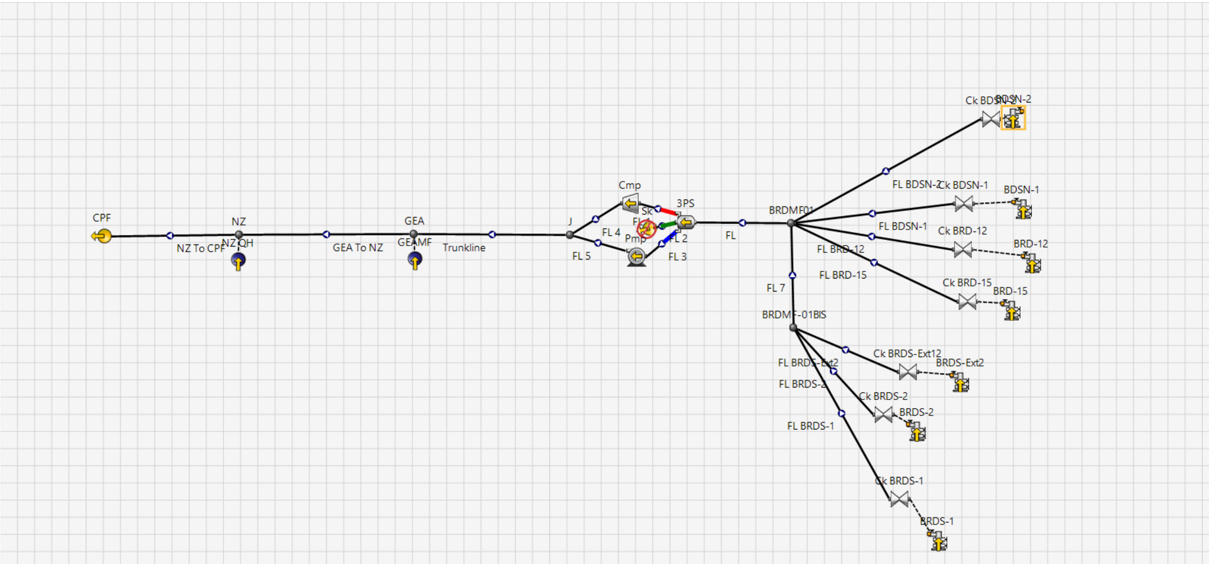


**Figure IV.19:** Network schematic of Boosting Model.

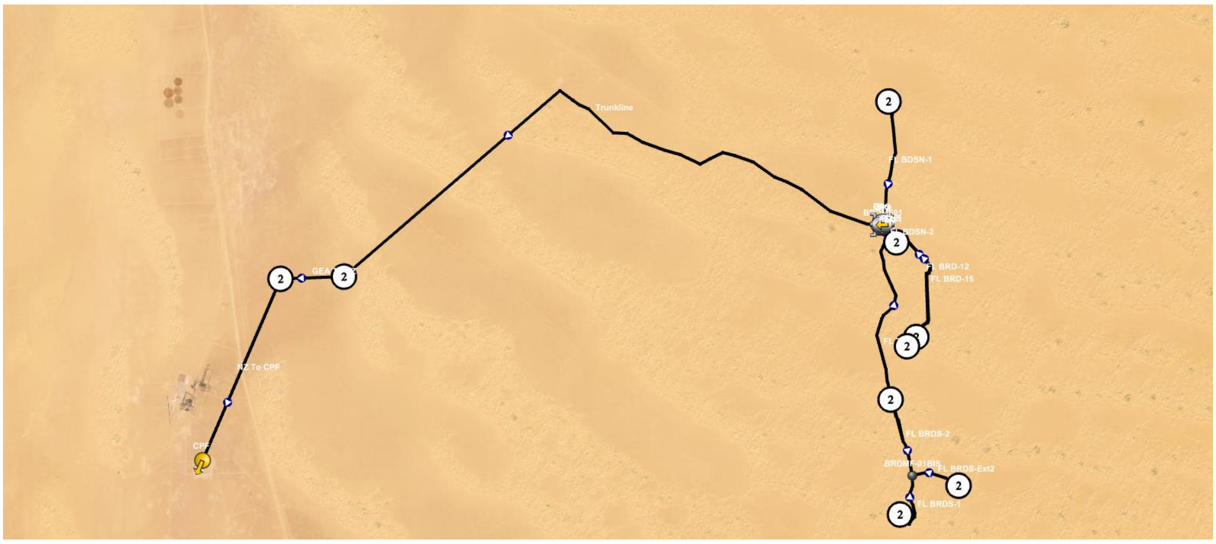


**Figure IV.20:** GIS of Boosting Model.

To enhance the accuracy and approximation of well-design simulations in PIPESIM, we employ well-technical sheets as a reference guide. These technical sheets provide comprehensive information about the well's characteristics, including its geometry, formation properties, fluid properties, and production data. By incorporating this information into PIPESIM, we can refine the well design model and achieve a more realistic representation of the well.

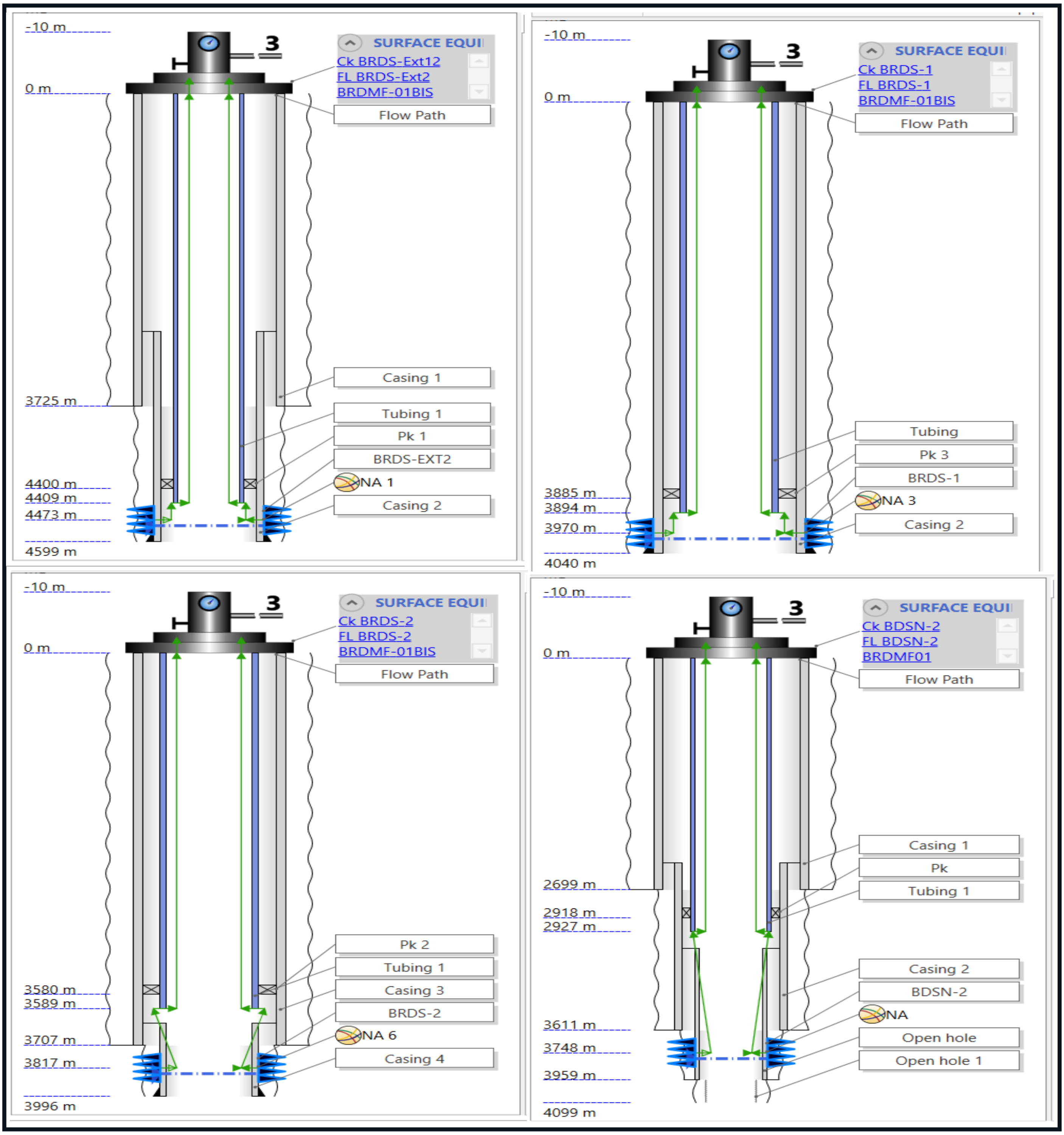
-10 m
0 m
3725 m
4400 m
4409 m
4473 m
4599 m
3
SURFACE EQUI
Ck BRDS-Ext12
FL BRDS-Ext2
BRDMF-01BIS
Flow Path
Casing 1
Tubing 1
Pk 1
BRDS-EXT2
NA 1
Casing 2
-10 m
0 m
3885 m
3894 m
3970 m
4040 m
SURFACE EQUI
Ck BRDS-1
FL BRDS-1
BRDMF-01BIS
Flow Path
Tubing
Pk 3
BRDS-1
NA 3
Casing 2
-10 m
0 m
3580 m
3589 m
3707 m
3817 m
3996 m
SURFACE EQUI
Ck BRDS-2
FL BRDS-2
BRDMF-01BIS
Flow Path
Pk 2
Tubing 1
Casing 3
BRDS-2
NA 6
Casing 4
-10 m
0 m
2699 m
2918 m
2927 m
3611 m
3748 m
3959 m
4099 m
SURFACE EQUI
Ck BDSN-2
FL BDSN-2
BRDMF01
Flow Path
Casing 1
Pk
Tubing 1
Casing 2
BDSN-2
NA
Open hole
Open hole 1

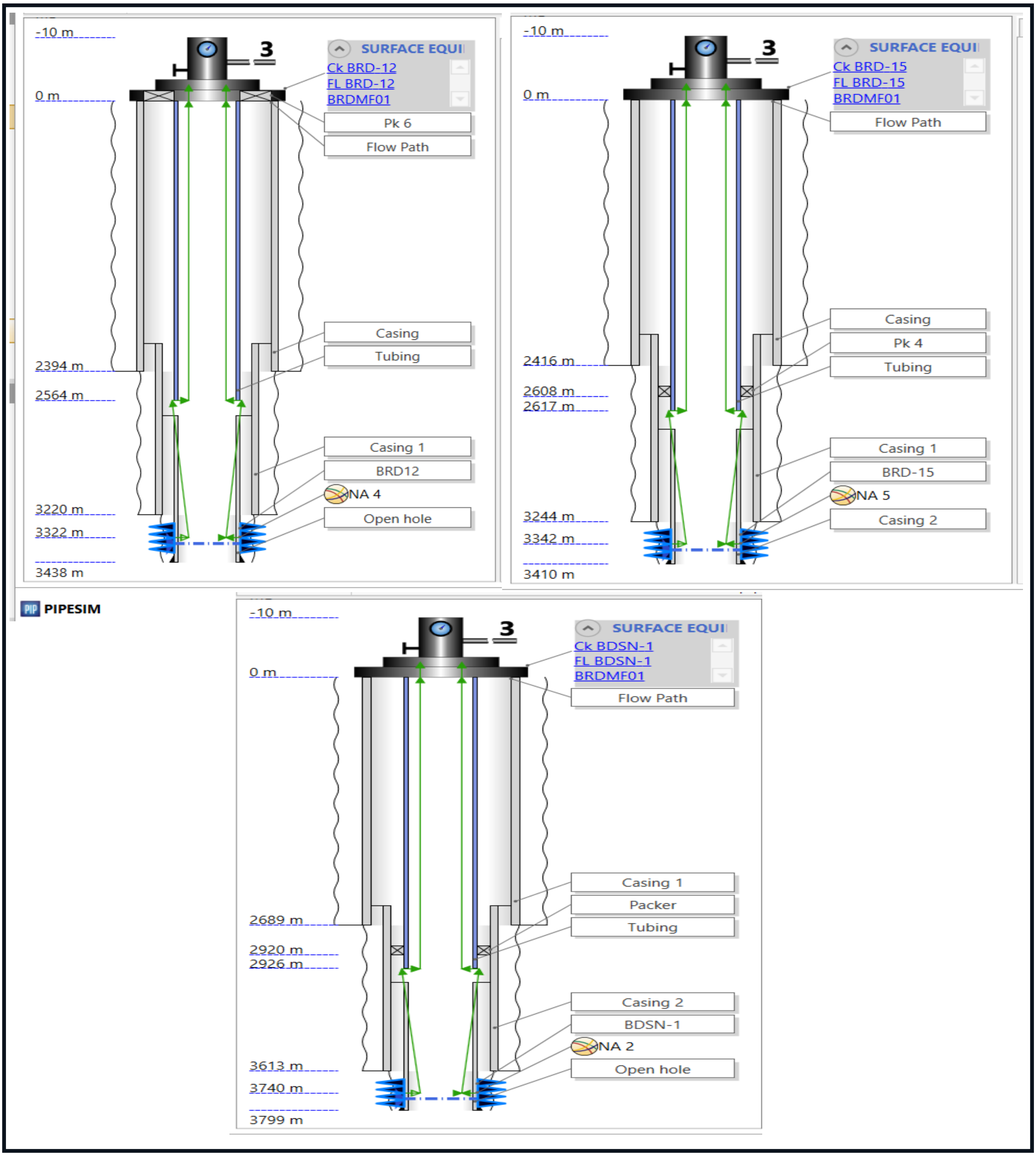


**Figure IV.21**: PIPESIM models of candidate wells.

### IV.2.3 Wellhead Pressure simulation

Generating reservoir performance curves (IPR) for individual wells using well-test data and the PIPESIM software is crucial for optimizing well production and reservoir management strategies.

PIPESIM utilizes the multi-rate method, a common technique for generating IPR curves, the core of this method lies in determining the coefficients “c” and “n”.

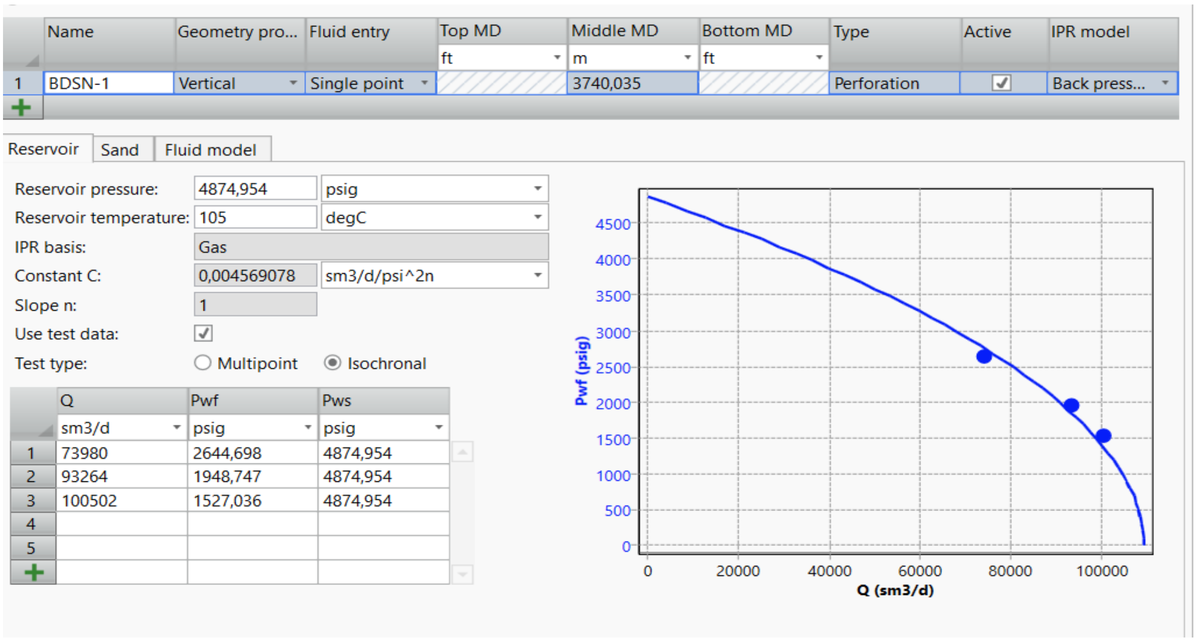


**Figure IV.22:** Curve IPR of BDSN-01

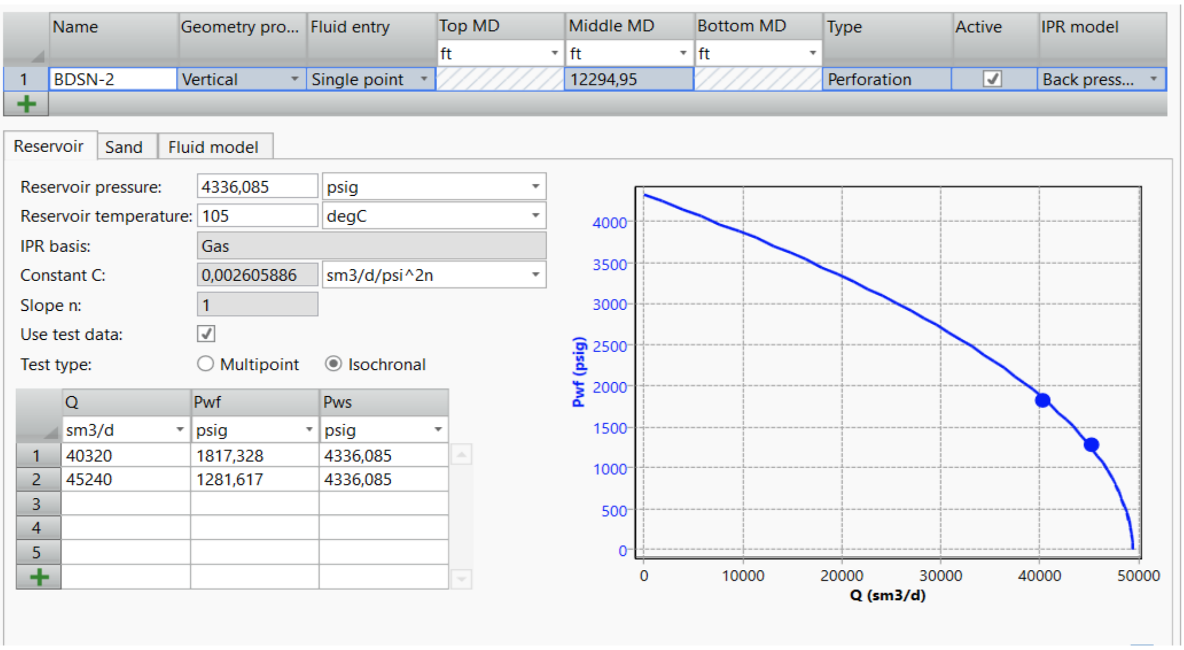


**Figure IV.23:** Curve IPR of BDSN-02.

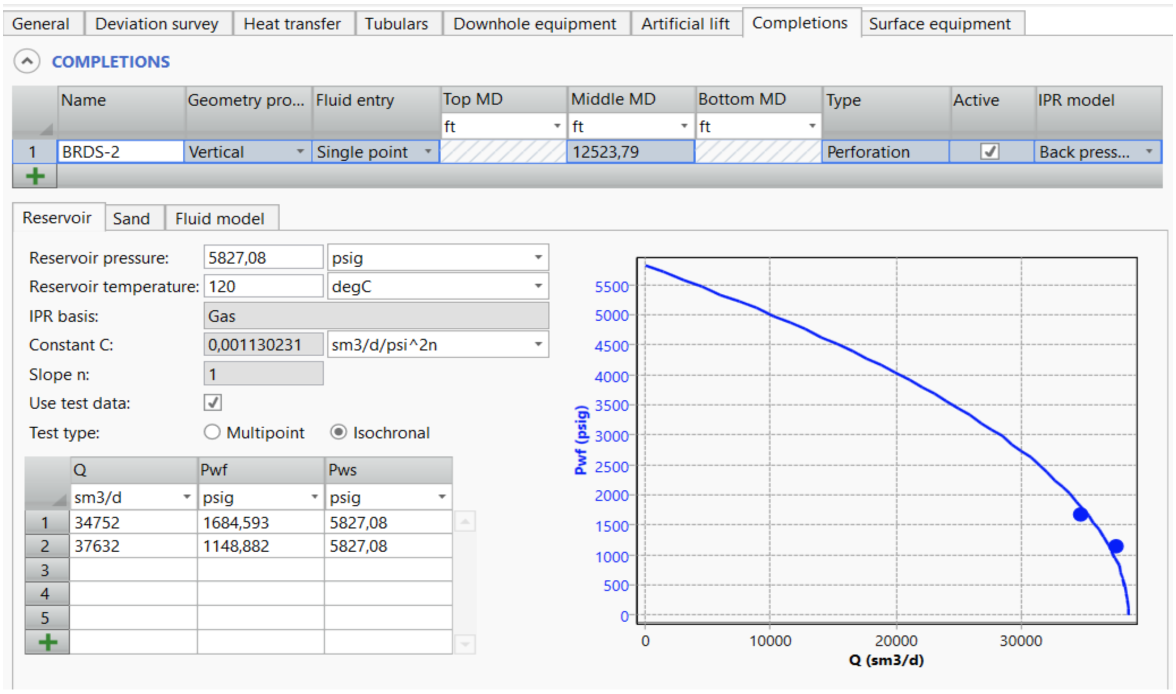


**Figure IV.24:** Curve IPR of BRDS-2.

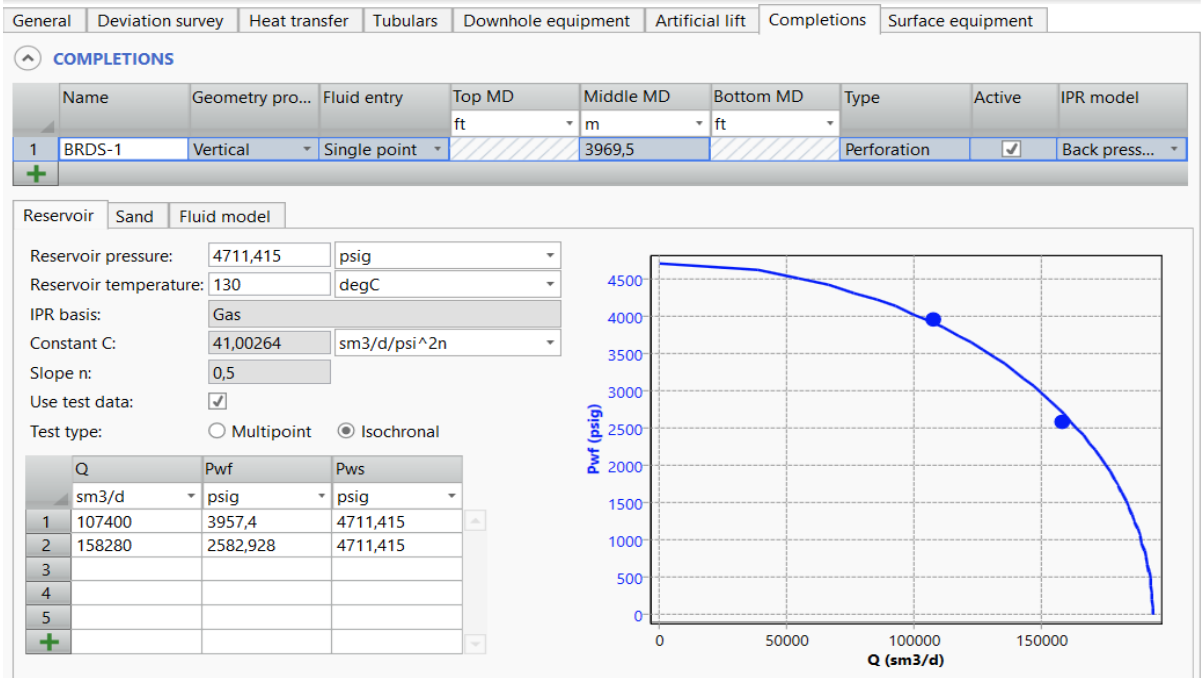


**Figure IV.25:** Curve IPR of BRDS-01.

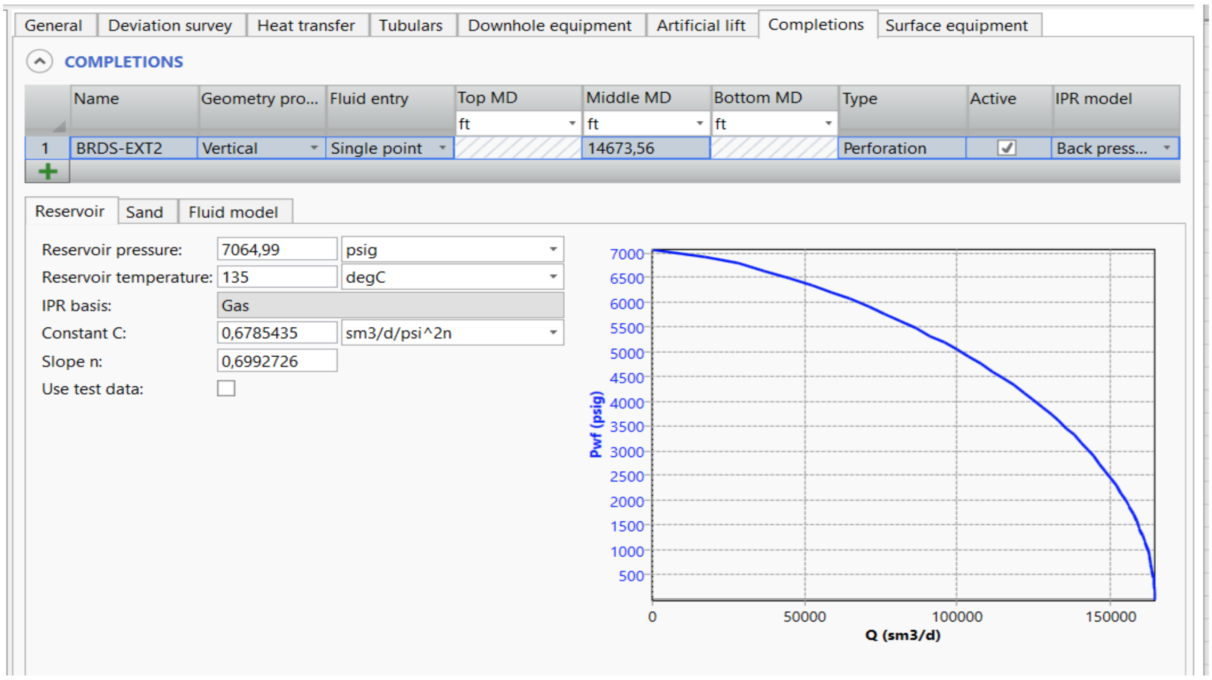


**Figure IV.26:** Curve IPR of BRDS-Ext02.

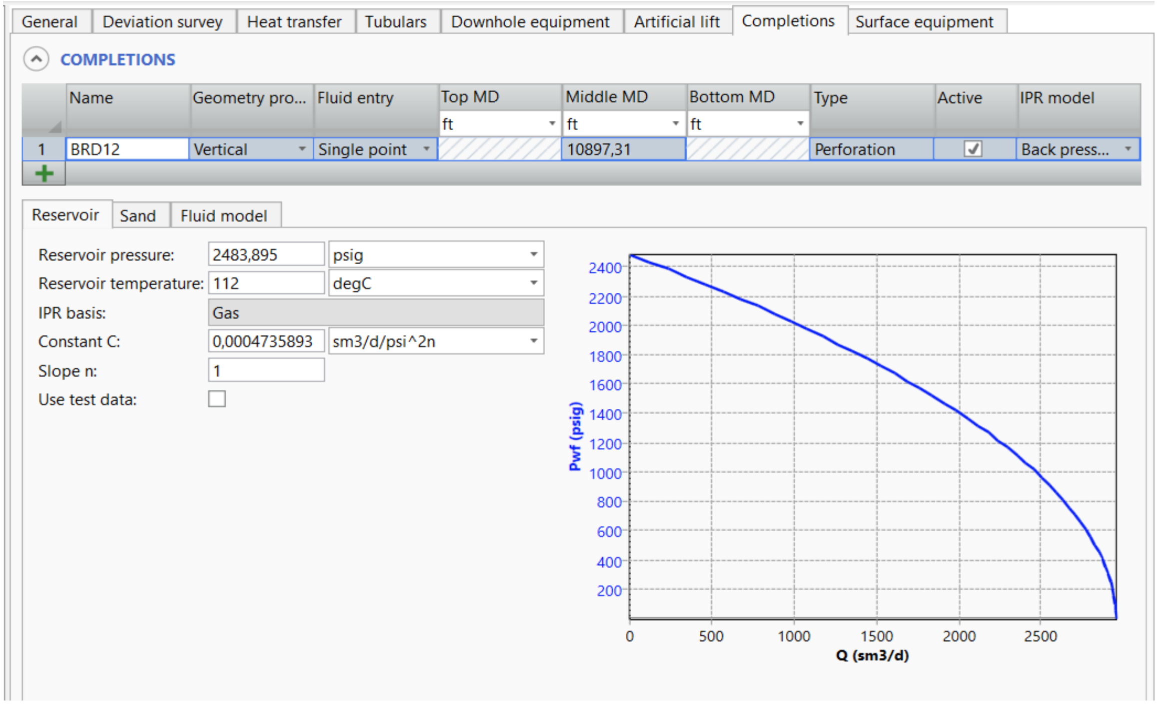


**Figure IV.27:** Curve IPR of BRD-12.

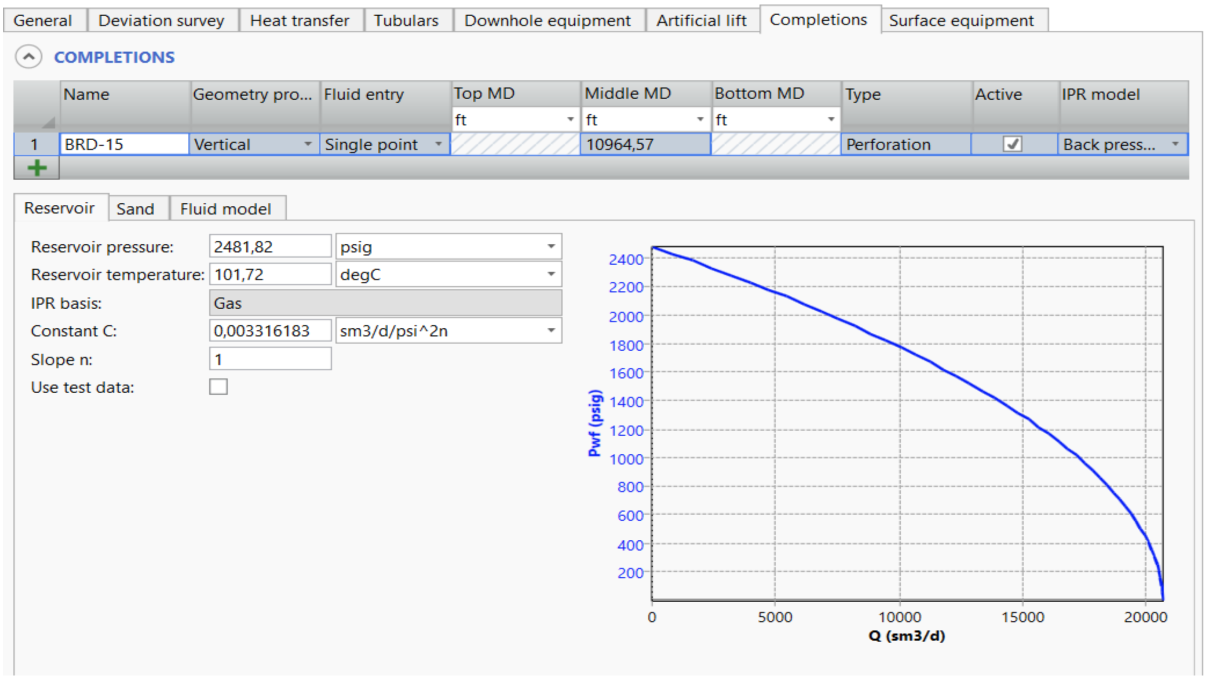


**Figure IV.28:** Curve IPR of BRD-15.

**NB:** For the wells BRD-15, BRD-12, and BRDS-EXT2, the constants "c" and "n" are calculated solely by the reservoir pressure due to the lack of recent well-test data.

**Table IV.3:** Summary of IPR calculation results.

| Wells | AOF | C | N |
| --- | --- | --- | --- |
| **BRD-12** | 2956,495 | 0,0004735893 | 1 |
| **BRD-15** | 20667,7 | 0,003316183 | 1 |
| **BRDS-1** | 193782,1 | 41,00264 | 0,5 |
| **BRDS-2** | 38570,42 | 0,001130231 | 1 |
| **BDSN-1** | 109239,6 | 0,004569078 | 1 |
| **BDSN-2** | 49327,01 | 0,002605886 | 1 |
| **BRDS-Ext2** | 164435,4 | 0,6785435 | 0,6992726 |

### IV.2.4 PVT Data Inputs

In the context of simulation using PIPESIM, we employed PVT (pressure, volume, temperature) data to enhance our understanding of the fluid's behavior and accurately represent it within the simulation. By incorporating PVT data, we can enhance the model's ability to select appropriate correlations, characterize fluid properties, and predict flow behavior with greater precision.

**Table IV.4:** Composition of reservoir fluids.

| Reservoirs / Compositions | TAGS NORTH | | TAGS WEST | | TAGS MAIN | |
|---|---|---|---|---|---|---|
| **Methane** | 81,446 | 81,446 | 81,383 | 80,71869 | 82,453 | 82,453 |
| **Ethane** | 5,652 | 5,652 | 6,353 | 6,301142 | 6,614 | 6,614 |
| **Propane** | 2,497 | 2,497 | 2,814 | 2,79103 | 2,706 | 2,706 |
| **Isobutane** | 0,64 | 0,64 | 0,617 | 0,6119635 | 0,662 | 0,662 |
| **Butane** | 1,015 | 1,015 | 1,076 | 1,067217 | 0,897 | 0,897 |
| **Isopentane** | 0,639 | 0,639 | 0,574 | 0,5693145 | 0,51 | 0,51 |
| **Pentane** | 0,43 | 0,43 | 0,423 | 0,4195471 | 0,339 | 0,339 |
| **Benzene** | 0,103 | 0,103 | 0,128 | 0,1269552 | 0,071 | 0,071 |
| **Hexane** | 0,826 | 0,826 | 0,704 | 0,6982534 | 0,596 | 0,596 |
| **Toluene** | 0,048 | 0,048 | 0,087 | 0,0862898 | 0,079 | 0,079 |
| **Methylcyclohexane** | 0 | 0 | 0,1 | 0,0991837 | 0 | 0 |
| **Heptane** | 0,777 | 0,777 | 0,64 | 0,6347758 | 0,571 | 0,571 |
| **P-Xylene** | 0,027 | 0,027 | 0,05 | 0,0495919 | 0,054 | 0,054 |
| **Ethylbenzene** | 0,004 | 0,004 | 0,009 | 0,0089265 | 0,007 | 0,007 |
| **O-Xylene** | 0,018 | 0,018 | 0,03 | 0,0297551 | 0,027 | 0,027 |
| **Octane** | 0,698 | 0,698 | 0,578 | 0,5732819 | 0,546 | 0,546 |
| **Nonane** | 0,514 | 0,514 | 0,402 | 0,3987185 | 0,373 | 0,373 |
| **Decane** | 0,461 | 0,461 | 0,406 | 0,4026859 | 0,367 | 0,367 |
| **Undecane** | 0,366 | 0,366 | 0,323 | 0,3203634 | 0,285 | 0,285 |
| **Dodecane** | 0,291 | 0,291 | 0,257 | 0,2549022 | 0,225 | 0,225 |
| **Tridecane** | 0,253 | 0,253 | 0,228 | 0,2261389 | 0,202 | 0,202 |
| **Tetradecane** | 0,203 | 0,203 | 0,186 | 0,1844817 | 0,161 | 0,161 |
| **Pentadecane** | 0,172 | 0,172 | 0,161 | 0,1596858 | 0,137 | 0,137 |
| **Hexadecane** | 0,137 | 0,137 | 0,131 | 0,1299307 | 0,11 | 0,11 |
| **Heptadecane** | 0,133 | 0,133 | 0,129 | 0,127947 | 0,107 | 0,107 |
| **Octadecane** | 0,103 | 0,103 | 0,103 | 0,1021592 | 0,082 | 0,082 |
| **Nonadecane** | 0,075 | 0,075 | 0,075 | 0,0743878 | 0,058 | 0,058 |
| **Nitrogen** | 1,044 | 1,044 | 0,654 | 0,6486615 | 0,539 | 0,539 |
| **Carbon Dioxide** | 0,995 | 0,995 | 1,799 | 1,784315 | 0,923 | 0,923 |
| **neo-Pentane** | 0,019 | 0,019 | 0,015 | 0,0148776 | 0,014 | 0,014 |
| **C20+** | 0,414 | 0,414 | 0,388 | 0,3848328 | 0,285 | 0,285 |

## IV.2.5 Data Matching

The selection of an appropriate vertical flow correlation is crucial for building a reliable well model in PIPESIM, a reservoir simulation software. This correlation should minimize the relative error between simulated and measured well performance data. PIPESIM offers a variety of correlations to choose from.

**Table IV.5:** Vertical flow correlations

| Correlation | Wells |
|---|---|
| LedaFlow v. 1.4 3-Phase | BDSN-2 |
| LedaFlow v. 1.4 2-Phase | BDSN-1 |
| Gray (modified) | BRD-12 |
| Govier, Aziz [Tulsa (Legacy 1989)] | BRD-15 |
| Govier, Aziz & Fogarasi | BRDS-Ext2 |
| Gomez | BRDS-2 |
| Duns & Ros [Tulsa (Legacy 1989)] | BRDS-1 |

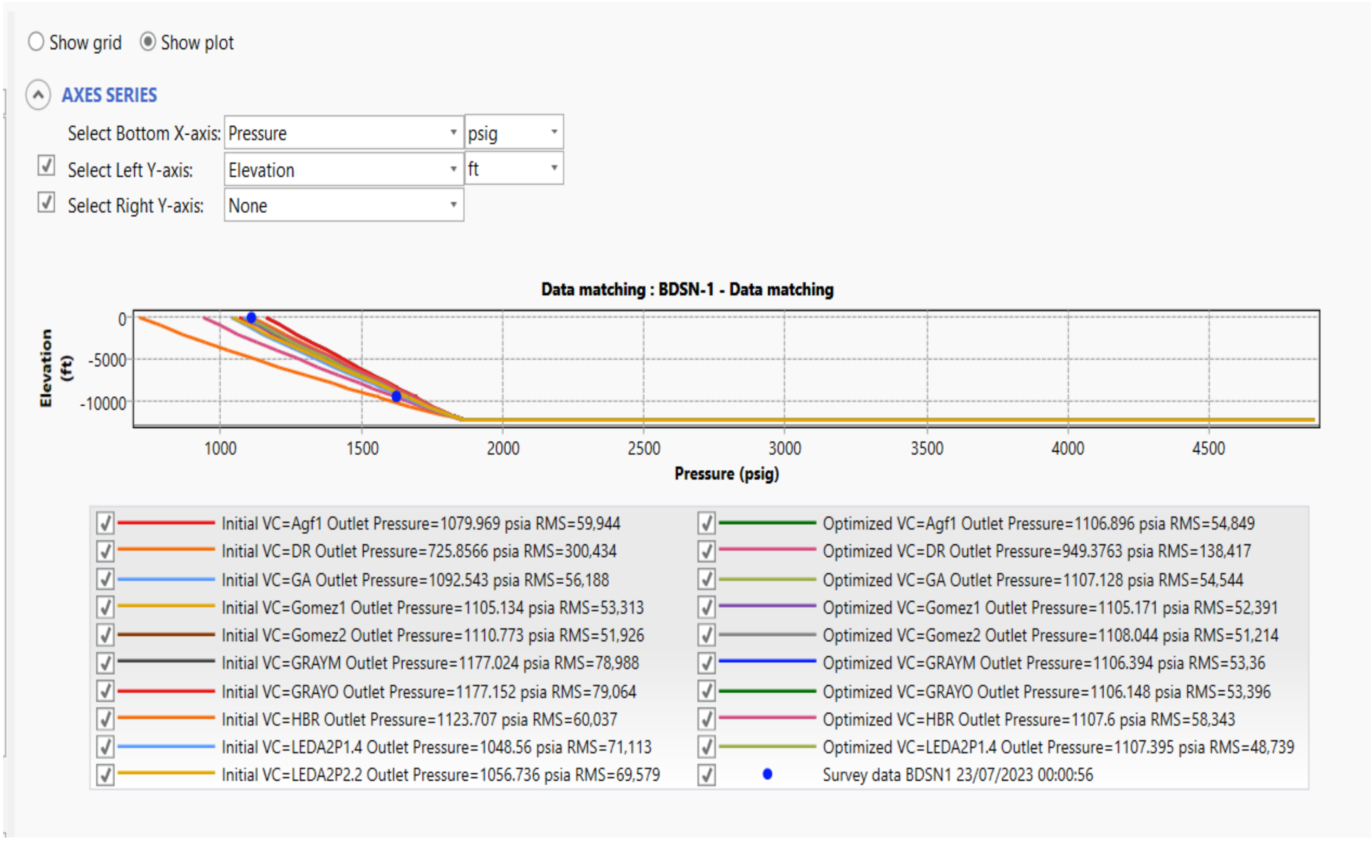


Data matching

Name: BDSN-1 - Data matching

Description:

Data matching | Engine console | Profile results | Results summary

| | Vertical multiphase correlation | Calibrated vertical friction factor | Calibrated vertical holdup factor | Calibrated U value multiplier | Initial pressure RMS | Calibrated pressure RMS | Initial temperature RMS | Calibrated temperature RMS | Initial holdup RMS | Calibrated holdup RMS | Initial total RMS | Calibrated total RMS |
|---|---|---|---|---|---|---|---|---|---|---|---|---|
| 1 | LedaFlow v. 1.4 2-Phase | 2 | 0.819576 | 1.101745 | 54.39241 | 32.571946 | 16.720689 | 16.167115 | 0 | 0 | 71.113099 | 48.739061 |
| 2 | LedaFlow v. 1.4 3-Phase | 2 | 0.819576 | 1.101745 | 54.39241 | 32.571946 | 16.720689 | 16.167115 | 0 | 0 | 71.113099 | 48.739061 |
| 3 | Gomez Enhanced | 2 | 1.000394 | 1.187494 | 35.386079 | 35.350071 | 16.539433 | 15.863916 | 0 | 0 | 51.925512 | 51.213987 |
| 4 | Gomez | 2 | 0.994729 | 1.086791 | 36.788816 | 36.213541 | 16.523989 | 16.177778 | 0 | 0 | 53.312804 | 52.391319 |
| 5 | Gray (modified) | 1.110854 | 1.379899 | 1.130811 | 62.585891 | 37.352416 | 16.402129 | 16.007433 | 0 | 0 | 78.98802 | 53.359849 |
| 6 | Gray (original) | 1.149784 | 1.378334 | 1.126622 | 62.662046 | 37.375104 | 16.401906 | 16.021064 | 0 | 0 | 79.063952 | 53.396167 |
| 7 | LedaFlow v. 2.2 2-Phase | 0.509749 | 0.825361 | 1.177009 | 52.972505 | 38.034802 | 16.606343 | 15.86074 | 0 | 0 | 69.578848 | 53.895542 |
| 8 | LedaFlow v. 2.2 3-Phase | 0.509749 | 0.825361 | 1.177009 | 52.972505 | 38.034802 | 16.606343 | 15.86074 | 0 | 0 | 69.578848 | 53.895542 |
| 9 | Govier, Aziz [Tulsa (Legacy 1989)] | 0.5 | 1.071717 | 0.817282 | 38.011283 | 36.282912 | 16.504139 | 17.658058 | 0 | 0 | 54.515422 | 53.94097 |
| 10 | Govier, Aziz & Fogarasi | 0.774288 | 0.958861 | 0.844219 | 39.653658 | 37.106043 | 16.534572 | 17.437829 | 0 | 0 | 56.18823 | 54.543872 |
| 11 | Aziz Govier Fogarasi | 0.5 | 0.93223 | 0.872348 | 43.390535 | 37.61521 | 16.55347 | 17.233764 | 0 | 0 | 59.944006 | 54.848974 |
| 12 | Hagedorn & Brown | 1.407351 | 1.046709 | 1.294424 | 43.614647 | 42.800114 | 16.421929 | 15.542417 | 0 | 0 | 60.036576 | 58.342531 |
| 13 | Duns & Ros [Tulsa (Legacy 1989)] | 0.5 | 0.5 | 0.942922 | 282.713236 | 121.101403 | 17.540424 | 17.20109 | 0 | 0 | 300.25366 | 138.302492 |
| 14 | Duns & Ros [Baker Jardine] | 0.5 | 0.5 | 0.942922 | 282.893281 | 121.215789 | 17.540328 | 17.200793 | 0 | 0 | 300.433609 | 138.416582 |

**Figure IV.29**: Data Matching of BDSN-1.

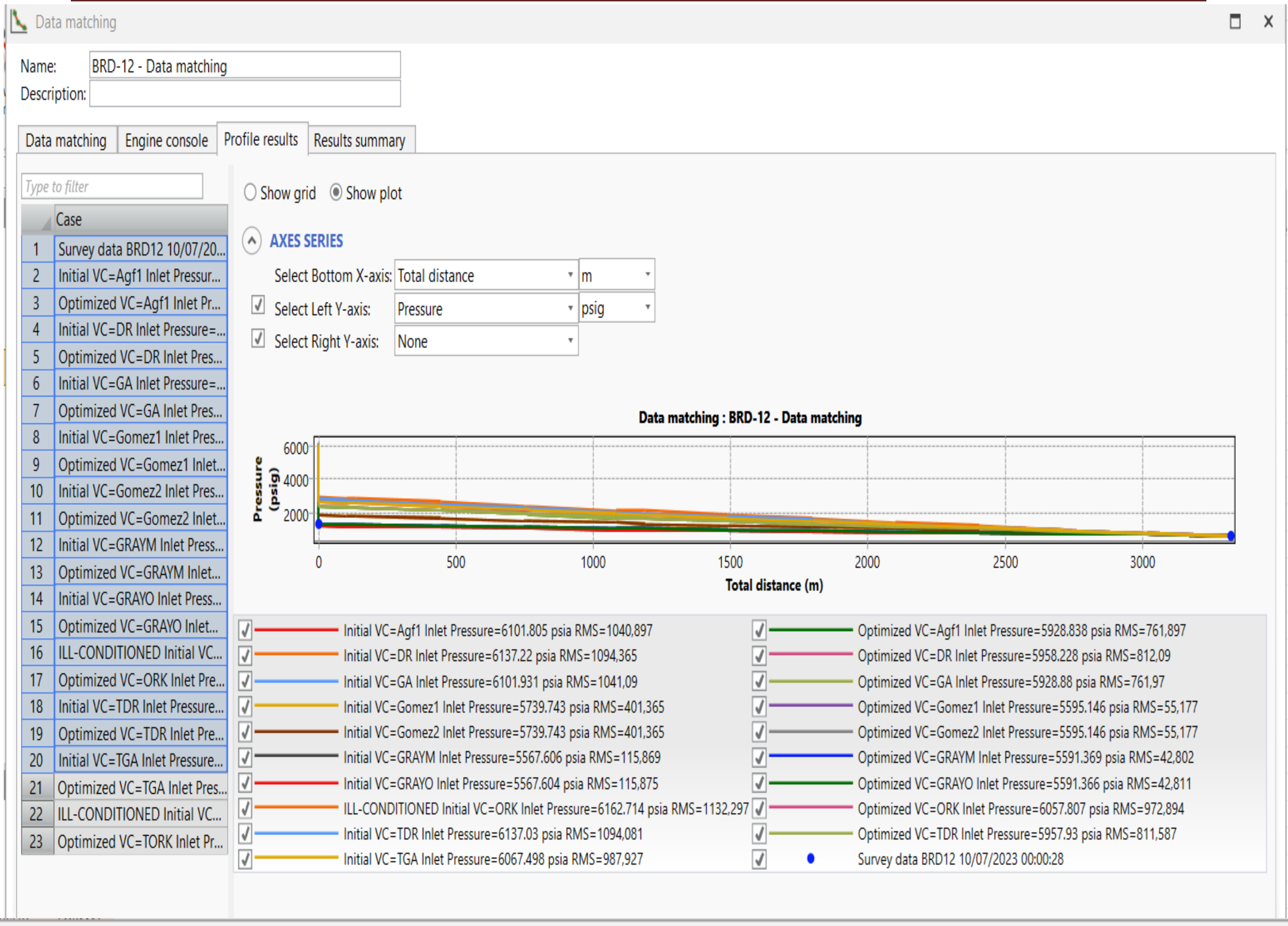


Data matching

Name: BRD-12 - Data matching

Description:

Data matching | Engine console | Profile results | Results summary

Type to filter

| | Vertical multiphase correlation | Calibrated vertical friction factor | Calibrated vertical holdup factor | Calibrated U value multiplier | Initial pressure RMS | Calibrated pressure RMS | Initial temperature RMS | Calibrated temperature RMS | Initial holdup RMS | Calibrated holdup RMS | Initial total RMS | Calibrated total RMS |
|---|---|---|---|---|---|---|---|---|---|---|---|---|
| 1 | Gray (modified) | 1.23335 | 1.263827 | 2.963099 | 72.014754 | 0.344823 | 43.854127 | 42.45722 | 0 | 0 | 115.868881 | 42.802044 |
| 2 | Gray (original) | 1.23335 | 1.263827 | 2.963099 | 72.020554 | 0.353187 | 43.854271 | 42.457425 | 0 | 0 | 115.874825 | 42.810613 |
| 3 | Gomez | 2 | 0.5 | 0.1 | 366.913396 | 10.584329 | 34.451972 | 44.592463 | 0 | 0 | 401.365368 | 55.176792 |
| 4 | Gomez Enhanced | 2 | 0.5 | 0.1 | 366.913396 | 10.584329 | 34.451972 | 44.592463 | 0 | 0 | 401.365368 | 55.176792 |
| 5 | Govier, Aziz [Tulsa (Legacy 1989)] | 0.608914 | 0.5 | 0.1 | 962.041834 | 664.260979 | 25.885406 | 30.974659 | 0 | 0 | 987.92724 | 695.235638 |
| 6 | Aziz Govier Fogarasi | 0.612603 | 0.5 | 0.1 | 1015.56738 | 732.062857 | 25.329914 | 29.834328 | 0 | 0 | 1040.897295 | 761.897185 |
| 7 | Govier, Aziz & Fogarasi | 0.609256 | 0.5 | 0.1 | 1015.761733 | 732.136033 | 25.327898 | 29.833479 | 0 | 0 | 1041.08963 | 761.969512 |
| 8 | Duns & Ros [Tulsa (Legacy 1989)] | 1.371952 | 0.5 | 0.1 | 1069.358301 | 782.373375 | 24.723134 | 29.21359 | 0 | 0 | 1094.081435 | 811.586966 |
| 9 | Duns & Ros [Baker Jardine] | 1.371952 | 0.5 | 0.1 | 1069.645296 | 782.883303 | 24.72002 | 29.207069 | 0 | 0 | 1094.365316 | 812.090372 |
| 10 | Orkiszewski [Baker Jardine] | 0.5 | 0.5 | 10 | 1107.891883 | 946.706747 | 24.405391 | 26.187494 | 0 | 0 | 1132.297273 | 972.894242 |
| 11 | Orkiszewski [Tulsa (Legacy 1989)] | 0.5 | 0.5 | 10 | 1107.891923 | 946.706973 | 24.452744 | 26.187492 | 0 | 0 | 1132.344667 | 972.894465 |

**Figure IV.30**: Data Matching of BRD-12.

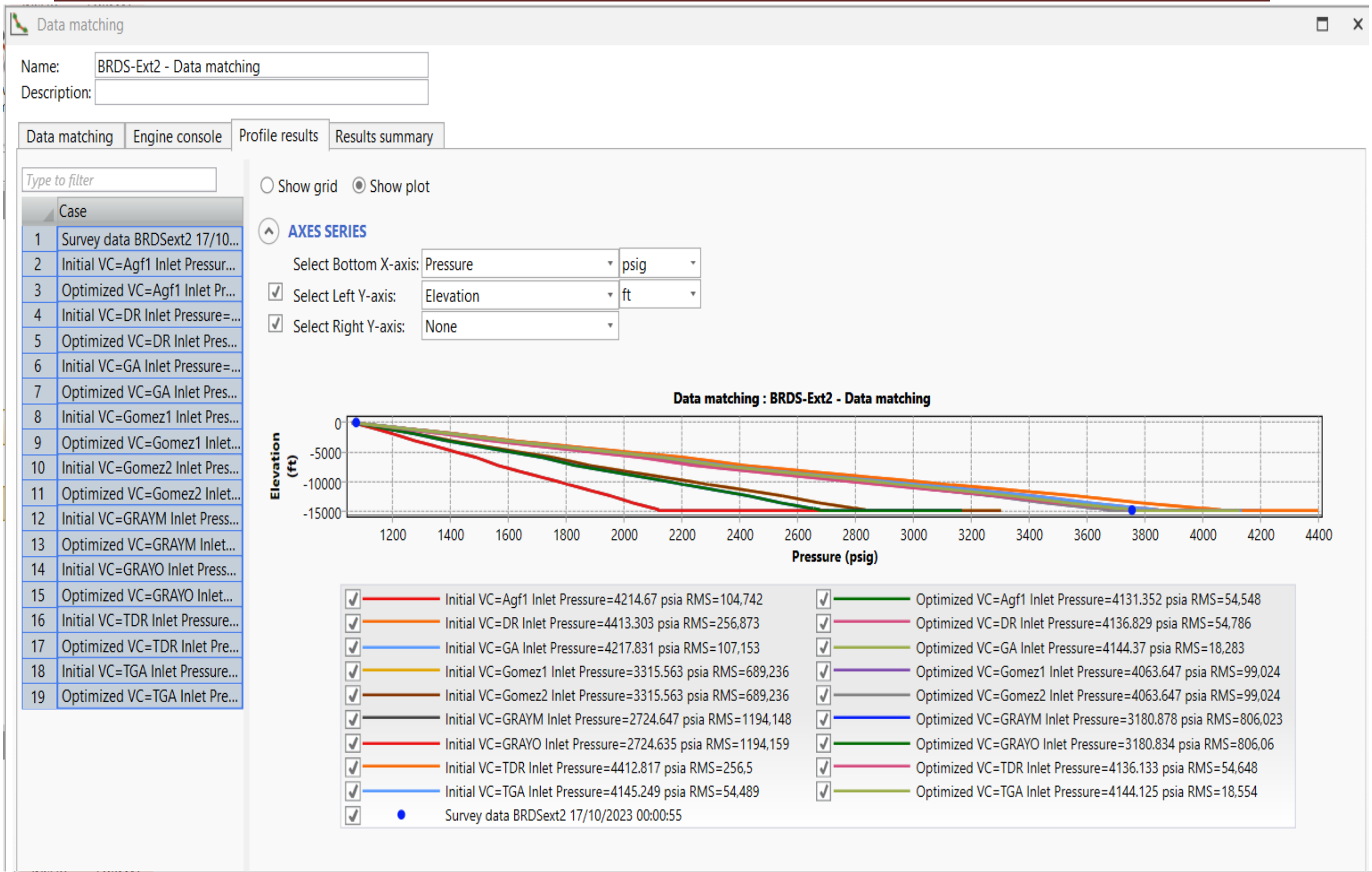


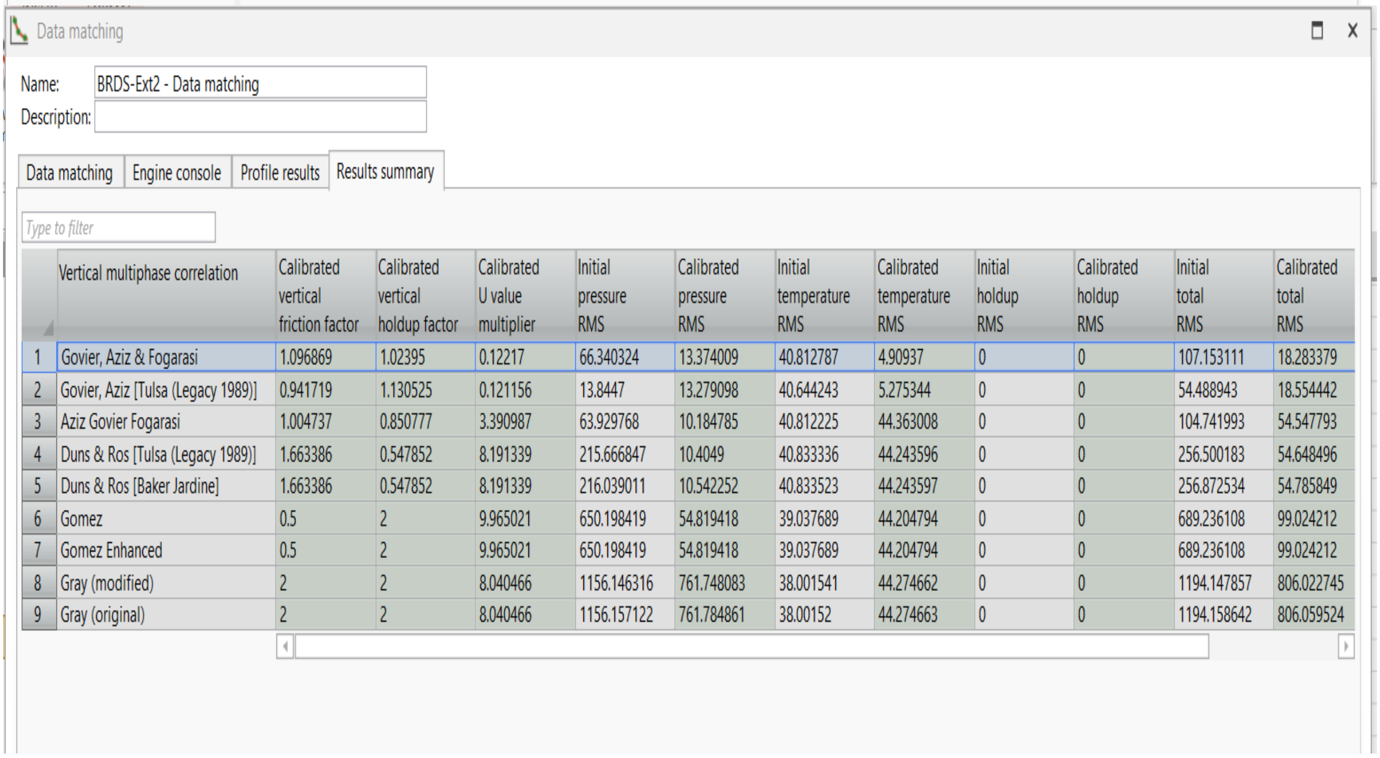


| | Vertical multiphase correlation | Calibrated vertical friction factor | Calibrated vertical holdup factor | Calibrated U value multiplier | Initial pressure RMS | Calibrated pressure RMS | Initial temperature RMS | Calibrated temperature RMS | Initial holdup RMS | Calibrated holdup RMS | Initial total RMS | Calibrated total RMS |
|---|---|---|---|---|---|---|---|---|---|---|---|---|
| 1 | Govier, Aziz & Fogarasi | 1.096869 | 1.02395 | 0.12217 | 66.340324 | 13.374009 | 40.812787 | 4.90937 | 0 | 0 | 107.153111 | 18.283379 |
| 2 | Govier, Aziz [Tulsa (Legacy 1989)] | 0.941719 | 1.130525 | 0.121156 | 13.8447 | 13.279098 | 40.644243 | 5.275344 | 0 | 0 | 54.488943 | 18.554442 |
| 3 | Aziz Govier Fogarasi | 1.004737 | 0.850777 | 3.390987 | 63.929768 | 10.184785 | 40.812225 | 44.363008 | 0 | 0 | 104.741993 | 54.547793 |
| 4 | Duns & Ros [Tulsa (Legacy 1989)] | 1.663386 | 0.547852 | 8.191339 | 215.666847 | 10.4049 | 40.833336 | 44.243596 | 0 | 0 | 256.500183 | 54.648496 |
| 5 | Duns & Ros [Baker Jardine] | 1.663386 | 0.547852 | 8.191339 | 216.039011 | 10.542252 | 40.833523 | 44.243597 | 0 | 0 | 256.872534 | 54.785849 |
| 6 | Gomez | 0.5 | 2 | 9.965021 | 650.198419 | 54.819418 | 39.037689 | 44.204794 | 0 | 0 | 689.236108 | 99.024212 |
| 7 | Gomez Enhanced | 0.5 | 2 | 9.965021 | 650.198419 | 54.819418 | 39.037689 | 44.204794 | 0 | 0 | 689.236108 | 99.024212 |
| 8 | Gray (modified) | 2 | 2 | 8.040466 | 1156.146316 | 761.748083 | 38.001541 | 44.274662 | 0 | 0 | 1194.147857 | 806.022745 |
| 9 | Gray (original) | 2 | 2 | 8.040466 | 1156.157122 | 761.784861 | 38.00152 | 44.274663 | 0 | 0 | 1194.158642 | 806.059524 |

**Figure IV.31**: Data Matching of Ext-2.

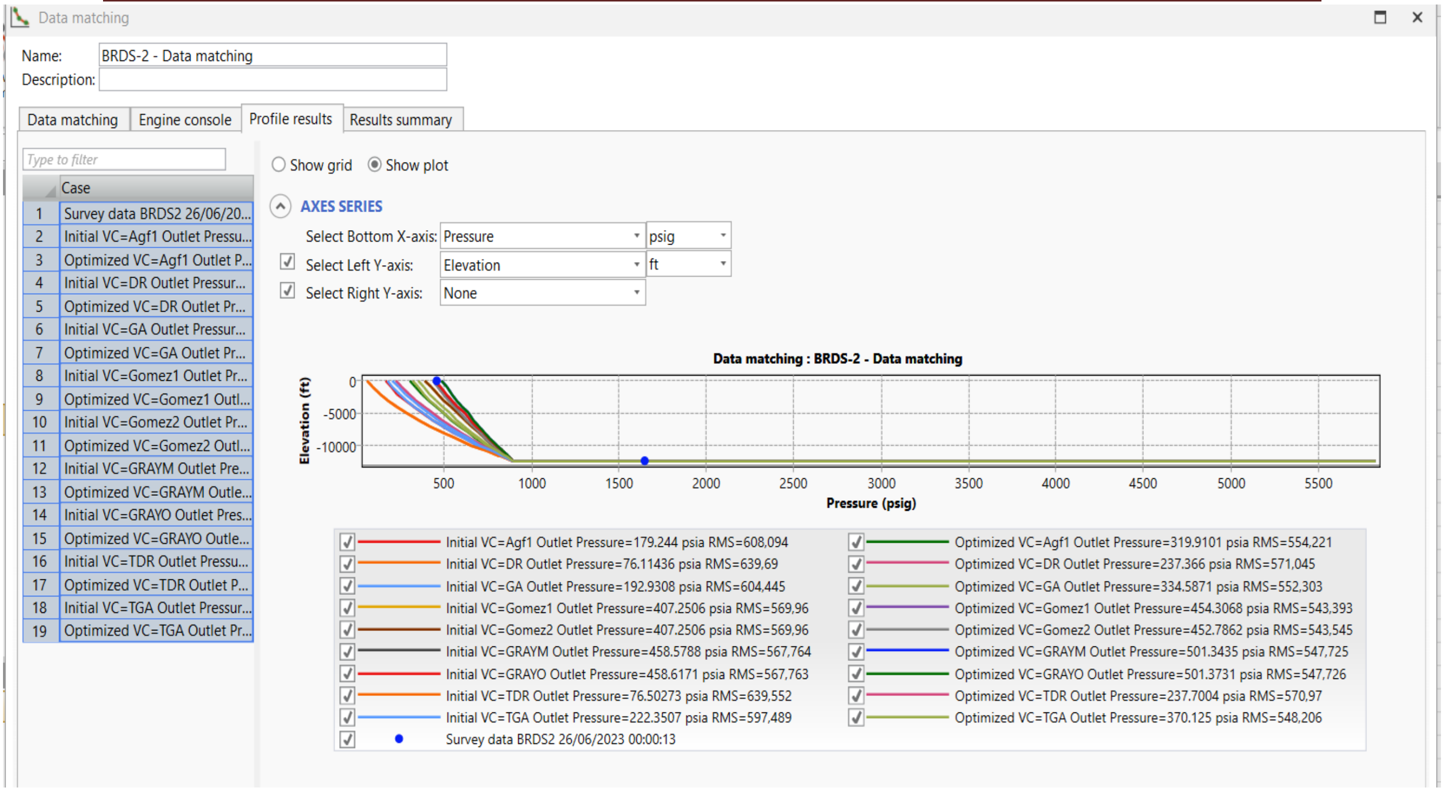


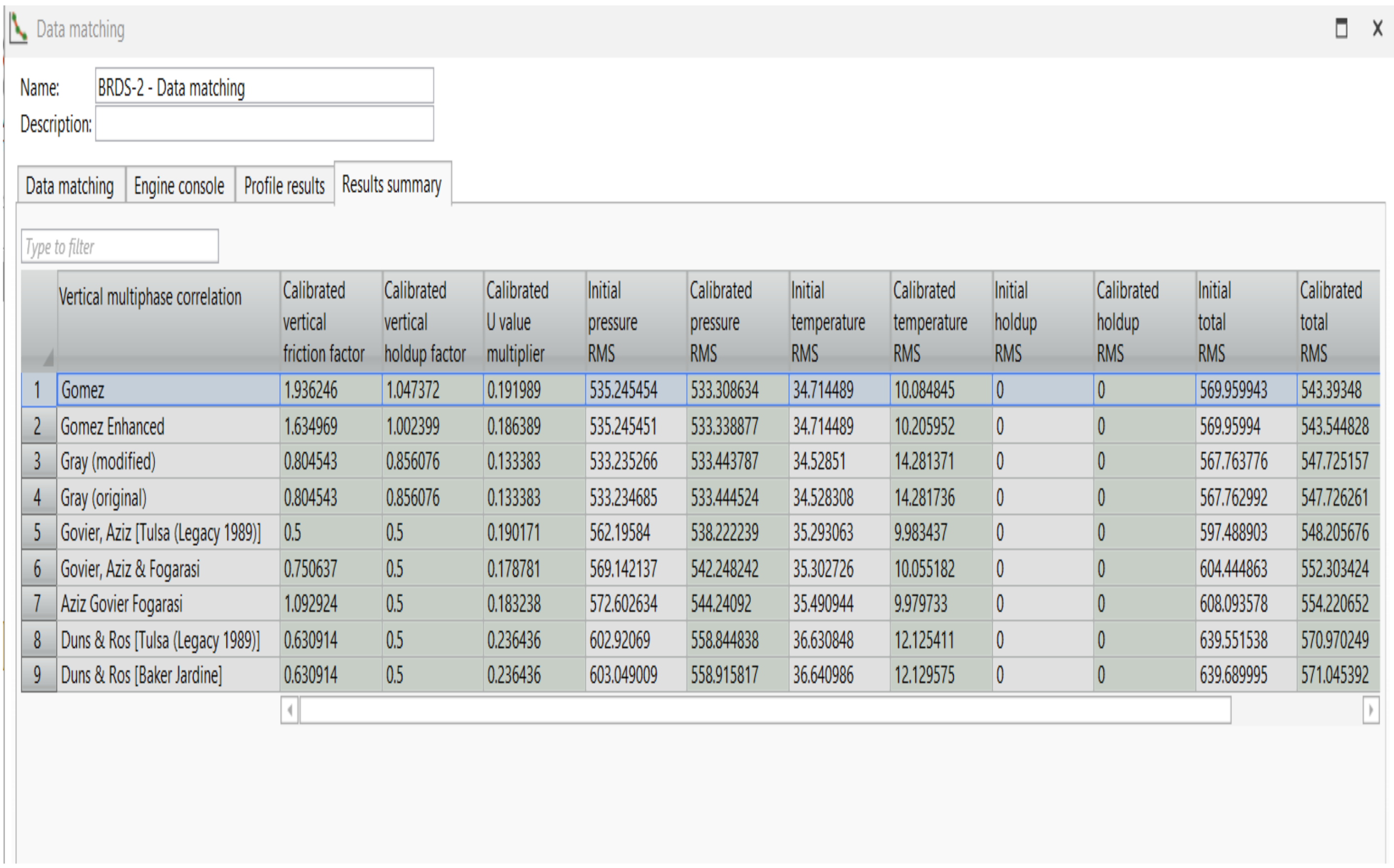


| | Vertical multiphase correlation | Calibrated vertical friction factor | Calibrated vertical holdup factor | Calibrated U value multiplier | Initial pressure RMS | Calibrated pressure RMS | Initial temperature RMS | Calibrated temperature RMS | Initial holdup RMS | Calibrated holdup RMS | Initial total RMS | Calibrated total RMS |
|---|---|---|---|---|---|---|---|---|---|---|---|---|
| 1 | Gomez | 1.936246 | 1.047372 | 0.191989 | 535.245454 | 533.308634 | 34.714489 | 10.084845 | 0 | 0 | 569.959943 | 543.39348 |
| 2 | Gomez Enhanced | 1.634969 | 1.002399 | 0.186389 | 535.245451 | 533.338877 | 34.714489 | 10.205952 | 0 | 0 | 569.95994 | 543.544828 |
| 3 | Gray (modified) | 0.804543 | 0.856076 | 0.133383 | 533.235266 | 533.443787 | 34.52851 | 14.281371 | 0 | 0 | 567.763776 | 547.725157 |
| 4 | Gray (original) | 0.804543 | 0.856076 | 0.133383 | 533.234685 | 533.444524 | 34.528308 | 14.281736 | 0 | 0 | 567.762992 | 547.726261 |
| 5 | Govier, Aziz [Tulsa (Legacy 1989)] | 0.5 | 0.5 | 0.190171 | 562.19584 | 538.222239 | 35.293063 | 9.983437 | 0 | 0 | 597.488903 | 548.205676 |
| 6 | Govier, Aziz & Fogarasi | 0.750637 | 0.5 | 0.178781 | 569.142137 | 542.248242 | 35.302726 | 10.055182 | 0 | 0 | 604.444863 | 552.303424 |
| 7 | Aziz Govier Fogarasi | 1.092924 | 0.5 | 0.183238 | 572.602634 | 544.24092 | 35.490944 | 9.979733 | 0 | 0 | 608.093578 | 554.220652 |
| 8 | Duns & Ros [Tulsa (Legacy 1989)] | 0.630914 | 0.5 | 0.236436 | 602.92069 | 558.844838 | 36.630848 | 12.125411 | 0 | 0 | 639.551538 | 570.970249 |
| 9 | Duns & Ros [Baker Jardine] | 0.630914 | 0.5 | 0.236436 | 603.049009 | 558.915817 | 36.640986 | 12.129575 | 0 | 0 | 639.689995 | 571.045392 |

**Figure IV.32:** Data Matching of BRDS-2.

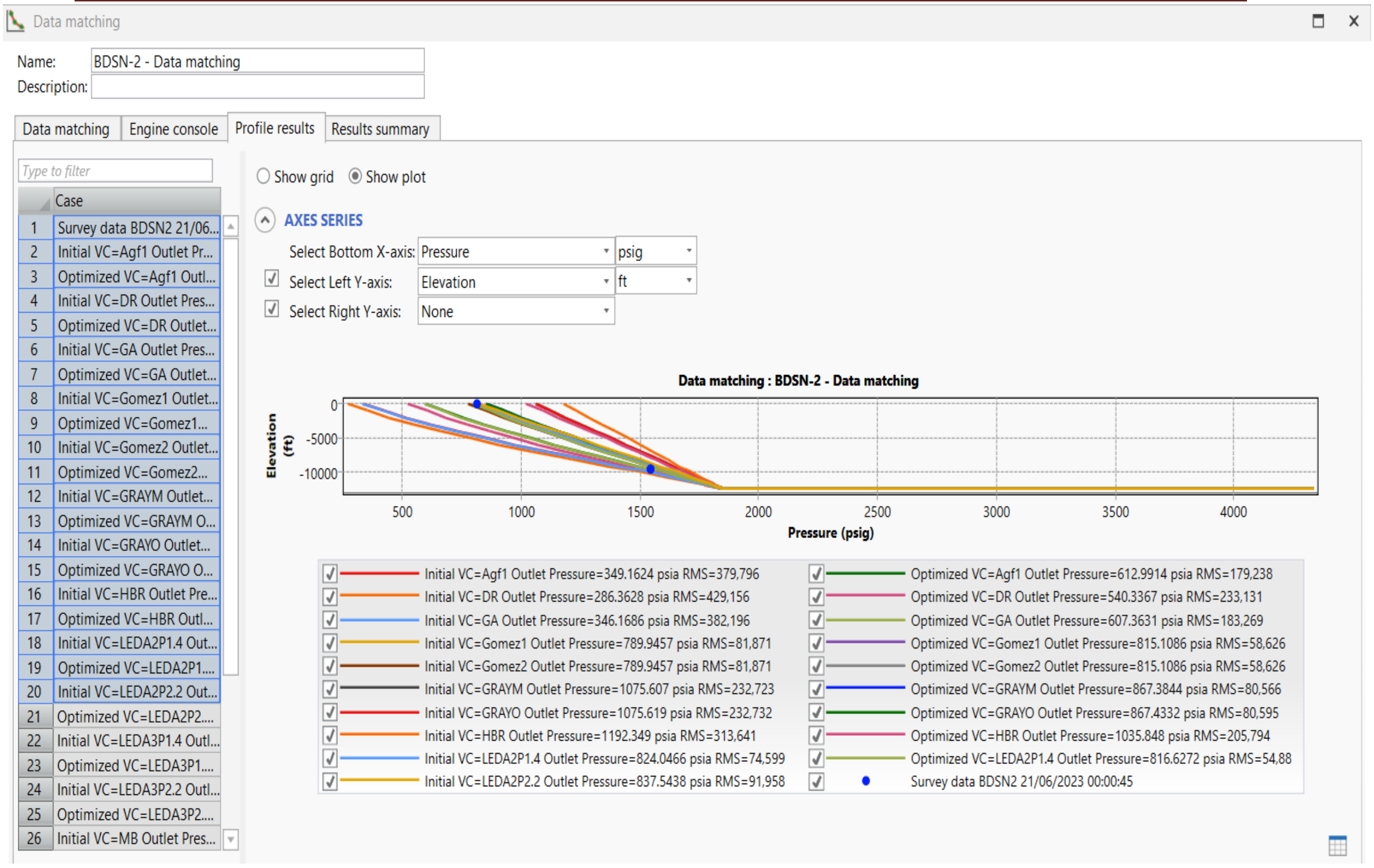


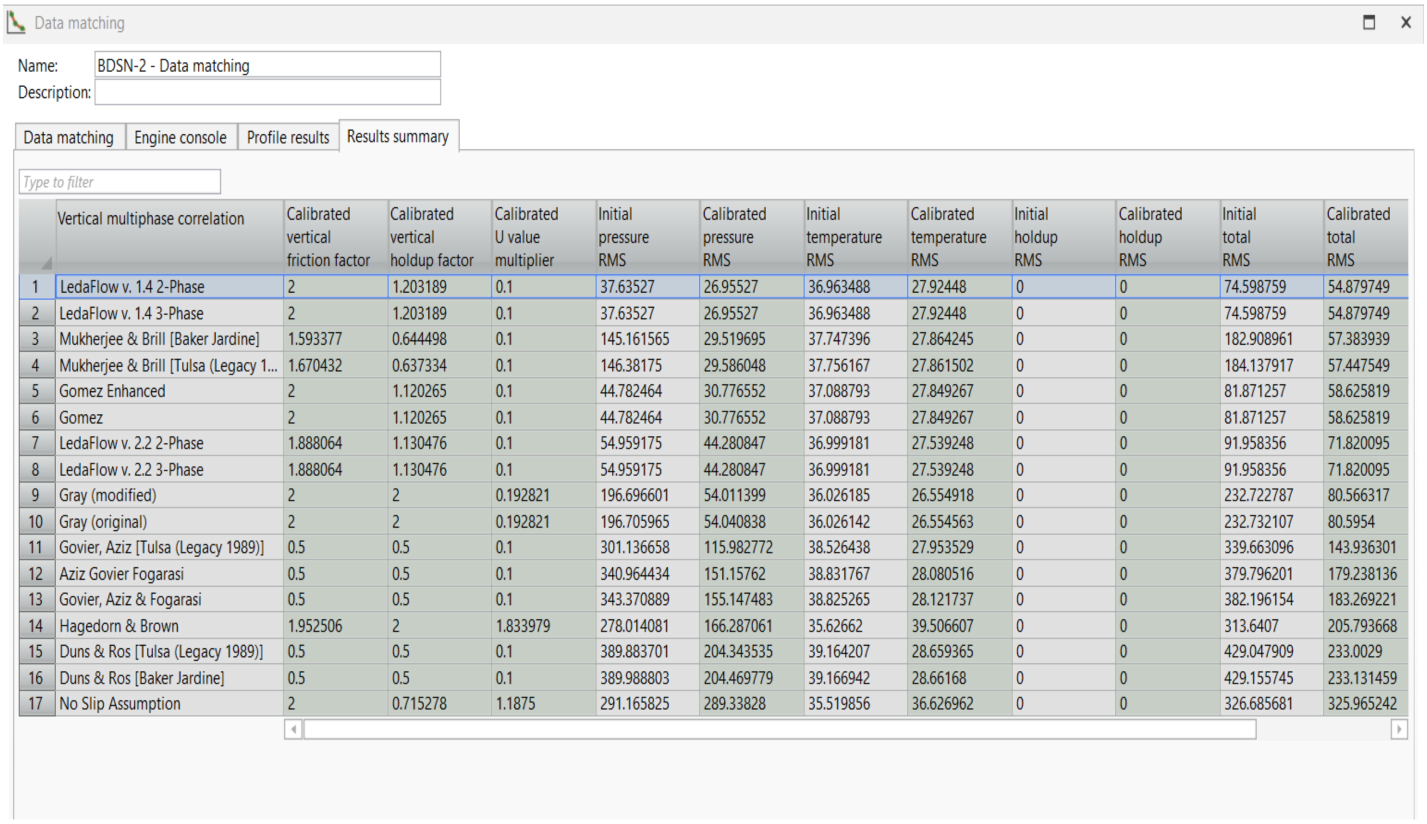


| | Vertical multiphase correlation | Calibrated vertical friction factor | Calibrated vertical holdup factor | Calibrated U value multiplier | Initial pressure RMS | Calibrated pressure RMS | Initial temperature RMS | Calibrated temperature RMS | Initial holdup RMS | Calibrated holdup RMS | Initial total RMS | Calibrated total RMS |
|---|---|---|---|---|---|---|---|---|---|---|---|---|
| 1 | LedaFlow v. 1.4 2-Phase | 2 | 1.203189 | 0.1 | 37.63527 | 26.95527 | 36.963488 | 27.92448 | 0 | 0 | 74.598759 | 54.879749 |
| 2 | LedaFlow v. 1.4 3-Phase | 2 | 1.203189 | 0.1 | 37.63527 | 26.95527 | 36.963488 | 27.92448 | 0 | 0 | 74.598759 | 54.879749 |
| 3 | Mukherjee & Brill [Baker Jardine] | 1.593377 | 0.644498 | 0.1 | 145.161565 | 29.519695 | 37.747396 | 27.864245 | 0 | 0 | 182.908961 | 57.383939 |
| 4 | Mukherjee & Brill [Tulsa (Legacy 1... | 1.670432 | 0.637334 | 0.1 | 146.38175 | 29.586048 | 37.756167 | 27.861502 | 0 | 0 | 184.137917 | 57.447549 |
| 5 | Gomez Enhanced | 2 | 1.120265 | 0.1 | 44.782464 | 30.776552 | 37.088793 | 27.849267 | 0 | 0 | 81.871257 | 58.625819 |
| 6 | Gomez | 2 | 1.120265 | 0.1 | 44.782464 | 30.776552 | 37.088793 | 27.849267 | 0 | 0 | 81.871257 | 58.625819 |
| 7 | LedaFlow v. 2.2 2-Phase | 1.888064 | 1.130476 | 0.1 | 54.959175 | 44.280847 | 36.999181 | 27.539248 | 0 | 0 | 91.958356 | 71.820095 |
| 8 | LedaFlow v. 2.2 3-Phase | 1.888064 | 1.130476 | 0.1 | 54.959175 | 44.280847 | 36.999181 | 27.539248 | 0 | 0 | 91.958356 | 71.820095 |
| 9 | Gray (modified) | 2 | 2 | 0.192821 | 196.696601 | 54.011399 | 36.026185 | 26.554918 | 0 | 0 | 232.722787 | 80.566317 |
| 10 | Gray (original) | 2 | 2 | 0.192821 | 196.705965 | 54.040838 | 36.026142 | 26.554563 | 0 | 0 | 232.732107 | 80.5954 |
| 11 | Govier, Aziz [Tulsa (Legacy 1989)] | 0.5 | 0.5 | 0.1 | 301.136658 | 115.982772 | 38.526438 | 27.953529 | 0 | 0 | 339.663096 | 143.936301 |
| 12 | Aziz Govier Fogarasi | 0.5 | 0.5 | 0.1 | 340.964434 | 151.15762 | 38.831767 | 28.080516 | 0 | 0 | 379.796201 | 179.238136 |
| 13 | Govier, Aziz & Fogarasi | 0.5 | 0.5 | 0.1 | 343.370889 | 155.147483 | 38.825265 | 28.121737 | 0 | 0 | 382.196154 | 183.269221 |
| 14 | Hagedorn & Brown | 1.952506 | 2 | 1.833979 | 278.014081 | 166.287061 | 35.62662 | 39.506607 | 0 | 0 | 313.6407 | 205.793668 |
| 15 | Duns & Ros [Tulsa (Legacy 1989)] | 0.5 | 0.5 | 0.1 | 389.883701 | 204.343535 | 39.164207 | 28.659365 | 0 | 0 | 429.047909 | 233.0029 |
| 16 | Duns & Ros [Baker Jardine] | 0.5 | 0.5 | 0.1 | 389.988803 | 204.469779 | 39.166942 | 28.66168 | 0 | 0 | 429.155745 | 233.131459 |
| 17 | No Slip Assumption | 2 | 0.715278 | 1.1875 | 291.165825 | 289.33828 | 35.519856 | 36.626962 | 0 | 0 | 326.685681 | 325.965242 |

**Figure IV.33:** Data Matching of BDSN-2

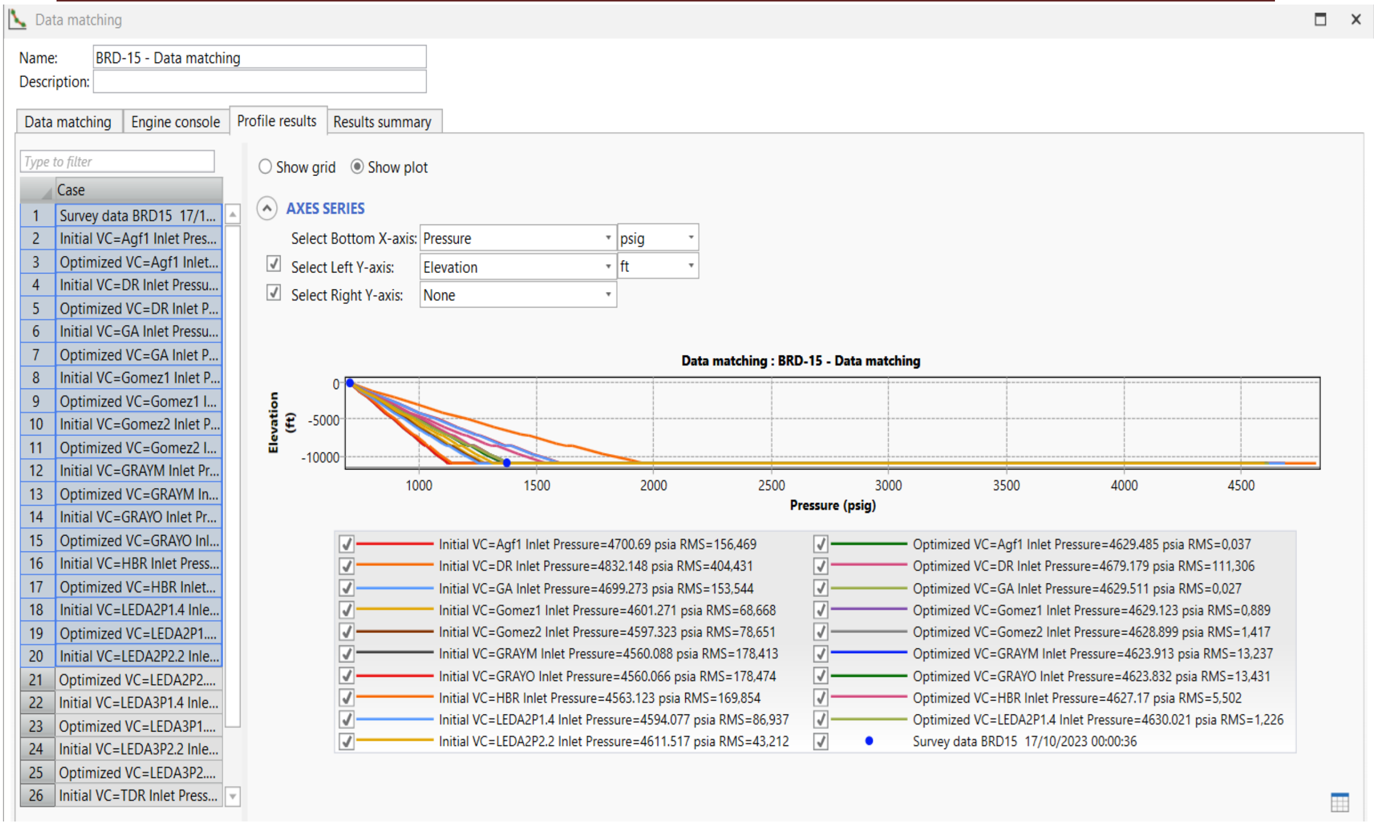


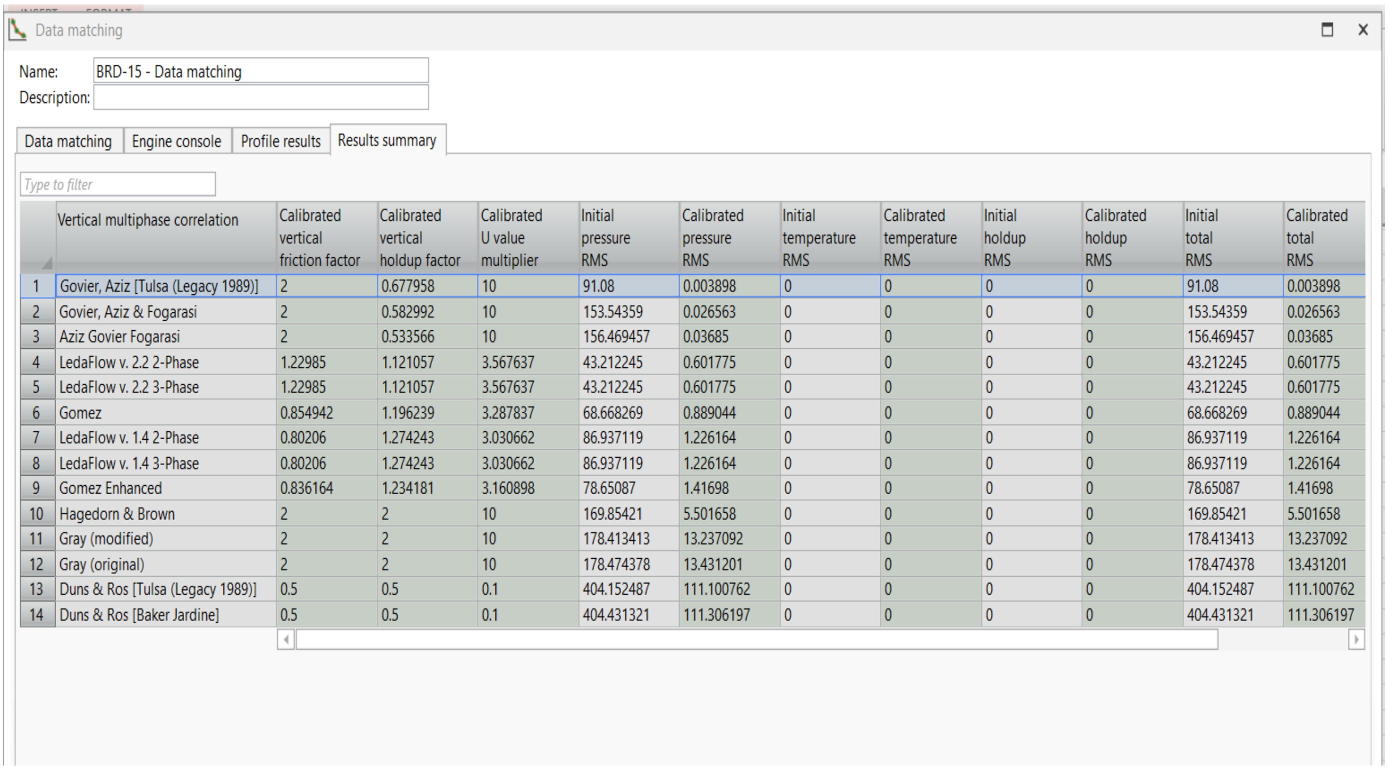

| | Vertical multiphase correlation | Calibrated vertical friction factor | Calibrated vertical holdup factor | Calibrated U value multiplier | Initial pressure RMS | Calibrated pressure RMS | Initial temperature RMS | Calibrated temperature RMS | Initial holdup RMS | Calibrated holdup RMS | Initial total RMS | Calibrated total RMS |
|---|---|---|---|---|---|---|---|---|---|---|---|---|
| 1 | Govier, Aziz [Tulsa (Legacy 1989)] | 2 | 0.677958 | 10 | 91.08 | 0.003898 | 0 | 0 | 0 | 0 | 91.08 | 0.003898 |
| 2 | Govier, Aziz & Fogarasi | 2 | 0.582992 | 10 | 153.54359 | 0.026563 | 0 | 0 | 0 | 0 | 153.54359 | 0.026563 |
| 3 | Aziz Govier Fogarasi | 2 | 0.533566 | 10 | 156.469457 | 0.03685 | 0 | 0 | 0 | 0 | 156.469457 | 0.03685 |
| 4 | LedaFlow v. 2.2 2-Phase | 1.22985 | 1.121057 | 3.567637 | 43.212245 | 0.601775 | 0 | 0 | 0 | 0 | 43.212245 | 0.601775 |
| 5 | LedaFlow v. 2.2 3-Phase | 1.22985 | 1.121057 | 3.567637 | 43.212245 | 0.601775 | 0 | 0 | 0 | 0 | 43.212245 | 0.601775 |
| 6 | Gomez | 0.854942 | 1.196239 | 3.287837 | 68.668269 | 0.889044 | 0 | 0 | 0 | 0 | 68.668269 | 0.889044 |
| 7 | LedaFlow v. 1.4 2-Phase | 0.80206 | 1.274243 | 3.030662 | 86.937119 | 1.226164 | 0 | 0 | 0 | 0 | 86.937119 | 1.226164 |
| 8 | LedaFlow v. 1.4 3-Phase | 0.80206 | 1.274243 | 3.030662 | 86.937119 | 1.226164 | 0 | 0 | 0 | 0 | 86.937119 | 1.226164 |
| 9 | Gomez Enhanced | 0.836164 | 1.234181 | 3.160898 | 78.65087 | 1.41698 | 0 | 0 | 0 | 0 | 78.65087 | 1.41698 |
| 10 | Hagedorn & Brown | 2 | 2 | 10 | 169.85421 | 5.501658 | 0 | 0 | 0 | 0 | 169.85421 | 5.501658 |
| 11 | Gray (modified) | 2 | 2 | 10 | 178.413413 | 13.237092 | 0 | 0 | 0 | 0 | 178.413413 | 13.237092 |
| 12 | Gray (original) | 2 | 2 | 10 | 178.474378 | 13.431201 | 0 | 0 | 0 | 0 | 178.474378 | 13.431201 |
| 13 | Duns & Ros [Tulsa (Legacy 1989)] | 0.5 | 0.5 | 0.1 | 404.152487 | 111.100762 | 0 | 0 | 0 | 0 | 404.152487 | 111.100762 |
| 14 | Duns & Ros [Baker Jardine] | 0.5 | 0.5 | 0.1 | 404.431321 | 111.306197 | 0 | 0 | 0 | 0 | 404.431321 | 111.306197 |

**Figure IV.34:** Data Matching of BRD-15

### IV.2.6 Simulation Results

The results presented here in summarize the outcomes of PIPESIM simulations conducted for the project, specifically focusing on the performance of the employed Booster and the resulting flowrates and pressure characteristics for the designated candidate wells.

**Table IV.6:** Results of PIPESIM simulation.

| Name | Pressure(out) | Temperature °C | ST oil rate | ST Water rate | ST gas rate | ST gas GOR | ST Water CUT |
|---|---|---|---|---|---|---|---|
| | Psig | | SM3/d | SM3/d | SM3/d | SM3/SM3 | % |
| BDSN-1 | 112,8601 | 87,58207 | 42,23273 | 0 | 96777,74 | 2291,534 | 0 |
| BDSN-2 | 96,52816 | 84,53686 | 17,05269 | 0 | 44112,52 | 2586,836 | 0 |
| BRD12 | 86,96652 | 86,40932 | 4,432331 | 0 | 13720,32 | 3095,51 | 0 |
| BRD-15 | 102,7197 | 80,83314 | 18,81405 | 0 | 58239,08 | 3095,51 | 0 |
| BRDS-1 | 171,2682 | 122,4592 | 118,7227 | 0 | 164483,9 | 1385,446 | 0 |
| BRDS-2 | 94,45031 | 103,2312 | 26,27636 | 0 | 36404,49 | 1385,446 | 0 |
| BRDS-EXT2 | 124,8975 | 118,0181 | 73,46516 | 0 | 156702,5 | 2133,018 | 0 |

To evaluate the effectiveness of our proposed methodology (Boosting Method), we conducted a comparative analysis of the simulation results obtained from PIPESIM with the actual data from previous well tests. The comparison is presented in the form of graphs, allowing for a clear visualization of the performance and accuracy of our approach.

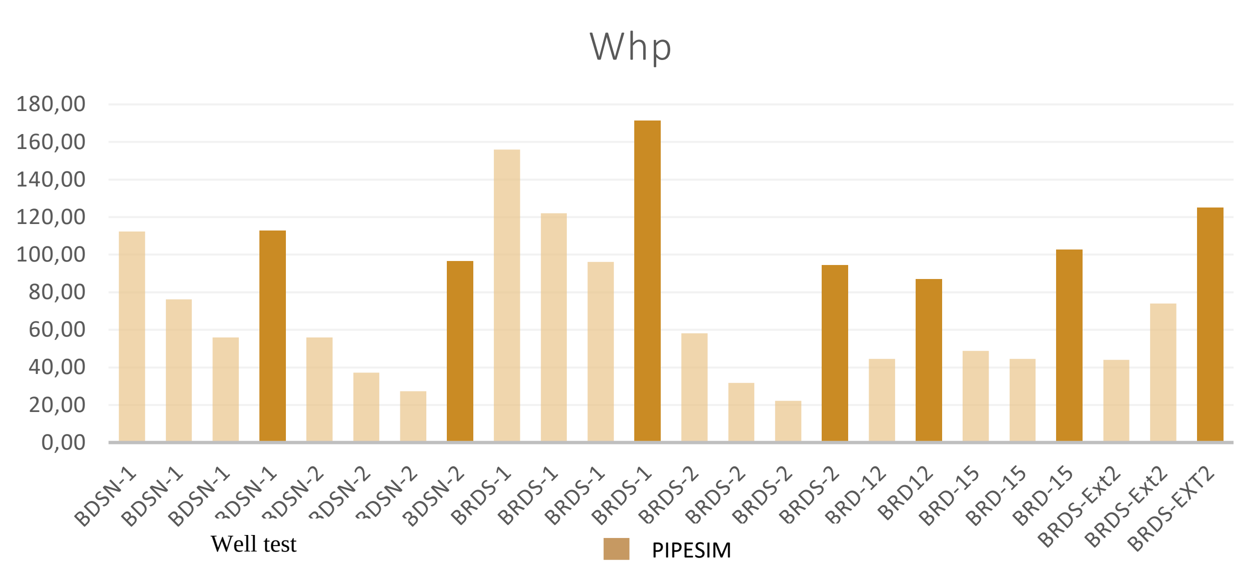


**Figure IV.35:** Well-test data VS PIPESIME simulation results of Whp.

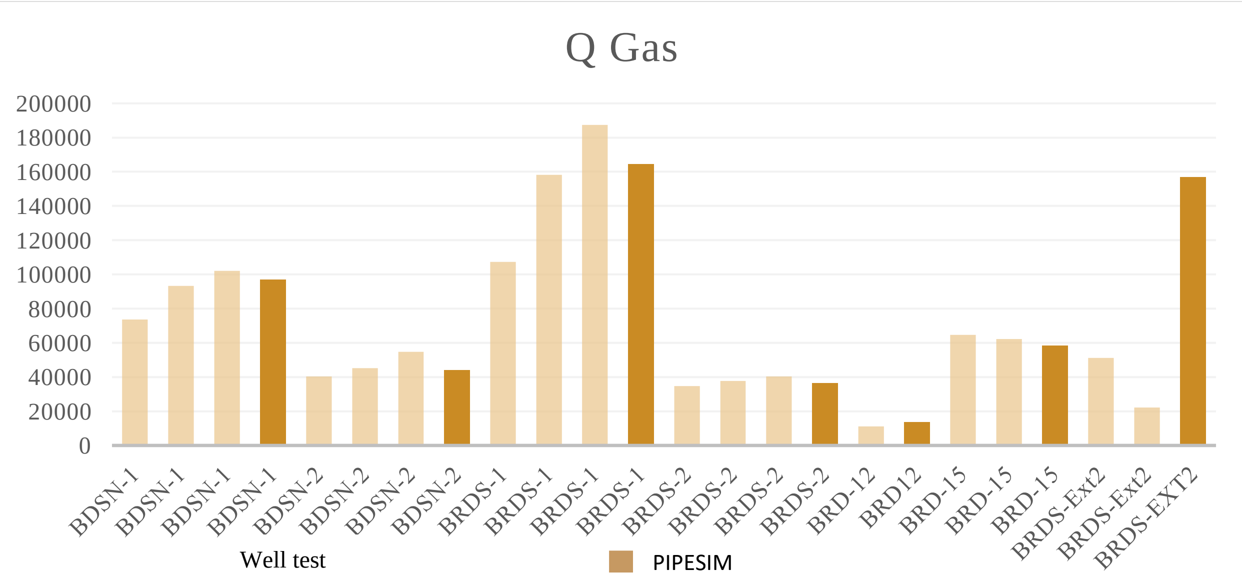


**Figure IV.36:** Well-test data VS PIPESIME simulation results of Qg.

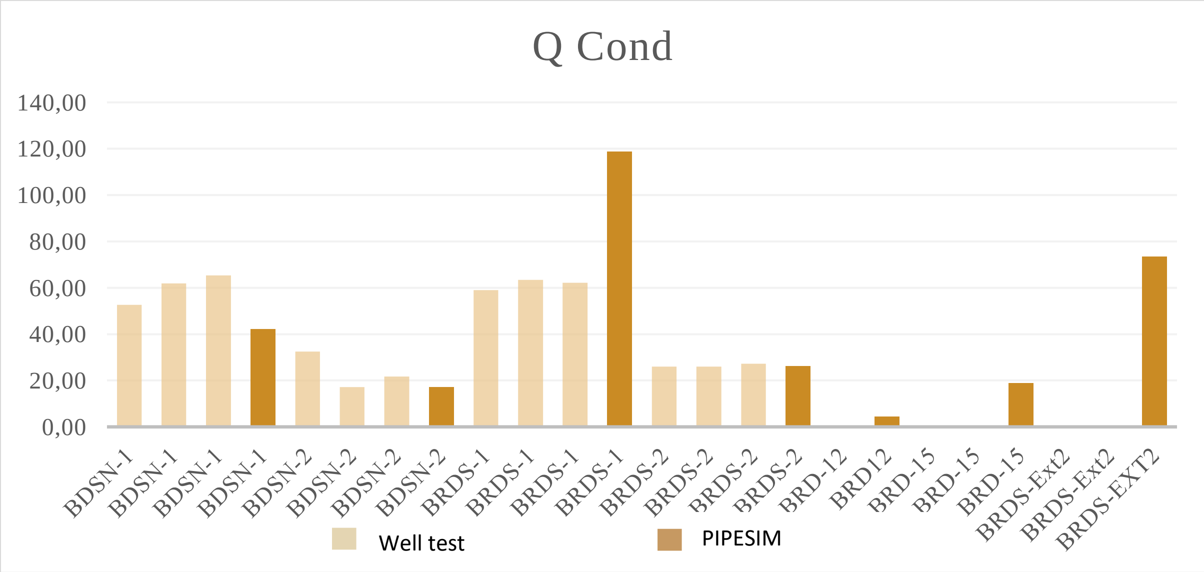


**Figure IV.37:** Well-test data VS PIPESIME simulation results of Qcond.

The simulation results validate the Booster suitability for the project and confirm its ability to deliver the required flow rates to the candidate wells. The flow and pressure analysis provides a comprehensive understanding of the fluid dynamics within the pipeline network, ensuring safe and efficient operation.

## IV.3 The Economic Study

It is essential to conduct an economic evaluation of any operation to justify its implementation on wells. This involves calculating the total cost of this particular operation on the one hand, and on the other hand, calculating the possible daily gain of the production expected from the wells. This will enable us to determine the amount of time necessary to recover our investment and begin generating profits from the project.

### IV.3.1 Estimation of the costs associated with the booster unit

In order to calculate the total costs associated with installing the Booster unit, it is necessary to know:

- The daily rental price of the Booster unit: is 13000 to 14000 USD $
- The duration for which the unit needs to be installed (NPT): it takes approximately 20 days to set up and install the boosting unit which during the wells well not produce.

**NB:**

- The booster daily rental cost includes the setup cost of the booster unit and all its related expenses (labour, equipment, etc.).
- We chose the maximum cost possible of the booster (which amounts to 14000 USD$), to represent the daily rental expenses of the booster in our study. In order to account for the highest potential financial losses in this project.

### IV.3.2 The expected average daily production and income

Based on our simulation using the PIPESIM software we were able to estimate the expected average daily production rate of our candidate wells after using a boosting unit, as highlighted in the table below. This data allows us to estimate the probable daily income of this project:

**Table IV.7:** Expected average daily production for rate natural gas, condensate and GPL.

| **Products** | | **Natural Gaz** | **Condensate** | **GPL** | **Total daily income** |
|---|---|---|---|---|---|
| **Daily rates** | | **mmBtu** | **TM** | **TM** | |
| | | 21307,6247 | 102,761982 | 53,0936907 | |
| **Daily income** | **USD$** | 271106,4972 | 54533,2148 | 21502,94473 | 347 142,66 |
| | **DZD** | 36431291,1 | 7328173,405 | 2889565,713 | 46 649 030,22 |

**NB:**

The data in our calculations is based on the average base price of natural gas, condensate and GPL in May 2024.

**Table IV.8:** The base price of natural gas, condensate and GPL in May 2024

| Products | Natural Gaz | Condensate | GPL |
|---|---|---|---|
| Unit | USD $/mmBtu | USD $/TM | USD $/TM |
| Base price | 12,72345 | 530,675 | 405 |

1Sm3 =0.04 mmBtu

1USD= 134,38 DZD (As of 25/05/2024)

### IV.3.3 The Net Gain of the Boosting Project

The total net gain of the project is equal to the expected production rate in a day minus the daily rental cost of the booster multiplied by the number of operating days minus the total lost during the installation period. We can formulate it as such in equation IV.1:

$$\textbf{Total net gain} = \left(\text{Total daily production income} - \text{daily rental for boosting unit}\right) \times \text{Number of operating days} - \text{Total lost costs during the installation of the booster} \quad \textbf{(IV.1)}$$

Where:

$$\textbf{Total lost costs during the installation of the booster} = \text{NPT} \times \left(\text{Daily rental cost} + \text{Total daily production income}\right) = 7222853{,}2\ \text{USD\$} \quad \textbf{(IV.2)}$$

As we can see all the elements in formula **IV.1** are known aside from the number of operating days, which we need to determine in order to estimate the point at which we will cover our investment and begin to make a profit from this project. Our goal is to reach where the total production income is higher than boosting unit expenses.

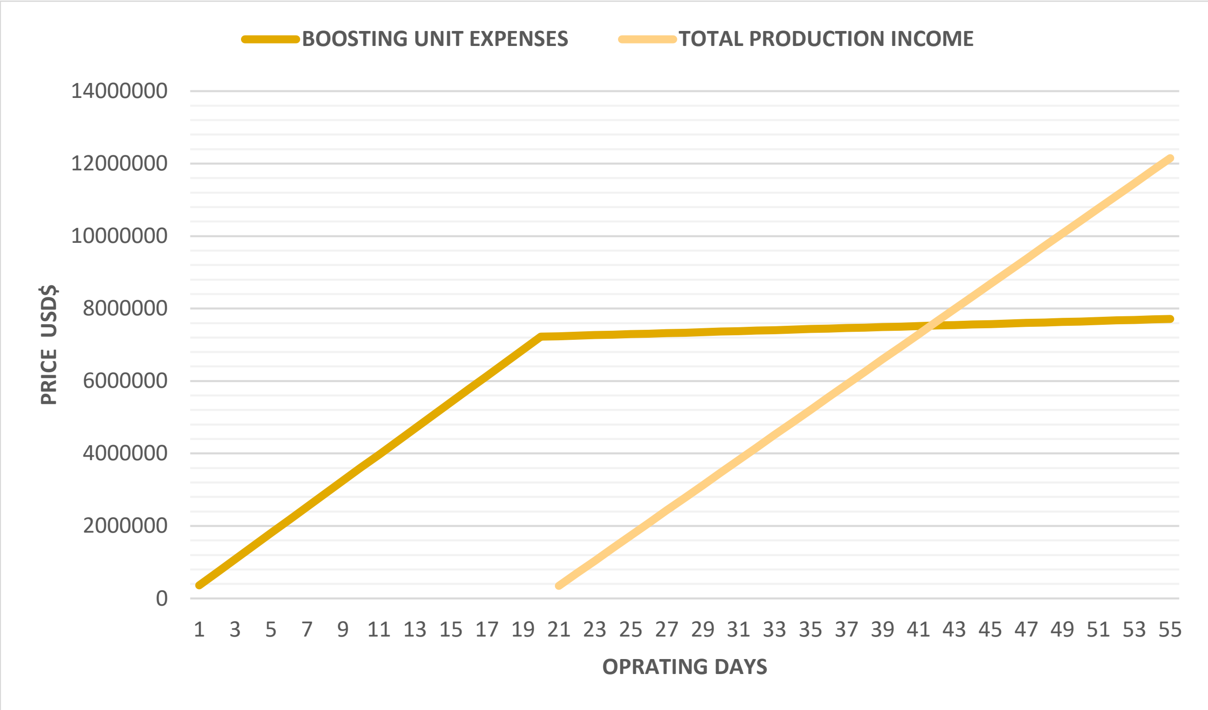


**Figure IV.38:** Boosting unit expenses vs. total production income curve.

Even though we still have a system rental cost, the daily profitability will eventually cover it. As it is shown in Figure IV.38 the investment will be paid off relatively quickly. According to our calculations, after approximately 22 days of production, we begin to make a profit. Therefore, it's clear that the booster project has the potential to be profitable long term.

# Conclusion

# Conclusion

While a definitive assessment of the booster unit's efficiency for the seven candidate wells (BRDS-1, BRDS-2, BDSN-1, BDSN-2, BRD-12, BRD-15, BRDS-Ext2) requires further analysis, the technology presents a compelling case for boosting production rates.

Our research demonstrates a significant increase in gas and, particularly, condensate flow rates. Notably, the use of a booster unit eliminates the wells' distance as a production obstacle. We were able to achieved an average flow rate of 568474.9 Sm3/day, demonstrating the booster's effectiveness.

Furthermore, our economic evaluation indicates a remarkably short payback period. Within approximately 21 days, following this period, production profits will significantly exceed the initial investment.

This translates to a highly cost-effective solution that overcomes distance limitations and boosts overall production efficiency.

Additionally, the unit optimizes flow conditions, minimizing energy consumption and potentially extending the reservoir's productive life. This translates to long-term cost savings and a sustained revenue stream.

However, the most significant economic benefit likely arises during a critical period of reservoir pressure decline. Here, the booster unit acts as a countermeasure, preventing production decline and ensuring economically viable well performance – a crucial factor for maintaining profitability.

Ultimately, a cost-effectiveness analysis alongside a detailed reservoir engineering study will determine the optimal timing for implementing the booster unit. However, our research results strongly suggest that this technology can be an effective method that maximize production efficiency, extends wells life, and ultimately boosts their bottom line.

# Recommendations

To ensure a more accurate study and realisation of this project, we would like to add some suggestions:

- We propose using Machine Learning to provide better evaluations of the results obtained based on the modeling of PIPESIM and MBAL Software.
- We suggest the possibility of creating a new LP manifold that connects the candidates wells to the LP inlet of the processing facility (CPF).
- For the well BRD-1, we recommend using another boosting unit to increase its pressure.
- Another potential solution for BRD-1 is to create a new pipeline that connects it to the HP BRD-MF01 to boost it with the other wells.
- Boosting methods offer a temporary solution to the current reservoir pressure decline. Therefore, it's crucial to consider and potentially use other production optimization methods that often involve direct intervention at the reservoir level.

# References


**[1]** YEBBOU, K. (2017) *CHARACTERIZATION OF THE UPPER TRIAS CLAY-SANDSTONE RESERVOIR (TAGS) OF THE BRIDES FIELD GASSI TOUIL REGION*. Professional end-of-training project to obtain an engineer diploma specializing in petroleum geology.

**[2]** Bouchair, A. and Zaimen, K. (2017) *Geological context and Estimated reserves of the TAGI deposit in the Toual field - Gassi Touil*. Thesis. Université Mohammed Seddik Benyahia -Jijel.

**[3]** CHAMM, Mlle.Z. (2016) *Geological and Petrophysical Assessment of the Silurian Clayey Sandstone Reservoir Unit F6-M2 of the Gassi Taouil Oil Field in the Berkin Basin*. National Polytechnic School.

**[4]** KICHE, M. and HADRI, A. (2021) *SEDIMENTOLOGICAL STUDY AND THE PETROPHYSICAL ASPECT OF THE F6 (SAG) RESERVOIRS OF THE TOUAL GASSI TOUIL FIELD*. Université Mouloud Mammeri de Tizi-Ouzou.

**[5]** DAHEM, M.E., ALKOSHAB, A. and DOUAIR, Z. (2018) *Development & study of connection of wells in the Gassi -Touil region*. Master degree thesis. Kasdi Merbah.

**[6]** SONATRACH (2016) *Implementation report for the Brides Nord-2 (BDSN-2) borehole (March 2016) Exploration production activity Exploration division Assets direction East-Berkine west department - Gassi Touil project*. Sonatrach.

**[7]** Ahmed, T. and Meehan, D.N. (no date) *Advanced Reservoir Management and Engineering*. Second Edition.

**[8]** PennState (no date) *Drive Mechanisms in Gas Reservoirs, PennState, College of earth and Mineral Science*. Available at: https://www.e-education.psu.edu/png301/node/624 (Accessed: 29 May 2024).

**[9]** M. Rafiqul, I. (2022) *Reservoir Development*.

**[10]** SONATRACH ‘documents’.

**[11]** SONATRACH *Wells technical sheets*. Technical sheets.

**[12]** SONATRACH ‘Well test data’.

**[13]** Boyce and Maurice (2006) *Centrifugal Compressors: Selection and Application Guide for Engineers and Procurment Specialists*. Gulf Professional Publishing.

**[14]** Heise and Lorenz (1996) ‘Screw Compressors: Theory, Selection and Application’. Springer.

**[15]** EXPRO (2023) ‘Expro Production Enhancement, On Demand Compression – JV Gas’, 2 March.

**[16]** Lichtenstein and Klaus (2004) *Centrifugal Compressors for Process Industries: A Tutorial*. Elsevier.

**[17]** Bloch, Heinz P and Alan R, B. (2015) *A Practical Guide to Compressor Technology*. Elsevier.

**[18]** PETEX ‘MBAL ANALYTICAL RESERVOIR ENGINEERING TOOLKIT PETROLEUM ENGINEERING SOFTWARE’.

**[19]** Bhadariya, V. and Sapale, P. (2019) ‘Reservoir Performance Prediction using Integrated Production Modelling’, *International Journal of Recent Technology and Engineering (IJRTE)*, 1 November. Available at: https://www.researchgate.net/publication/337465384_Reservoir_Performance_Prediction_using_Integrated_Production_Modelling (Accessed: 29 May 2024).

**[20]** ‘RESERVOIR SIMULATION USING MBAL (A CASE STUDY OF RZD FIELD)’.

**[21]** SCHLUMBERGER *Pipesim New Features, SCHLUMBERGER*. Available at: https://www.software.slb.com/products/pipesim/features (Accessed: 2 June 2024).

**[22]** SCHLUMBERGER *Pipesim steady-state Multiphase flow simulator, SCHLUMBERGER*. Available at: https://www.software.slb.com/products/pipesim (Accessed: 2 June 2024).

# Annex

| BDSN-2 | FICHE TECHNIQUE | COORDONEES UTM | X= 309 835,5 m |
|---|---|---|---|
| | | | Y= 3 389 551,62 m |
| | RESERVOIR TAGS | COUPE TECHNIQUE | Zsol = 199,33 m |
| | | | Ztab = 210 m |

## EQUIPEMENTS DE SURFACE

| DESIGNATION | | TYPE & DIMENSIONS |
|---|---|---|
| PLAQUE DE BASE | | 20" 3K |
| CASING SPOOL | | 20" 3K x 13"5/8 5K |
| TUBING HEAD | | 13"5/8 5K x 11" - 5K |
| ADAPTEUR | | 11" 5K x 4"1/16 - 5K |
| Lower Master Valve | | 4"1/16 - 5K CAMERON |
| Upper Master Valve (Hydraulic) | | 4"1/16 - 5K STREAM FLO |
| Arbre de noel | Cross | 4"1/16 - 5K CAMERON |
| | Wing valve | 4"1/16 - 5K STREAM FLO |
| | Lateral Valve | 4"1/16 - 5K CAMERON |
| | Swab valve | 4"1/16 - 5K CAMERON |
| | Top cap | 4"1/16 - 5K CAMERON |

## EQUIPEMENTS DE FOND

| N | DESIGNATION | LONG | TOP |
|---|---|---|---|
| 1 | Tubing hanger WP 4 ½ N.VAM 13.15# | 0,485 | 0,00 |
| 2 | Pup Joint | 1,244 | 0,49 |
| 3 | 2 Tubing 4.5" 15.1#13Cr V.Top | 23,701 | 1,73 |
| 4 | Pup Joint 4.5" 15.1#13Cr | 0,900 | 25,43 |
| 5 | Flow coupling 4"1/2 | 1,785 | 26,33 |
| **6** | **TRSSV 4"½ 15.10 # VAM TOP PIN 3.688"** | **1,365** | **28,12** |
| 7 | Flow coupling 4'' ½ 15.10 # VAM TOP | 1,795 | 29,48 |
| 8 | 243 Tubing 4.5" 15.1#13Cr V.Top | 2873,136 | 31,28 |
| 9 | **Halliburton 3.688" R nipple** | 0,375 | 2904,41 |
| **10** | Tubing 4.5" 15.1#13Cr V.Top | **11,852** | **2904,79** |
| 11 | Pup Jt 4.5" 15.1#13Cr | 0,980 | 2916,64 |
| 12 | Ratch Latch 4'' ½ 13.50 # VAM TOP | 0,590 | 2917,62 |
| 13 | **7" MHR Packer OD= 5.875" ID =3.875"** | **1,815** | 2918,21 |
| **14** | Mill Out Extension 5" 18.00# NEW VAM | 1,585 | **2920,02** |
| 15 | Reducing adapter | 0,304 | 2921,61 |
| 16 | Flow coupling 4'' ½ 15.10 # VAM TOP | 1,795 | 2921,91 |
| 17 | **Otis RN nipple 4''½ 15.10# VAMTOP Box X Pin 3.688 X 3.456 NO GO** | 0,425 | 2923,71 |
| 18 | Perforated pup joint 4'' ½ 15.10 # VAM TOP | 3,020 | **2924,13** |
| 19 | Mule Guide Shoe 4'' ½ 15.10 # VAM TOP | 0,305 | 2927,15 |
| 20 | End of complétion | | 2927,46 |

## OBSERVATIONS

**Appareil :** WDI 814

**Forage :** du 21/03/2016 au 26/07/2016

**Completion :** 26/07/2016

| Date | Diam | Dens | Type | Pénét | Top (m) | Bottom (m) | Réservoir |
|---|---|---|---|---|---|---|---|
| | | | | | 3736 | 3742,5 | |
| | | | | | 3747,5 | 3756 | TAGS |
| | | | | | 3757,5 | 3759 | |

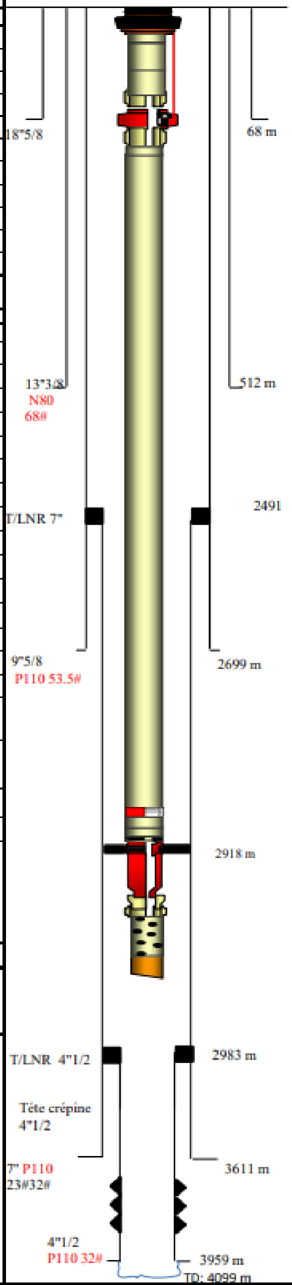


Mise à jour le 29/11/2019 par Sce Tpuits

| BRD 15 | FICHE TECHNIQUE | COORDONEES UTM | X= 310490.01<br>Y= 3 381830.15 |
|---|---|---|---|
| | RESERVOIR TAGS | COUPE TECHNIQUE | Haut TR_Sol = 7,68 m |

## EQUIPEMENT DE SURFACE

| DESIGNATION | TYPE & DIMMENSION |
|---|---|
| **P/Base FMC casing head housting** | 20" 3K x 13"5/8 CHH 5K |
| **Tubing Head Cameron** | 13"5/8 x 11"-5K |
| **Adapter Cameron** | 11"-5K x 4"1/16-5K |
| **ARBRE NOEL** | 4"1/16-5K |
| **VANNE HYDRAULIQUE** | 2 Vannes 4"1/16-5K: 2VM+VL |

## EQUIPEMETS DE FOND

| N | DESIGNATION | LONG | TOP |
|---|---|---|---|
| 1 | Tbg hanger 11″ NOM. H BPV, 3"900 MIN Bore, L Tle=0.67 (olive filetée 4"1/2NVAM (F)x4"1/2 N-Vam (F)15.10# BTM | 0,481 | 0,000 |
| 2 | Réd 4"1/2NVam MxVamTop M 13.50# 13%cr M80,ID=3.920 | 1,228 | 0,481 |
| 3 | 01 Tbg 4"1/2 vam top 13.50 # 13% cr VM 80 | 26,617 | 1,709 |
| 5 | Pup joint 4"1/2 vam top 13.50 # 13% cr VM80 | 0,888 | 28,326 |
| 6 | Pup joint 4"1/2 vam top 13.50 # 13% cr VM80 | 0,894 | 29,214 |
| 7 | Flow coupling 13% Cr C 95 -4"500- 13.50 # VAM TOP FXM | 1,796 | 30,108 |
| 8 | **TRSSV 4″1/2 Vam Top 13.50# -7500 psi avec siège intégré 3"688** | **1,366** | **31,904** |
| 9 | Flow coupling 13% Cr C 95 -4"500- 13.50 # VAM TOP FXM | 1,757 | 33,270 |
| 10 | 202 Tubing 4"1/2 vam top 13.50 # 13% cr -N80- ID=3"920 | 2554,626 | 35,027 |
| 11 | Pup joint 4"1/2 vam top 13.50 # -13% cr- VM 80 | 1,423 | 2589,653 |
| 12 | **Siége R 3"688 L_ Nipple 4″1/2 - 13.50#VAMTOP FXM** | **0,378** | **2591,076** |
| 13 | Pup joint 4"1/2 vam top 13.50 # 13% cr VM 80 | 1,476 | 2591,454 |
| 14 | 1 tbg 4"1/2 vam top 13.50 # 13% cr N 80 | 12,645 | 2592,930 |
| 15 | Pup joint 4"1/2 vam top 13.50 # 13% cr VM 80 | 1,420 | 2605,575 |
| 16 | Ratch latch 4"1/2 OD -13.50# VAM TOP model seals 13% cr | 0,593 | 2606,995 |
| 17 | **Packer MHR 7"23-32# max, OD 5"875, ID 3.875 ( L=1.82M) Bas Packer 1.02M - Haut packer 0.80M** | **1,815** | **2607,588** |
| 18 | Millout extention 5"18# N VAM M x M | 1,665 | 2609,403 |
| 19 | Réd 5" 18# N VAM x 4 1/2" VAM TOP 13.50# F x M | 0,305 | 2611,068 |
| 20 | Flow Cp 4.5" Vam Top B.P 15.10 #13Cr | 1,795 | 2611,373 |
| 21 | **Siége type RN 4″ 1/2 N VAM 13.5 # 13% Cr ID= 3.688 NO GO 3.456 F x M** | **0,426** | **2613,168** |
| 22 | Tube perforé 4"1/2 VAM TOP 13.5# 13% Cr VM 80 | 3,020 | 2613,594 |
| 23 | Mule Shoe Guide 4″.96 VAM TOP 13.5# VM 13% Cr ID:4″ | 0,305 | 2616,614 |

## PERFORATIONS

| DATE | PHASI | TIR | TYPE | PEN | EHD | TOP | BTM |
|---|---|---|---|---|---|---|---|
| 27/07/2012 | 60° | 6SPF | 2"7/8 Power Jet Omega | 36" | 0,34" | 3327<br>3354 | 3331<br>3357 |

## CASING

| Hole Size | 26" | 16" | 12"1/4 | 8"1/2 | 5"7/8 |
|---|---|---|---|---|---|
| Casing Size | 18"5/8 | 13"3/8 | 9"5/8 | 7" | 4"1/2 |
| Casing Con | BTC | BTC | N VAM | N VAM | N VAM |

**OBSERVATIONS :**

Puits foré par ENAFOR 06 : Haut TR- = 7.68 M
Début de forage le : 24/04/2012, Fin de forage le : 21/06/2012
Puits sous saumure densité 1.30
Espace annulaire 18"5/8 x 13"3/8 cimenté au jour
Espace annulaire 13"3/8 x 9"5/8 sous boue à l'huile d: 1.05
Espace annulaire 9"5/8 x 4"1/2 sous saumure d: 1.30
**String Elongation 1,18 m, String compréssion 5T soit -0,53 m**

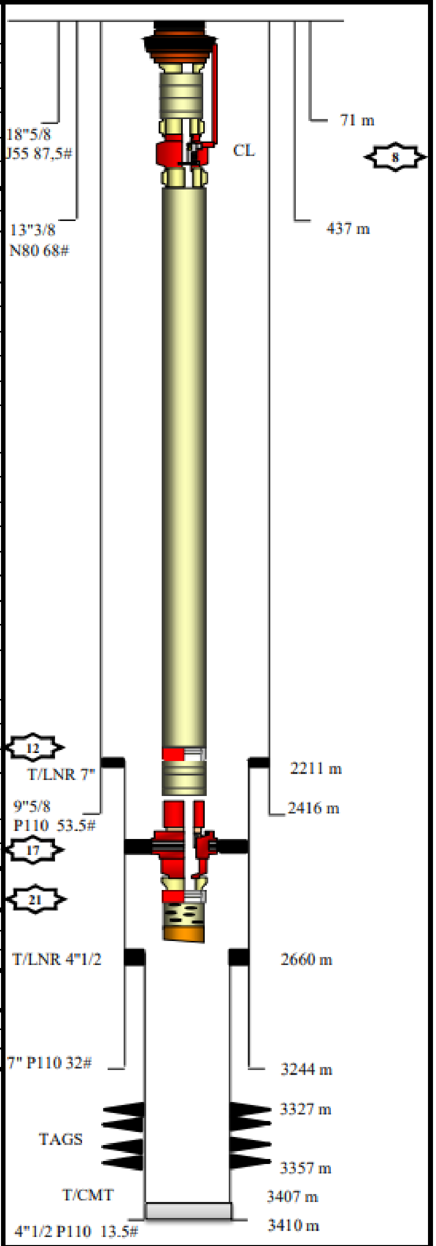


**Mise à jour par Sce tech Puits le 19/03/14**

| BRDS-1 | FICHE TECHNIQUE | COORDONEES UTM | X= 309 735.91<br>Y= 3 369 439.64 |
|---|---|---|---|
| | RESERVOIR SILURIEN B2 | COUPE TECHNIQUE | Zsol = 209 m<br>Ztab = 219.95 m |

## EQUIPEMENT DE SURFACE

| DESIGNATION | TYPE & DIMENSIONS |
|---|---|
| PLAQUE DE BASE | 20"3/4-3K |
| CASING HEAD | 20"3/4-3K x 13"5/8-5K |
| DSA | 13"5/8-5K x 13"5/8-10K |
| CASING SPOOL | 13"5/8-10K x 11" 15K |
| PACK OFF FLANGE | 11"5/8-15K x 11" 10K |
| TUBING HEAD | 11" x 7"1/16 10K- FMC |
| ADAPTEUR | 7"1/16 10K x 4"1/16 10K - FMC |
| ARBRE DE NOEL | 4"1/16-10K - FMC |
| VANNES HYDRAULIQUES | 4"1/16 10K (VMS+VL) - FMC |

## EQUIPEMENTS DE FOND

| N° | DESIGNATION | LONG | TOP |
|---|---|---|---|
| 1 | Tubing hanger 4.5" 13.5# VAM FMC | 0,457 | 0,000 |
| 2 | Pup Joint X/Over 4.5" NVAM-V TOP | 1,285 | 0,457 |
| 3 | 326 Tubing Jt 4.5" 13,50 # 13Cr L13 V TOP | 3868,767 | 1,742 |
| **4** | **Halliburton 3.688" R nipple 4.5" 15.10# VAM TOP** | **0,376** | **3870,509** |
| 5 | Tubing Jt 4.5" 13,50 # 13Cr L13 V TOP | 11,849 | 3870,885 |
| 6 | Pup Joint 4.5" 13,50 # 13Cr V TOP | 2,019 | 3882,734 |
| 7 | Ratch Latch | 0,527 | 3884,753 |
| **8** | **7" MHR Packer** | **1,943** | **3885,280** |
| 9 | Mill Out Extension | 1,590 | 3887,22 |
| 10 | Red.adapter | 0,305 | 3888,81 |
| 11 | Flow coupling 4.5" Vam Top B.P 13Cr | 1,755 | 3889,12 |
| **12** | **Halliburton 3.688" RN nipple 15.10# (NO GO 3,456)** | **0,425** | **3890,87** |
| 13 | Perforated Pup Joint 4.5" 15,10 # | 2,979 | 3891,30 |
| 14 | Mule Shoe Guide | 0,215 | 3894,28 |
| 15 | Fin complétion | | **3894,49** |

## PERFORATIONS

| DATE | DIAM | DENS | TYPE | PENETR | TOP | BTM | RESERVOIR |
|---|---|---|---|---|---|---|---|
| 03/04/2010 | 4"5/8 | 5 | SDP JRC | 43" | 3934,0 | 3936,0 | Silurien "B2 Sommet" |
| 02/04/2010 | | | | | 3940,0 | 3946,0 | |
| | | | | | 3959,0 | 3963,0 | |
| 23/03/2010 | 4"1/2 | 5 | SDP JRC | 43" | 3996,0 | 4005,0 | Silurien "B2 base" |
| 08/03/2010 | | | | | 4070,0 | 4073,0 | Silurien"B1" |
| | | | | | 4076,0 | 4081,0 | |
| | | | | | 4096,0 | 4100,0 | |
| | | | | | 4108,0 | 4112,0 | |
| 16/02/2010 | | | | | 4190,0 | 4198,0 | Silurien "A2" |
| 15/02/2010 | | | | | 4202,0 | 4205,5 | |
| | | | | | 4209,0 | 4213,0 | |

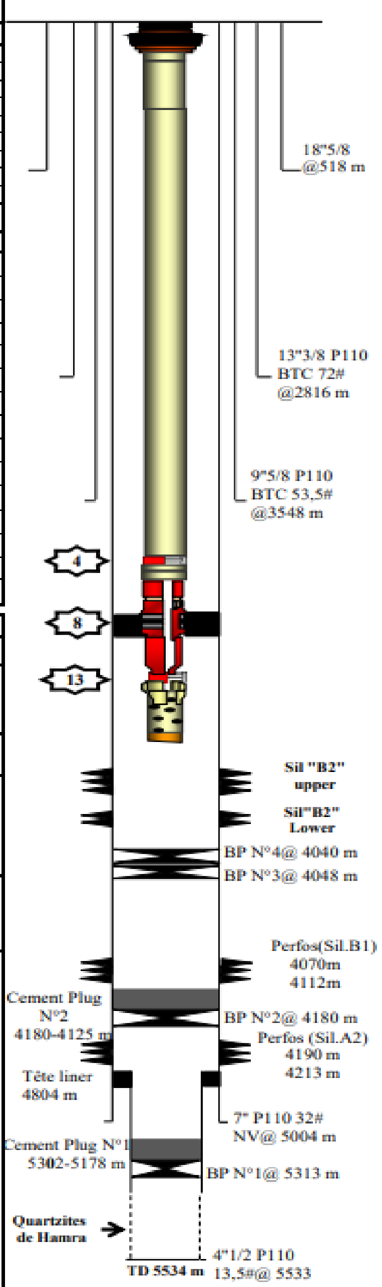


**OBSERVATIONS :**

Completion faite par Rig ENF-16

Début forage: 01/05/2009 , Fin de sondage: 14/04/2010,TD sondeur : 5534m (Niveau atteint : Quartzite de Hamra "QH")

**Work Over "ENF 34"** (Du 07/02 au 22/03/2018) : Complétion du puits dans le réservoir Silurien B2. String compression 7T: -0,810 m, Tubing stretch : 3,520 m ;

Rig Elevation à T.D Bolts = 6,650 m.

Mise à jour le 24/08/2019 par Sce T.puits

Capture d'écran et croquis

| BRDS-2 | FICHE TECHNIQUE | COORDONEES UTM | X= 309 195.86 m<br>Y= 3 377 926.46 m |
|---|---|---|---|
| | Réservoir Silurien F6-B2 | COUPE TECHNIQUE | H table = 8,15m |

## EQUIPEMENTS DE SURFACE

| Désignation | Fabricant | Type/modèle/PN | Dimension nominale | Série | Observation |
|---|---|---|---|---|---|
| **Casing Head Housing** | | | 20"3/4 | 3K | |
| **Casing Spool** | | | 20"3/4 x 13"5/8 | 3K x 5K | |
| **Casing Spool** | | | 13"5/8 x 11" | 5K x 10K | |
| **Pack-off Flange Adapter** | | | 11" | 10K x 5K | |
| **Tubing Head** | **FMC** | | 11" x 7"1/16 | 5K | |
| **Adaptateur** | **FMC** | | 7"1/16 x 4"1/16 | 5K | |
| **Suspension** | | **Olive** | 7"1/16 | 5K | |
| **Vanne maitresse inférieure** | **FMC** | | 4"1/16 | 5K | Manuelle |
| **Vanne maîtresse supérieure** | **FMC** | | 4"1/16 | 5K | Hydraulique |
| **Croix** | **Cameron** | | 4"1/16 | 5K | |
| **Vannes latérale (côte produc** | **FMC** | | 4"1/16 | 5K | Hydraulique |
| **Vannes latérale (côte kill)** | **Cameron** | | 4"1/16 | 5K | Manuelle |
| **Vanne de curage** | **Cameron** | | 4"1/16 | 5K | Manuelle |
| **Top Cap** | **FMC** | | 4"1/16 | 5K | |

## EQUIPEMETS DE FOND

| N | DESIGNATION | LONG | TOP |
|---|---|---|---|
| 1 | **Olive 7"1/16 NOM, 4"1/2N-Vam down F x 4"1/2 LTC UP F;BPV MIN BORE 3"900** | **0,445** | **0,00** |
| 2 | 351 Tubing 4.5" 13.5# SM85 N,VAM | 3566,571 | 0,445 |
| 3 | **Nipple R 3.688"** | **0,355** | **3567,02** |
| 4 | 01 Tubing 4.5" 13.5# SM85 N,VAM | 10,206 | 3567,371 |
| 5 | 01PUPS JOINT 4.5" 13.5#13Cr | 1,469 | 3577,577 |
| 6 | Ratch Latch | 0,590 | 3579,046 |
| 7 | **7" MHR Packer** | **1,817** | **3579,636** |
| 8 | Mill Out Extension | 1,590 | 3581,453 |
| 9 | Red.adapter | 0,304 | 3583,043 |
| 10 | Flow Cp 4.5" Vam Top B.P 13Cr | 1,795 | 3583,347 |
| 11 | **Nipple RN 3.456" NO-GO 4"1/2 13.50# V,TOP** | **0,424** | **3585,142** |
| 12 | Perforated Pup Jt 4.5" 13,50# 13CR VAM TOP P8.30 | 2,947 | 3585,566 |
| 13 | Mule Shoe Guide 4.5" 13,50# VAM TOP | 0,303 | 3588,513 |
| 14 | End of completion | | 3588,816 |

## PERFORATIONS

| DATE | DIAM | DENS | TYPE | PENETRATION | TOP | BTM | REMARQUE |
|---|---|---|---|---|---|---|---|
| - | 0,33" | 6spf | Gun 2"7/8 | 41,2" | 3758 m | 3767 m | TAGI Perfos squeezées |
| | 0.33" | 6spf | Gun 2"7/8 | 41,2" | 3802.5 m<br>3812.5 m<br>3827.5 m | 3807 m<br>3815 m<br>3832 m | Silurien F6-B2<br>Perfos ouvertes |

**OBSERVATIONS :**

Debut de Forage : 11/04/2015 , Fin de Forage : 17/10/2015
Debut de completion 06/10/2015 , Fin de completion 17/10/2015
Puits producteur du Gaz et Condensat

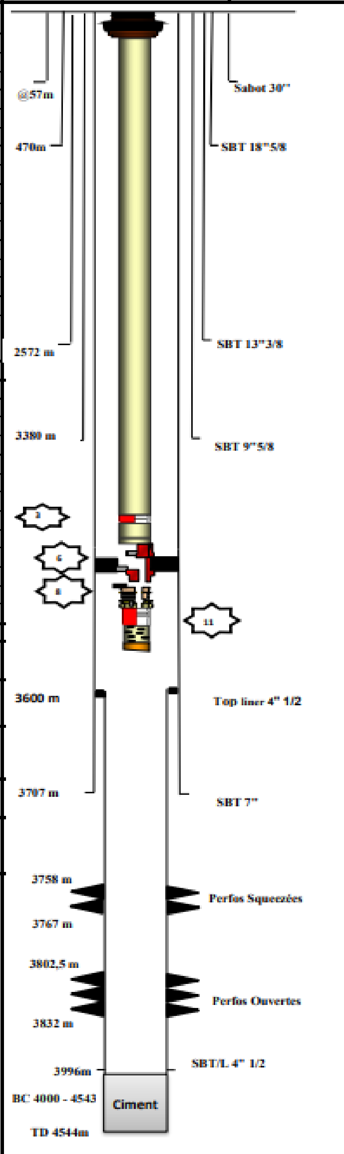


Mise à jour le 11/10/2019 par service tech-puits

| BDSN-1 | FICHE TECHNIQUE | COORDONNEES UTM | X= 309 392,52 m |
|---|---|---|---|
| | | | Y= 3 400 212,78 m |
| | RESERVOIR TAGS | COUPE TECHNIQUE | Zsol = 195 m |
| | | | Ztab = 205,82 m |

**EQUIPEMENT DE SURFACE**

| DESIGNATION | TYPE & DIMENSIONS |
|---|---|
| **TUBING HEAD** | 13"5/8 5K x 11" 5K - Crown |
| **ADAPTATEUR** | 11" 5K x 4"1/16 5K- FMC |
| **Vannes hydrauliques** | LMS + UHMV 4 1/16" 5K - FMC |
| **X mas Tree** | 4"1/16 5K - FMC |
| **Wing valve** | 4"1/16 5K - Hydraulic FMC |
| **Swab valve** | 4"1/16 5K - FMC |
| **Top cap** | 4"1/16 5K - CROWN |

**EQUIPEMENTS DE FOND**

| N | DESIGNATION | LONG | TOP |
|---|---|---|---|
| 1 | Olive Crown 11" taraudée 4"1/2 NV B x 4"3/4 ACME | 0,485 | 0,00 |
| 2 | Pup Joint | 1,060 | 0,49 |
| 3 | 310 joints de tubing 4.5" New Vam P110 13,5# | 2905,425 | 1,55 |
| **4** | **OTIS L. Nipple R 4"1/2 New Vam** | **0,350** | **2906,97** |
| 5 | Pup Jt 4.5" | 2,060 | 2907,32 |
| 6 | Joint Tubing 4.5" | 9,280 | 2909,38 |
| 7 | Baker Anchol Seal 4"1/2 New Vam | 0,900 | 2918,66 |
| **8** | **Baker Hydraulic Packer SABL3 7" 32-38#** | **1,740** | **2919,56** |
| 10 | Reducing adapter 4"1/2 NV x 5" VAM | 0,210 | 2921,30 |
| 9 | Mill Out Extension 5" VAM | 1,700 | 2921,51 |
| 11 | Flow coupling 4"1/2 NV | 1,800 | 2923,21 |
| **12** | **OTIS L. Nipple RN 4"1/2 New Vam** | **0,390** | **2925,01** |
| 14 | Mule Guide Shoe 4'' ½ New Vam | 0,600 | 2925,40 |
| 15 | End of completion | | 2926,00 |

**OBSERVATIONS**

Completion réalisée par l'appareil TP-139

| Date | Diam | Dens | Type | Pénét | Top (m) | Bottom (m) | Réservoir |
|---|---|---|---|---|---|---|---|
| | | | | | 3732,5 | 3747,5 | TAGS |

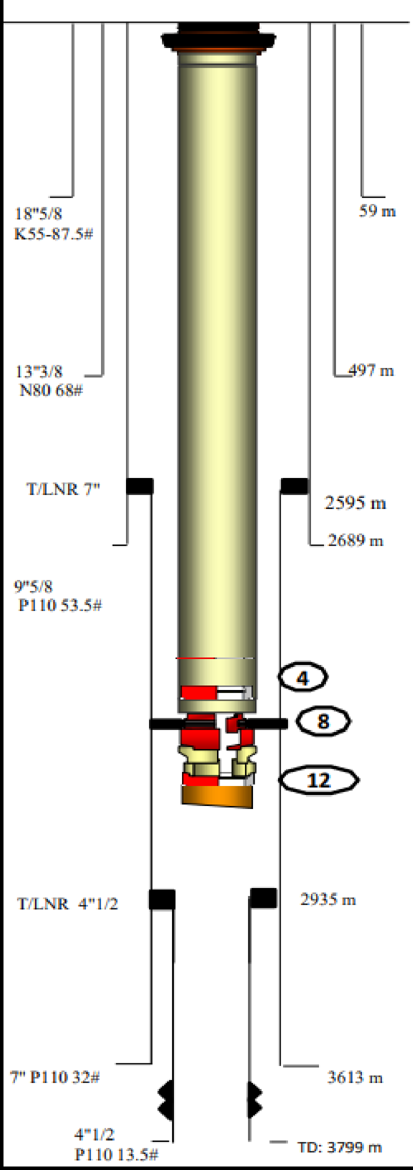


Mise à jour le 15/10/2019 par Sce Tpuits

# BRD 12

## FICHE TECHNIQUE

### RESERVOIR TAGS

| COORDONEES UTM | X= 311 175, 000 |
|---|---|
| | Y= 3 382 500, 000 |
| COUPE TECHNIQUE | Zsol = 190 m |
| | Ztab= 197,9 m |

### EQUIPEMENT DE SURFACE

| DESIGNATION | TYPE & DIMMENSION |
|---|---|
| COMPACT CSG HOUSING R-TOOL | 13"5/8-5K (BX 160), WP: 6500 psi |
| ADAPTER AVEC VANNE | 13"5/8 -5K x 4"1/16-5K |
| SUSPENSION | OLIVE 13"3/8 NOM BPV 3"980 |
| ARBRE NOEL | 4"1/16-5K CAMERON |
| VANNE HYDRAULIQUE CAMERON | 2 Vannes 4"1/16-5K: 2VM+VL |

### EQUIPEMETS DE FOND

| N | DESIGNATION | LONG | TOP |
|---|---|---|---|
| 1 | SSMC 13"5/8 Cam Tbg Hanger, 4"1/2 Vam top F with 4" BPV, type H & 1/4" CL port , ID: 3"870 | 0,500 | 0,00 |
| 1 | P/ J 4"1/2' Vam Top 13,5# 13% Cr-L80 OD: 4"968, ID: 3"795 | 1,460 | 0,50 |
| 1 | 01 tbg 4 1/2" 13,5# 13%Cr-L80 Vam top, OD: 4"968, ID: 3"795 | 12,250 | 1,96 |
| 2 | P/ J 4"1/2' Vam Top 13,5# 13% Cr-L80 OD: 4"968, ID: 3"795 | 1,510 | 14,21 |
| 3 | 01 tbg 4 1/2" 13,5# 13%Cr-L80 Vam top, OD: 4"968, ID: 3"795 | 12,020 | 15,72 |
| 4 | P/ J 4"1/2' Vam Top 13,5# 13% Cr-L80 OD: 4"968, ID: 3"795 | 1,510 | 27,74 |
| 5 | F/Cpling 4 1/2" 13,5# 13%Cr-C95 V top, OD: 5,128, ID: 3,795 | 1,760 | 29,25 |
| **6** | **TRSSV Hall 3,688" NE Self Equalizing OD: 6,970, 7500 PSI, 13,50# 13%Cr** | **1,370** | **31,01** |
| 7 | F/ Cpling 4 1/2" 13,5# 13%Cr- C95 V top, OD: 5,128, ID: 3,795 | 1,750 | 32,38 |
| 8 | P/ J 4"1/2' Vam Top 13,5# 13% Cr-L80 OD: 4"968, ID: 3"795 | 1,590 | 34,13 |
| 9 | 206 Tbg 4"1/2' V top 13,5# 13%Cr-L80, OD: 4,968, ID: 3,795 | 2475,00 | 35,72 |
| 10 | P/ J 4"1/2' Vam Top 13,5# 13% Cr-L80 OD: 4"968, ID: 3"795 | 1,400 | 2510,72 |
| **11** | **Siege 4"1/2 Vam Top 13,50# type R 3,688"Hallib, OD: 4"982, 12K psi wp** | **0,380** | **2512,12** |
| 12 | P/ J 4"1/2' Vam Top 13,5# 13% Cr-L80 OD: 4"968, ID: 3"795 | 1,580 | 2512,50 |
| 13 | P/ J 4"1/2' Vam Top 13,5# 13% Cr-L80 OD: 4"968, ID: 3"795 | 1,500 | 2514,08 |
| 14 | Ratch latch Nitrile seal Assembly 4"1/2 Vam Top Hallib OD:5"290, ID: 3"867- 13,50# 13%Cr 7500 psi wp | 0,590 | 2515,58 |
| **15** | **Hallibur 7"23-32# MHR Packer assy HNBR OD:5"875, ID:3"875-7500 psi wp Nitrile Elastomers,13%Cr FW** | **1,810** | **2516,17** |
| 16 | Millout Extension 5" 18# New Vam MxM 13% Cr 10000 Psi wp,OD: 5"035, ID: 4"220 | 0,990 | 2517,98 |
| 17 | Adaptor 5"18# N-Vam F x 4"1/2 Vam Top M 13,50# , 13% Cr 8540 psi wp , OD: 5"610, ID: 3,884 | 0,310 | 2518,97 |
| 18 | P/ J 4"1/2' Vam Top 13,5# 13% Cr-L80 OD: 4"968, ID: 3"795 | 1,590 | 2519,28 |
| 19 | 02 tbg 4 1/2" 13,5# 13%Cr-L80 Vam top, OD: 4"968, ID: 3"795 | 24,390 | 2520,87 |
| 20 | P/ J 4"1/2' Vam Top 13,5# 13% Cr-L80 OD: 4"968, ID: 3"795 | 1,500 | 2545,26 |
| **21** | **Siege 4"1/2 Vam Top 13,50# type R 3,688"Hallib, OD: 5"003,12000 psi wp, 13% Cr** | **0,380** | **2546,76** |
| 22 | P/ J 4"1/2' Vam Top 13,5# 13% Cr-L80 OD: 4"968, ID: 3"795 | 1,590 | 2547,14 |
| 23 | 01 tbg 4 1/2" 13,5# 13%Cr-L80 Vam top, OD: 4"968, ID: 3"795 | 11,980 | 2548,73 |
| 24 | P/J Perforé 4"1/2 Vam Top 13,5# 13% Cr-L80 OD: 4"968, ID:3"795 | 3,020 | 2560,71 |
| 25 | Sbt 4 1/2" Vam Top 13% Cr 13,50# , OD: 4,960, ID: 3,867 | 0,300 | 2563,73 |

### PERFORATIONS

| DATE | PHASI | TIR | TYPE | PEN | EHD | TOP | BTM |
|---|---|---|---|---|---|---|---|
| 11/02/2012 | 60° | 6SPF | 3"1/2 SHAPED CHARGE | 34,46" | 0,35" | 3311 | 3312 |
| | | | | | | 3313,5 | 3320 |
| | | | | | | 3324 | 3332 |

**OBSERVATIONS :**
Rig name : TP 200, Début forage le 25/08/2006, Fin forage le 07/02/2007, Bouchon de ciment à 3382 m, **15000 Lbs compression**

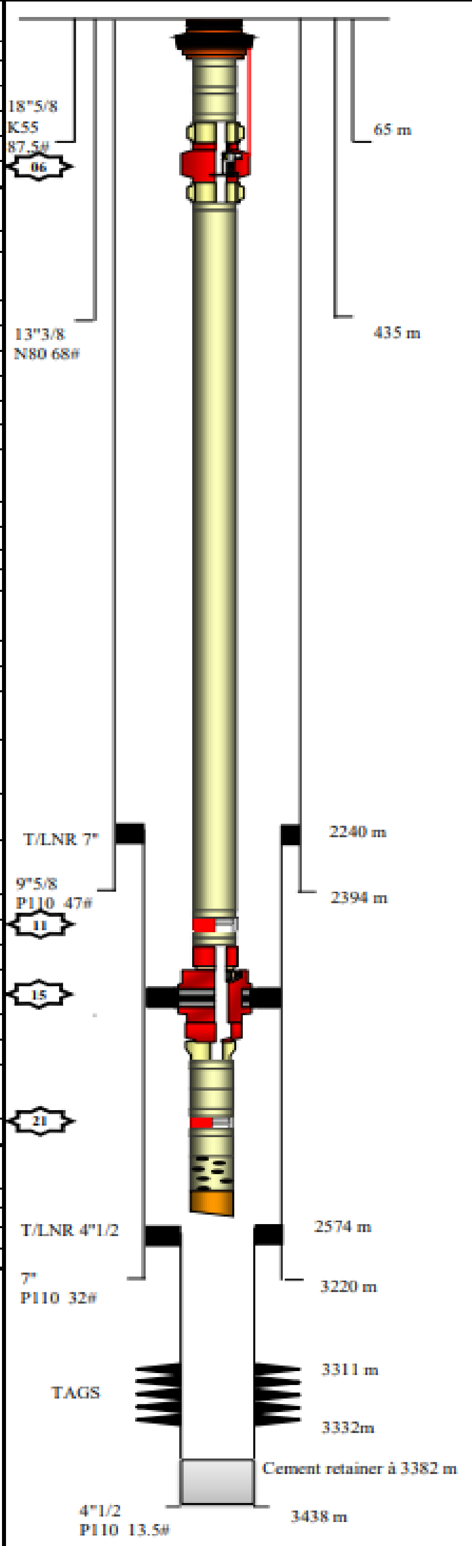


**Mise a jour le 06/05/2014 par Sce Tpuits**

| BRDS-Ext2 | FICHE TECHNIQUE<br>RESERVOIR SILURIEN F6-A2 | COORDONNEES UTM | X= 314 128,965 m<br>Y= 3 371 490,006 m |
|---|---|---|---|
| | | COUPE TECHNIQUE | Zsol = 212,495 m<br>Ztab = 222,495 m |

## EQUIPEMENTS DE SURFACE

| DESIGNATION | Fabricant | Modèle | Dimension nominale | Série | Observations |
|---|---|---|---|---|---|
| Plaque de base | | | 20"3/4 | 3K | |
| Casing Spool | | | 20"3/4 x 13"5/8 | 3K x 5K | |
| Tubing Head | Streamflo | | 13"5/8 x 11" | 5K x 10K | |
| Adaptateur | FMC | | 11" x 4"1/16 | 10K | |
| Vanne maitresse Inf | FMC | | 4"1/16 | 10K | Manuelle |
| Vanne maitresse Sup | FMC | | 4"1/16 | 10K | Hydraulique |
| Croix | FMC | | 4"1/16 | 10K | |
| Vanne latérale de production | FMC | | 4"1/16 | 10K | Hydraulique |
| Vanne latérale (Kill side) | FMC | | 4"1/16 | 10K | Manuelle |
| Vanne de curage | FMC | | 4"1/16 | 10K | Manuelle |
| Top cap | FMC | | 4"1/16 | 10K | |

## EQUIPEMENTS DE FOND

| N | DESIGNATION | LONG | TOP |
|---|---|---|---|
| 1 | FMC TUBING HANGER | 0,530 | 0,000 |
| 2 | 2 Jts Tbg 4.5" 13.5#13Cr NEWVAM VM 85 | 20,288 | 0,530 |
| 3 | X-Over 13,50# 13CR NEW VAM Box x VAM TOP Pin | 1,780 | 20,818 |
| 4 | Pup joint 4 1/2" 15.1# 13Cr L80 VAM TOP BxP | 1,982 | 22,598 |
| 5 | Flow Coupling 4.5" 15.1 #13Cr VAM TOP BxP | 1,755 | 24,580 |
| **6** | **6.97" NE 3.688" TRSSSV** | **2,280** | **26,335** |
| 7 | Flow Coupling 4.5" 15.1 #13Cr VAM TOP BxP | 1,759 | 28,615 |
| 8 | 4 joints tubing 4.5" 13.5# L13 VAM TOP | 47,428 | 30,374 |
| 9 | X-OVER 13,50# 13CR NEW VAM Pin x VAM Top Box | 1,870 | 77,802 |
| 10 | 347 joints tubing 4.5" 13.5#13Cr NEW VAM VM 85 | 3537,629 | 79,672 |
| 11 | X-OVER 13,50# 13 CR NEW VAM Box x VAM Top Pin | 1,944 | 3617,301 |
| 12 | 65 joints tubing 4.5" 13.5# L13 Vam Top | 766,335 | 3619,245 |
| **13** | **Siège R 3,688"** | **0,379** | **4385,580** |
| 14 | 4.5" 13.5# L13 VAM TOP | 11,584 | 4385,959 |
| 15 | Pup joint 4.5" 15.1#13Cr VAM TOP box | 1,982 | 4397,543 |
| 16 | Ratch Latch | 0,528 | 4399,525 |
| **17** | **7" MHR Packer** | **1,943** | **4400,053** |
| 18 | Mill Out Extension | 1,595 | 4401,996 |
| 19 | Adaptor Crossover 4.5" 15.1# NV B x VT P | 0,305 | 4403,591 |
| 20 | Flow Coupling 4.5" 15.1 #13Cr VAM TOP BXP | 1,755 | 4403,896 |
| **21** | **3.688" RN Nipple 3.456" No-go** | **0,425** | **4405,651** |
| 22 | 4.5" 15.1#13Cr Perforated PJ Vam T BxP | 2,976 | 4406,076 |
| 23 | Mule shoe | 0,214 | 4409,052 |
| 24 | Fin de complétion | | 4409,266 |

**OBSERVATIONS**

Début de forage: 12/11/2015; fin de forage: 10/04/2016 (Appareil ENF-32)
Début de complétion: 25/12/2018; fin de complétion: 14/02/2019 (Appareil ENF-34)

| Intervalle Perfos | Top (m) | Bottom (m) | Réservoir |
|---|---|---|---|
| 1ère série | 4128 | 4140,5 | Silurien B2 (squeezées) |
| 2ème série | 4468 | 4477 | Silurien A2 |

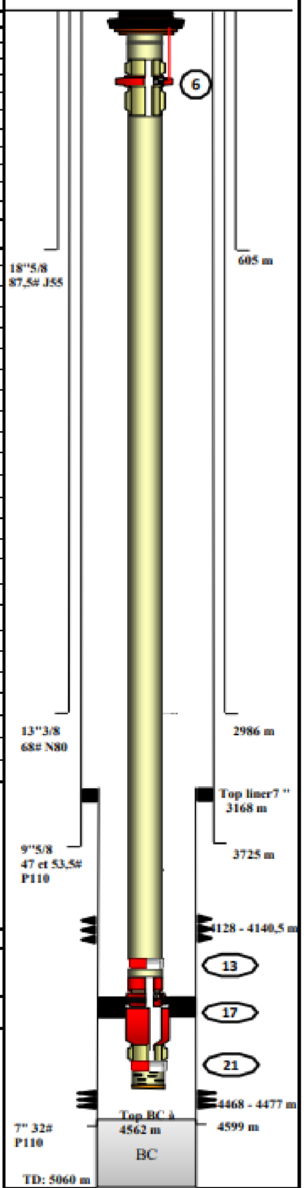


Mise à jour le 17/02/2019 par Sce Tpuits

**‘Sil B2’Reservoir**

| Constituants | MW (g/mole) | % molaire du gaz brut | ρ (g/m$^3$) |
|---|---|---|---|
| N2 | 28.014 | 4.643 | - |
| CO2 | 44.01 | 0.238 | - |
| C1 | 16.043 | 72.743 | - |
| C2 | 30.07 | 6.788 | - |
| C3 | 44.097 | 2.707 | - |
| iC4 | 58.124 | 0.679 | - |
| nC4 | 58.124 | 1.286 | - |
| iC5 | 72.151 | 0.736 | - |
| nC5 | 72.151 | 0.759 | - |
| C6 | 86.178 | 1.563 | 0.664 |
| C7 | 96 | 1.960 | 0.738 |
| C8 | 107 | 1.326 | 0.765 |
| C9 | 121 | 1.219 | 0.781 |
| C10 | 134 | 0.954 | 0.792 |
| C11 | 147 | 0.719 | 0.796 |
| C12 | 161 | 0.515 | 0.833 |
| C13 | 175 | 0.402 | 0.825 |
| C14 | 190 | 0.274 | 0.836 |
| C15 | 206 | 0.188 | 0.842 |
| C16 | 222 | 0.115 | 0.849 |
| C17 | 237 | 0.076 | 0.845 |
| C18 | 251 | 0.050 | 0.848 |
| C19 | 263 | 0.022 | 0.858 |
| C20 | 275 | 0.017 | 0.863 |
| C21 | 291 | 0.009 | 0.868 |
| C22 | 305 | 0.007 | 0.873 |
| C23+ | 350 | 0.006 | 0.877 |
| Total | | 100.00 | |

| Componen | Reservoir Fluid GEA | |
|---|---|---|
| | Wt % | Mole % |
| N2 | 1,12 | 1,02 |
| CO2 | 8,89 | 5,14 |
| H2S | 0,00 | 0,00 |
| C1 | 46,75 | 74,13 |
| C2 | 11,62 | 9,83 |
| C3 | 6,71 | 3,87 |
| i-C4 | 1,75 | 0,77 |
| n-C4 | 2,77 | 1,21 |
| i-C5 | 1,45 | 0,51 |
| n-C5 | 1,14 | 0,40 |
| C6 | 1,50 | 0,46 |
| Mcyclo-C5 | 0,10 | 0,03 |
| Benzene | 0,04 | 0,01 |
| Cyclo-C6 | 0,16 | 0,05 |
| C7 | 1,47 | 0,39 |
| Mcyclo-C6 | 0,31 | 0,08 |
| Toluene | 0,16 | 0,04 |
| C8 | 1,52 | 0,36 |
| C2-Benzen | 0,06 | 0,01 |
| mp-Xylene | 0,23 | 0,06 |
| o-Xylene | 0,06 | 0,01 |
| C9 | 1,21 | 0,26 |
| C10 | 1,35 | 0,26 |
| C11 | 1,10 | 0,19 |
| C12 | 0,98 | 0,16 |
| C13 | 0,87 | 0,13 |
| C14 | 0,77 | 0,10 |
| C15 | 0,70 | 0,09 |
| C16 | 0,60 | 0,07 |
| C17 | 0,54 | 0,06 |
| C18 | 0,49 | 0,05 |
| C19 | 0,43 | 0,04 |
| C20+ Mass % | | 14,99 |

| | PVT SiL A2 | |
|---|---|---|
| | wt% | mol% |
| $N_2$ | 0,299 | 0,312 |
| $CO_2$ | 5,198 | 3,454 |
| nC1 | 40,542 | 73,907 |
| nC2 | 9,166 | 8,913 |
| nC3 | 6,218 | 4,123 |
| iC4 | 2,458 | 1,237 |
| nC4 | 2,566 | 1,291 |
| neo-C5 | 0,041 | 0,017 |
| iC5 | 2,177 | 0,883 |
| nC5 | 1,026 | 0,416 |
| C6 | 2,247 | 0,763 |
| Benzene | 0,071 | 0,027 |
| C7 | 2,244 | 0,655 |
| Toluene | 0,333 | 0,106 |
| C8 | 2,353 | 0,602 |
| Ethylbenzene | 0,018 | 0,005 |
| M- and P- Xyle | 0,442 | 0,122 |
| O- Xylene | 0,130 | 0,036 |
| C9 | 1,836 | 0,419 |
| C10 | 2,169 | 0,446 |
| C11 | 1,831 | 0,343 |
| C12 | 1,524 | 0,262 |
| C13 | 1,539 | 0,244 |
| C14 | 1,377 | 0,203 |
| C15 | 1,276 | 0,176 |
| C16 | 1,101 | 0,142 |
| C17 | 1,165 | 0,142 |
| C18 | 0,988 | 0,113 |
| C19 | 0,770 | 0,084 |
| C20+ | 6,895 | 0,557 |

| Component | Calculated Fluid NZ QH | |
|---|---|---|
| | wt% | mol% |
| $N_2$ | 6,320 | 5,327 |
| $H_2S$ | <0.001 | <0.001 |
| $CO_2$ | 5,805 | 3,114 |
| C1 | 49,364 | 72,671 |
| C2 | 13,560 | 10,647 |
| C3 | 7,095 | 3,799 |
| iC4 | 1,795 | 0,729 |
| nC4 | 2,441 | 0,992 |
| neo-C5 | 0,067 | 0,022 |
| iC5 | 1,238 | 0,405 |
| nC5 | 0,959 | 0,314 |
| C6 | 1,531 | 0,419 |
| Benzene | 0,114 | 0,034 |
| C7 | 1,372 | 0,323 |
| Toluene | 0,072 | 0,018 |
| C8 | 1,322 | 0,273 |
| Ethylbenzene | 0,006 | 0,001 |
| m- and p- Xyle | 0,034 | 0,008 |
| o- Xylene | 0,024 | 0,005 |
| C9 | 0,995 | 0,183 |
| C10 | 0,931 | 0,154 |
| C11 | 0,776 | 0,117 |
| C12 | 0,657 | 0,091 |
| C13 | 0,593 | 0,076 |
| C14 | 0,493 | 0,059 |
| C15 | 0,423 | 0,047 |
| C16 | 0,345 | 0,036 |
| C17 | 0,328 | 0,032 |
| C18 | 0,257 | 0,024 |
| C19 | 0,182 | 0,016 |
| C20+ | 0,901 | 0,064 |